CALIFORNIA INSTITUTE OF TECHNOLOGY

ELECTRON TUBE AND MICROWAVE LABORATORY

A FIELD ANALYSIS OF THE M TYPE BACKWARD WAVE OSCILLATOR

by

Roy W. Gould

Technical Report No. 3

September 1955

A REPORT ON RESEARCH CONDUCTED UNDER

CONTRACT WITH THE OFFICE OF NAVAL RESEARCH

AND THE SPERRY GYROSCOPE COMPANY

A FIELD ANALYSIS OF THE M-TYPE BACKWARD WAVE OSCILLATOR

by

Roy W. Gould

CALIFORNIA INSTITUTE OF TECHNOLOGY

Pasadena, California

A Technical Report to the Office of Naval Research

and the

Sperry Gyroscope Company

September 1955

ACKNOWLEDGMENT

I wish to thank my associates with whom various aspects of this problem have been discussed and particularly Professor Lester M. Field for his continued interest in this investigation. My stay at the California Institute of Technology has been made possible through the financial support of the National Science Foundation and the Hughes Aircraft Company. Assistance with computation and preparation of the manuscript from Mr. Iwao Sugai; my wife, Bunny; and Mrs. Ruth Brown, is gratefully acknowledged.

II A FIELD ANALYSIS OF THE M TYPE BACKWARD WAVE OSCILLATOR

ABSTRACT

A field theory of electron beams focused by crossed electric and magnetic fields is given. The theory is basic to the understanding of the small signal behavior of crossed field electron devices. It is applied to explain the slipping stream, or diocotron, effect as a coupling of two surface waves of the electron beam, and to derive the start oscillation conditions of the M-type backward wave oscillator. It is found that the slipping stream effect can reduce the starting current by an appreciable factor. The results are compared with the thin beam theory which neglects space charge effects.

An analysis of a loaded strip transmission line is given, from which a method of representing space harmonic slow wave circuits by a surface admittance boundary condition is obtained. Forward and backward space harmonic interaction may be treated equally well.

TABLE OF CONTENTS

I. INTRODUCTION

The last few years have seen the invention of a host of new microwave amplifier and oscillator tubes. The small signal theory of tubes using electron beams focused by axial or longitudinal magnetic fields is now rather well developed (1),(2),(3),(4),(5). The theory of tubes using electron beams focused by crossed electric and magnetic fields is not so well developed, perhaps because this type of tube has not been so important until recently. The M-type (M for magnetron, because of the similar steady flow conditions) backward wave oscillator is likely to be very important because of its higher efficiency of conversion of d.c. energy to a.c. energy and its greater tuning rate than the longitudinally focused, or O-type (O for ordinary) backward wave oscillator. The operating characteristics and the theory of this new type of tube are summarized in reference (6).

The major contribution of this paper is to present a field analysis of M-type tubes which makes it possible to take into account space charge effects, that is, the effect on the motion of the charge of fields generated by the space charge. It is not possible to do this without a number of assumptions, to be discussed later, the principal one of which is that the unperturbed condition in the beam is a generalization of the planar Brillouin(7) state. While, in principal, this state can be realized in beam type tubes, it is doubtful whether most tubes fulfill this condition very closely.

Although this paper concentrates on the application of the theory to the M-type backward wave oscillator, the theory developed here is

fundamental to all M-type beam tubes. The diocotron, or slipping stream amplifier, is discussed briefly, inasmuch as some of the effects which it exhibits have a bearing on the backward wave oscillator discussion.

A schematic diagram of the M-type backward wave oscillator is shown in Figure 1. Electrons emitted from the cathode, C, are focused into a beam through the combined action of the magnetic field B_{ox}, and the electric field produced by the plate, P, the sole, S, and the slow wave circuit, or delay line, L. When the electrons travel to the right with a velocity approximately equal to the phase velocity of one of the space harmonics of a wave of the slow wave circuit, a strong modulation of the electrons occurs and they may give energy to the field, much as in a magnetron. If the energy flow of the circuit wave is to the left, this energy, reinforcing the modulation of the beam as it goes, is delivered to the transmission line connected to the circuit on the left, and ultimately delivered to a load. The circuit is terminated on the right, by T, so that there is no reflection of electromagnetic energy at this end of the circuit. The electrons are collected by K, after their passage through the interaction region.

In order for the modulation of the beam to reinforce, and for oscillations to increase with time until non-linearities limit the amplitude, the circuit wave and the electrons must have a certain relative velocity and the tube must be greater than a certain minimum length. The latter condition can also be interpreted to mean that, for a given length, a certain minimum current in the electron beam is required. These "start oscillation" conditions will be determined in this analysis.

The elementary theory neglects space charge effects (8), (9). This

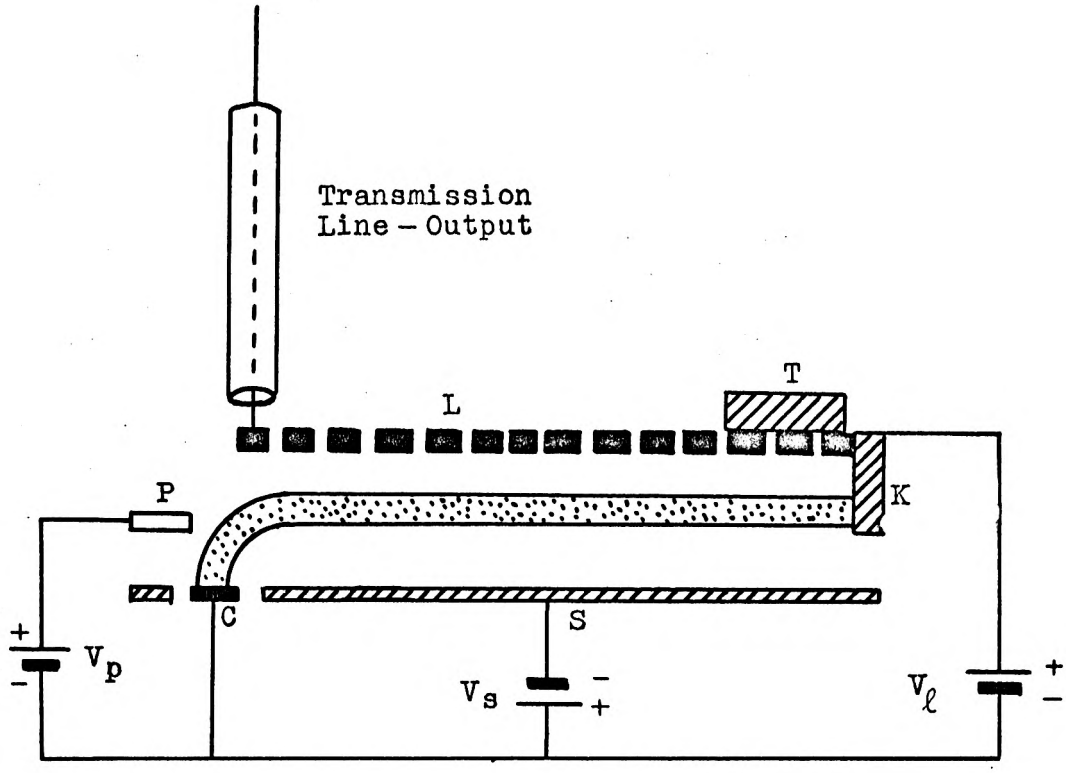

Figure 1. Schematic Structure of the Linear M-Type Backward Wave Oscillator

analysis studies the effects of space charge (particularly the slipping stream effect) on the start oscillation conditions. French workers report (6) that the current required to start oscillations is frequently only one-half or one-third the value predicted by the elementary theory and suggest that space charge effects are responsible. An approximate theory which they have devised (6),(10) to explain this result is discussed at the conclusion of this analysis.

In order to carry out the analysis it is necessary to make a number of assumptions. These are listed here for reference, although in many cases a more detailed discussion will be found at the point at which they are introduced.

1. All quantities are assumed to be independent of the x coordinate over the width of the tube w. Fringing fields are neglected, and it is assumed that the beam does not spread in this direction.

2. A self-consistent field method is used. The particle aspect of the electron is ignored by considering the motion of an equivalent charged fluid.

3. The analysis is non-relativistic. Non-relativistic equations of motion are used. Magnetic fields are neglected, except in Section V where the slow wave circuit is discussed. The electric field is assumed irrotational.

4. The analysis is restricted to small signals. All equations are linearized by neglecting the products of time-varying quantities. The t and z dependences are assumed to be $e^{j(\omega t - \beta z)}$, and superposition applies.

5. An equivalent surface charge density and surface current

density is used to take into account the deformation of the boundary of the electron beam.

6. Only a finite number of modes of propagation are used, so that it is not possible to meet all the boundary conditions on the motion of the electron beam at the point at which it enters the interaction region.

7. It is assumed that the electron beam affects only one of the circuit space harmonics. Thus the "rising sun" effect and operation near a circuit cutoff frequency is not analyzed, although the manner in which these two effects may be studied is outlined in Section V .

8. It is assumed that the steady state of the electron beam is the planar Brillouin state, or a modification of it, so that the steady or d.c. velocity of the beam is in the z direction only.

9. Numerical computations are carried out for small $\frac{\omega_p^2}{\omega_c^2}$ only, although there is reason to believe that the results would not be significantly different if $\frac{\omega_p^2}{\omega_c^2}$ were as large as unity.

10. The sole is assumed to be far from the beam in the numerical position of the analysis. This is not an essential assumption. Other cases may be calculated with no additional difficulty. Actually, it is desirable to have the beam close to sole and far from the circuit for high efficiency operation.

II. THE ELECTRONIC EQUATIONS

The equations obeyed by the field quantities in the interior of the electron beam will be derived in this section. The motion of the charge will be discussed from the Euler point of view, as well as from the Lagrange point of view, since some confusion exists in the literature where these methods have been applied to electron beam problems. Figure 2, shows the configuration to be analyzed.

Steady State of the Beam. It is assumed that the electric and magnetic forces balance at every point within the beam and that the flow is rectilinear. Thus

$$E_{oy} + u(y)\, B_{ox} = 0 \qquad \text{II.1}$$

where the velocity, u, may depend on y. The electric field, E_{oy}, varies with y because of the charge in the beam,

$$\frac{\partial E_o}{\partial y} = \frac{\rho_o}{\epsilon_o}\, s \qquad \text{II.2}$$

where the factor s has been introduced to account for the possibility of neutralization of the electron charge by ions. s is 1 when there are no ions, and 0 when the electron charge is completely neutralized. s might be termed the "slip" parameter since when $s = 0$, all electrons move with the same velocity, while when $0 < s \leq 1$, the upper electrons slip past the lower electrons. Differentiating II.1 with respect to y and combining with II.2, the gradient of the steady velocity is found to be

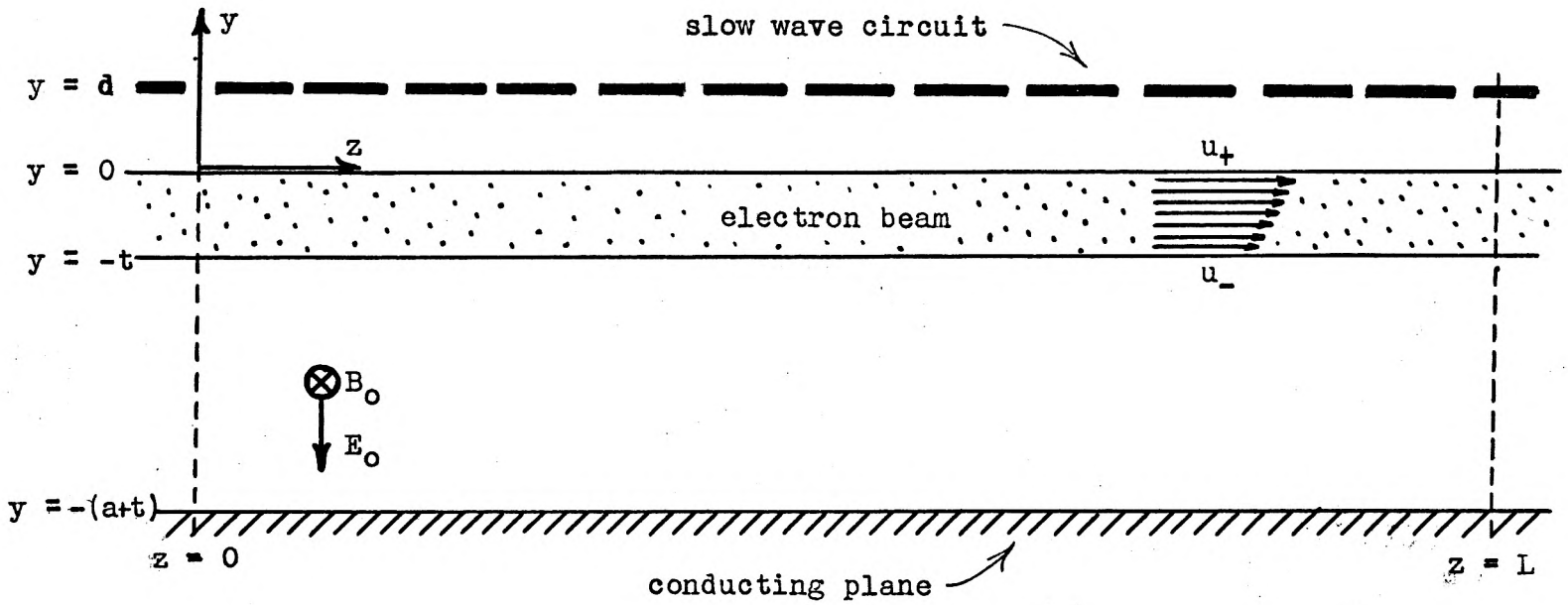

Figure 2. Configuration of the Model which is Analyzed

$$\frac{\partial u}{\partial y} = -\frac{1}{B_{ox}}\frac{\rho_o}{\epsilon_o} s = \frac{\omega_p^2}{\omega_c} s \qquad \text{II.3}$$

In the remainder of the analysis the velocity gradient will be denoted by

$$\Delta = \frac{\partial u}{\partial y} = \frac{\omega_p^2}{\omega_c} s \qquad \text{II.4}$$

It will be assumed that the sense of the steady magnetic field is as shown in Figure 2. However, reversing the magnetic field and the electric field simply changes the sign of ω_c .

It should be pointed out that the steady flow condition just described is somewhat more general than can be obtained if the electrons are emitted from a unipotential cathode, for in this case there is the additional restriction

$$\frac{1}{2} u^2 = \eta \phi_o \qquad \text{II.5}$$

where ϕ_o is the potential from which E_o is derived, measured from the cathode. It is easily shown that this additional restriction is compatible with II.3 only if $(\frac{\omega_p}{\omega_c})^2 s = 1$. Differentiating II.5 with respect to y and using II.1 ,

$$u \frac{\partial u}{\partial y} = \eta \frac{\partial \phi_o}{\partial y} = -\eta E_{oy} = \eta u B_{ox}$$

which may be written

$$\frac{\partial u}{\partial y} = \eta B_{ox} = \omega_c \ . \qquad \text{II.6}$$

This restriction means that in the absence of ions, the electron plasma frequency and the electron cyclotron frequency must be the same. This is the planar Brillouin condition (7). The more general condition II.3

will be assumed unless otherwise noted.

In practice, this type of steady flow is seldom realized, although in principle it can be obtained. The use of these steady flow conditions may be regarded as a working hypothesis, whose usefulness is to be determined by a comparison with the experimental results. It is true that in many physical problems some of the simpler results of a calculation do not depend particularly on the model chosen for the analysis, so long as the model is internally consistent. The field point of view makes possible an internally consistent analysis in which most of the approximations which must be made to solve the problem are mathematical approximations which have previously received careful scrutiny. The major physical assumption in this analysis is that the above steady flow conditions are realized.

In practical beams of this type the indication seems to be that the current densities are such as to make ω_p^2 considerably less than ω_c^2 and electrons do not follow linear trajectories. Perhaps some of the features of such a beam may be described satisfactorily by replacing it by a Brillouin flow beam with the same value of ω_p^2.

Perturbations from the Steady State. The linearized equations, in Eulerian form, for small perturbations from the steady state are

$$\frac{\partial \underline{v}_1}{\partial t} + (\underline{u} \cdot \nabla)\, \underline{v}_1 + (\underline{v}_1 \cdot \nabla)\, \underline{u} = -\eta (\underline{E}_1 + \underline{v}_1 \times \underline{B}_o) \qquad \text{II.7}$$

$$\frac{\partial \rho_1}{\partial t} + \nabla \cdot (\rho_o \underline{v}_1 + \underline{u} \rho_1) = 0 \qquad \text{II.8}$$

$$\epsilon_o \nabla \cdot \underline{E}_1 = \rho_1 \qquad \text{II.9}$$

$$\nabla \times \underline{E}_1 = 0 \ . \qquad \text{II.10}$$

The subscript 1 denotes the perturbation of a quantity, and the subscript 0 denotes the unperturbed or steady value of the quantity. The term $\underline{u} \times \underline{B}_1$ has been neglected in II.7 because it is of order $(u/c)^2$ smaller than $\underline{E}_1$. Equation II.10 is one of the Maxwell equations with the magnetic field, $\underline{B}_1$, neglected, and expresses the static approximation.

It will be convenient to assume that the t and z dependence of all quantities is given by the factor

$$e^{j(\omega t - \beta z)} \quad . \qquad \text{II.11}$$

In the remainder of the analysis, this dependence will be understood and the above factor omitted, except where required for clarity. The symbols for the field quantities are subsequently to be considered as phasors, denoting the amplitude and phase of the sinusoidal, or a.c., perturbation of the quantity in question.

Since $\nabla \times \underline{E}_1 = 0$, the electric field is derivable from a potential. Because of II.11 the z component of the electric field is just a constant times the potential, and it is possible to omit using a potential and express all quantities in terms of E_{1z}. For example, the x component of II.10 becomes

$$\frac{\partial E_{1z}}{\partial y} + j\beta E_{1y} = 0 \qquad \text{or} \qquad E_{1y} = -\frac{1}{j\beta} \frac{\partial E_{1z}}{\partial y} \quad . \qquad \text{II.12}$$

II.9 becomes

$$\frac{\partial E_{1y}}{\partial y} - j\beta E_{1z} = \frac{\rho_1}{\epsilon_0} \quad . \qquad \text{II.13}$$

Eliminating E_{1y} between these equations gives

$$\frac{\partial^2 E_{1z}}{\partial y^2} - \beta^2 E_{1z} = - j\beta \frac{\rho_1}{\epsilon_o} \quad , \qquad \text{II.14}$$

and II.8 may be solved for ρ_1

$$\rho_1 = - \frac{\rho_o \left(\frac{\partial v_{1y}}{\partial y} - j\beta v_{1z}\right)}{j(\omega - \beta u)} \quad . \qquad \text{II.15}$$

In component form II.7 is

$$j(\omega - \beta u)\, v_{1y} = - \eta (E_{1y} + v_{1z} B_{ox}) \qquad \text{II.16}$$

$$j(\omega - \beta u)\, v_{1z} + \Delta v_{1y} = -\eta (E_{1z} - v_{1y} B_{ox}) \, . \qquad \text{II.17}$$

The x equation is not required since the problem is assumed to be two-dimensional; $v_{1x} = 0$. Solving for v_{1y} and v_{1z} yields

$$v_{1y} = \frac{j(\omega - \beta u) E_{1y} - \omega_c E_{1z}}{\Omega^2} \qquad \text{II.18}$$

$$v_{1z} = \frac{j(\omega - \beta u) E_{1z} + (\omega_c - \Delta) E_{1y}}{\Omega^2} \quad , \qquad \text{II.19}$$

where $\Omega^2 = (\omega - \beta u)^2 - \omega_c(\omega_c - \Delta)$.

To obtain the differential equation obeyed by E_{1z} , substitute ρ_1 from II.15 into II.14, obtaining

$$\frac{\partial^2 E_{1z}}{\partial y^2} - \beta^2 E_{1z} = -\frac{\rho_o}{\epsilon_o} \frac{\beta\left(\frac{\partial v_{1y}}{\partial y} - j\beta\, v_{1z}\right)}{(\omega - \beta u)} \quad . \qquad \text{II.20}$$

Differentiating II.18 with respect to y , bearing in mind that u as well as E_{1y} and E_{1z} are functions of y , and using II.19 ,

$$\frac{\partial^2 E_{1z}}{\partial y^2} - \beta^2 E_{1z} = \frac{\omega_p^2}{\Omega^2}\left[\frac{\partial^2 E_{1z}}{\partial y^2} - \beta^2 E_{1z} + \frac{2\beta\Delta\left\{(\omega-\beta u)\frac{\partial E_{1z}}{\partial y} + \beta\omega_c E_{1z}\right\}}{\Omega^2}\right], \qquad \text{II.21}$$

which may be rewritten,

$$\left[1 - \frac{\omega_p^2}{\Omega^2}\right]\frac{\partial^2 E_{1z}}{\partial y^2} - 2\frac{\omega_p^2}{\Omega^4}\beta(\omega-\beta u)\Delta\frac{\partial E_{1z}}{\partial y} - \beta^2\left[1 - \frac{\omega_p^2}{\Omega^2} + \frac{2\omega_p^2\omega_c\Delta}{\Omega^4}\right]E_{1z} = 0 . \qquad \text{II.22}$$

This result may be obtained by another method, analogous to the Lagrangian description in hydrodynamics (11), in which the motion of an individual particle is described. The position of the electron is given by

$$\underline{r} = \underline{r}_o(a,b,c,t) + \underline{r}_1(a,b,c,t) \qquad \text{II.23}$$

where $\underline{r}_o(a,b,c,t)$ is the position of the electron in the absence of the small a.c. disturbances; a,b,c, are parameters which tell which electron is being described (for example, a,b,c, might be the xyz coordinates of the electron at $t = 0$); $\underline{r}_1$ is the a.c. perturbation of the electron position as a function of time.

The equation of motion of the electron is

$$\frac{d^2\underline{r}}{dt^2} = -\eta\left[\underline{E}(r) + \frac{d\underline{r}}{dt} \times \underline{B}(r)\right] \qquad \text{II.24}$$

where $\underline{E}(r) = \underline{E}_o(r) + \underline{E}_1(r)$

$\underline{B}(r) = \underline{B}_o(r) + \underline{B}_1(r)$ ($\underline{B}_1(r)$ may be neglected, however.)

$\underline{E}_o$ and $\underline{B}_o$ are the steady parts of the electric and magnetic fields and it is assumed that $\underline{E}_o(r_o) + \underline{u} \times \underline{B}_o(\underline{r}_o) = 0$ for all electrons so

that the unperturbed trajectories are straight lines. The linear, time-dependent part of the above equation is

$$\frac{d^2\underline{r}_1}{dt^2} = -\eta\left[\underline{E}_1(r_o) + (\underline{r}_1 \cdot \nabla)\,\underline{E}_o(\underline{r}_o) + \frac{d\underline{r}_1}{dt} \times \underline{B}_o\right] \quad . \qquad \text{II.25}$$

The first term arises from the change in $\underline{E}$ along the unperturbed trajectory, while the second term takes into account the fact that motion of the electron into a region where the d.c. field is different appears as an a.c. force on the electron since the motion is time varying. In the linear approximation $\underline{E}_1$ may be evaluated at its unperturbed position r_o . If $a,b,c,$ are the unperturbed electron coordinates at $t = 0$, the unperturbed coordinates at time t later are,

$$\begin{aligned} x_o &= a \\ y_o &= b \\ z_o &= c + u_o(b)t \quad . \end{aligned} \qquad \text{II.26}$$

Assuming the fields to vary as $e^{j\omega t}\, e^{-j\beta z}$ it is easily seen that in the linear approximation the time dependence of the force acting on the electron is $e^{j(\omega - \beta u)t}$ hence differentiation with respect to time, $\frac{d}{dt}$, is equivalent to multiplication by $j(\omega - \beta u)$. In component form II.25 becomes,

$$-(\omega - \beta u)^2\, y_1 = -\eta\left[E_{1y} + \frac{\partial E_{oy}}{\partial y}\, y_1 + j(\omega - \beta u)\, z_1\, B_{ox}\right] \qquad \text{II.27}$$

$$-(\omega - \beta u)^2\, z_1 = -\eta\left[E_{1z} - j(\omega - \beta u)\, y_1\, B_{ox}\right] \qquad \text{II.28}$$

($e^{j(\omega - \beta u)t}$ is understood.)

Solving for y_1 and z_1,

$$j(\omega - \beta u)\, y_1 = \frac{j(\omega - \beta u)\, E_{1y} - \omega_c\, E_{1z}}{\Omega^2} \qquad \text{II.29}$$

$$j(\omega - \beta u)\, z_1 = \frac{j(\omega - \beta u)\, \frac{\omega_c\ \Delta}{j(\omega - \beta u)}\, E_{1z} + \omega_c\, E_{1y}}{\Omega^2} \qquad \text{II.30}$$

where $\eta \frac{\partial E_o}{\partial y}$ has been replaced by the value obtained from II.2 and II.4,

$$\eta \frac{\partial E_o}{\partial y} = \eta \frac{\rho_o}{\epsilon_o}\, s = -\omega_p^2\, s = -\omega_c\, \Delta\,.$$

Notice that II.30 differs from II.19 although II.29 and II.18 are the same. II.18 and II.19 describe the velocity field at a particular point in space, while II.29 and II.30 describe the a.c. velocity of a particle whose unperturbed trajectory passes through this point, but whose perturbed trajectory does not.

The charge density in the vicinity of a particular particle is calculated from the Lagrange continuity equation

$$\rho = \frac{\rho_o}{\begin{vmatrix} \frac{\partial y}{\partial b} & \frac{\partial y}{\partial c} \\ \frac{\partial z}{\partial b} & \frac{\partial z}{\partial c} \end{vmatrix}}$$

using the particle positions,

$$y = b + y_1(u, E_{1y}\, E_{1z})\, e^{j(\omega - \beta u)t}\, e^{-j\beta c}$$

$$z = c + ut + z_1(u, E_{1y}\, E_{1z})\, e^{j(\omega - \beta u)t}\, e^{-j\beta c}\,.$$

Performing the indicated computations, and using $\frac{\partial u}{\partial b} = \Delta$,

$$\frac{\partial y}{\partial b} = 1 + \left[\frac{\partial y_1}{\partial u}\Delta + \frac{\partial y_1}{\partial E_{1y}}\frac{\partial E_{1y}}{\partial b} + \frac{\partial y_1}{\partial E_{1z}}\frac{\partial E_{1z}}{\partial b} - j\beta t\Delta y\right] e^{j(\omega-\beta u)t}\, e^{-j\beta c}$$

$$\frac{\partial y}{\partial c} = -j\beta y_1\, e^{j(\omega-\beta u)t}\, e^{-j\beta c}$$

$$\frac{\partial z}{\partial b} = \Delta t + \left[\frac{\partial z_1}{\partial u}\frac{\partial E_{1y}}{\partial b} + \frac{\partial z_1}{\partial E_{1z}}\frac{\partial E_{1z}}{\partial b}\right] e^{j(\omega-\beta u)t}\, e^{-j\beta c}$$

$$\frac{\partial z}{\partial c} = 1 - j\beta z_1\, e^{j(\omega-\beta u)t}\, e^{-j\beta c}$$

$$J = \frac{\partial y}{\partial b}\frac{\partial z}{\partial c} - \frac{\partial z}{\partial b}\frac{\partial y}{\partial c} = 1 + \left[\frac{\partial y_1}{\partial u}\Delta + \frac{\partial y_1}{\partial E_{1y}}\frac{\partial E_{1y}}{\partial b} + \frac{\partial y_1}{\partial E_{1z}}\frac{\partial E_{1z}}{\partial b} - j\beta t\Delta y_1 - j\beta z_1\right]$$

$$e^{j(\omega-\beta u)t}\, e^{-j\beta c} + j\beta\Delta t y_1\, e^{j(\omega-\beta u)t}\, e^{-j\beta c} + \text{second order terms.}$$

Thus

$$\rho \approx \frac{1}{1 + \left[\frac{\partial y_1}{\partial u}\Delta + \frac{\partial y_1}{\partial E_{1y}}\frac{\partial E_{1y}}{\partial b} + \frac{\partial y_1}{\partial E_{1z}}\frac{\partial E_{1z}}{\partial b} - j\beta z_1\right] e^{j(\omega-\beta u)t}\, e^{-j\beta c}}$$

$$\rho_1 = (\rho - \rho_o) = \rho_o\left[\frac{\partial y_1}{\partial u}\Delta + \frac{\partial y_1}{\partial E_{1y}}\frac{\partial E_{1y}}{\partial b} + \frac{\partial y_1}{\partial E_{1z}}\frac{\partial E_{1z}}{\partial b} - j\beta z_1\right] e^{j(\omega-\beta u)t}\, e^{-j\beta c} \qquad \text{II.31}$$

From II.29 and II.30

$$y_1 = \eta\left[\frac{E_{1y}}{\Omega^2} - \frac{\omega_c}{j(\omega-\beta u)}\frac{E_{1z}}{\Omega^2}\right]$$

$$z_1 = \eta\left[1 + \frac{\omega_c\,\Delta}{(\omega-\beta u)^2}\right]\frac{E_{1z}}{\Omega^2} + \eta\,\frac{\omega_c}{j(\omega-\beta u)}\frac{E_{1y}}{\Omega^2} \quad .$$

Thus

$$\frac{\partial y_1}{\partial u} = \eta\left\{\frac{+2\beta(\omega-\beta u)}{\Omega^4}\left[E_{1y} - \frac{\omega_c}{j(\omega-\beta u)}E_{1z}\right] - \frac{\omega_c\,\beta}{j(\omega-\beta u)^2}\frac{E_{1z}}{\Omega^2}\right\}$$

$$\frac{\partial y_1}{\partial E_{1y}} = \eta\,\frac{1}{\Omega^2} \qquad \frac{\partial y_1}{\partial E_{1z}} = -\eta\,\frac{\omega_c}{j(\omega-\beta u)}\frac{1}{\Omega^2} \quad .$$

Substituting into II.31 for ρ_1 ,

$$\rho_1 = -\rho_o \left\{ \begin{array}{l} \dfrac{2\beta\,\Delta(\omega-\beta u)}{\Omega^4}\left[E_{1y} - \dfrac{\omega_c}{j(\omega-\beta u)}E_{1z}\right] - \dfrac{\Delta\,\omega_c\,\beta}{j(\omega-\beta u)^2}\dfrac{E_{1z}}{\Omega^2} \\ + \dfrac{1}{\Omega^2}\dfrac{\partial E_{1y}}{\partial b} - \dfrac{\omega_c}{j(\omega-\beta u)}\dfrac{1}{\Omega^2}\dfrac{\partial E_{1z}}{\partial b} - j\beta\left[1+\dfrac{\omega_c\,\Delta}{(\omega-\beta u)^2}\right]\dfrac{E_{1z}}{\Omega^2} \\ - j\beta\,\dfrac{\omega_c}{j(\omega-\beta u)}\dfrac{E_{1y}}{\Omega^2} \end{array} \right\} \times e^{j(\omega-\beta u)t}\, e^{-j\beta c}$$

or

$$-\frac{j\beta}{\epsilon_o}\rho_1 = \frac{\omega_p^2}{\Omega^2}\left[\frac{\partial^2 E_{1z}}{\partial b^2} - \beta^2 E_{1z} + \frac{2\beta\,\Delta\,(\omega-\beta u)\dfrac{\partial E_{1z}}{\partial b} + \beta\omega_c\,E_{1z}}{\Omega^2}\right] \qquad \text{II.32}$$

where $E_{1y} = -\dfrac{1}{j\beta}\dfrac{\partial E_{1z}}{\partial b}$ has been used. This is an expression for the charge density in the vicinity of a given particle. Taking $c + u_o t = z$ to be a constant in this expression rather than c = constant, and $b = y$, the a.c. charge density at the point $(x, y + y_1 e^{j(\omega t - \beta z)}, z)$ is obtained. To a first approximation this is the a.c. charge density at the point x,y,z . II.32 is precisely the same as the right side of II.21. Thus the two methods give identical results, as they must, although they differ in detail.

This will now be compared with the method of Warnecke, Doehler and Bobot (12), which is in error. To compute the a.c. charge density they use $j(\omega-\beta u)y_1$ and $j(\omega-\beta u)z_1$ (II.29 and II.30), as the y and z components of a.c. velocity in the Eulerian continuity equation II.15, whereas the Lagrange continuity equation should be used. Another way of stating the difficulty is to note that II.29 and II.30 do not give the velocity at a fixed point in space (x,y,z) but rather the velocity at the point $(y + y_1,\ z + z_1)$. The velocity at (y,z) can be computed

from this however, if it is remembered that the particles which are at (y,z) came from an unperturbed position $(y - y_1, z - z_1)$ where the steady part of the z velocity is

$$u(y) = \frac{\partial u}{\partial y} y_1 = u(y) - \Delta y_1 \ .$$

This contributes to the a.c. velocity at the fixed point giving

$$v_{1y} = j(\omega - \beta u)\, y_1 \qquad \text{II.33}$$

$$v_{1z} = j(\omega - \beta u)\, z_1 - \Delta\, y_1 \ . \qquad \text{II.34}$$

Using II.29 and II.30 in II.34 gives exactly II.19 . The extra term in II.34 subtracts from the z component of velocity. This can be understood as follows: If the particles move upward, $y_1 > 0$, the z velocity of a given point will be less because the particles which are at this point have come from a point below where the steady velocity in the z direction is less (if $\Delta > 0$). This effect contributes to the a.c. velocity of the point since y_1 , the vertical displacement is an a.c. effect.

Discussion of the Differential Equation for E_{1z}. II.21 may be simplified in three special cases. First, if $s = 0$ all electrons have the same velocity, u . Because of the constant electric field, however, different electrons are at different electrostatic potentials, depending on their position in the beam. Since different electrons are at different potentials but all have the same velocity, they cannot have been emitted from a unipotential cathode with zero initial velocities. Thus the following analysis does not apply to a situation which is easily realized in practice. Nevertheless, it is instructive to consider this case in some detail because of its simplicity. This relatively simple case forms the

basis for discussion of the more complicated slipping stream case ($s \neq 0$) .

When $s = \Delta = 0$, II.21 reduces to

$$\left[1 - \frac{\omega_p^2}{(\omega - \beta u)^2 - \omega_c^2}\right]\left[\frac{d^2 E_{1z}}{dy^2} - \beta^2 E_{1z}\right] = 0 \quad . \qquad \text{II.35}$$

The solutions of this equation are of two types:

$$\text{(a)} \quad (\omega - \beta u)^2 = \omega_p^2 + \omega_c^2 \qquad \text{II.36}$$

$$\text{(b)} \quad \frac{d^2 E_{1z}}{dy^2} - \beta^2 E_{1z} = 0 \quad . \qquad \text{II.37}$$

Solutions of type (a) have a charge density in the interior of the beam associated with them. In a coordinate system which moves with the electrons all disturbances of this type oscillate with the frequency $\sqrt{\omega_p^2 + \omega_c^2}$. These disturbances are the plasma oscillations of the beam, modified by the magnetic field (when ω_c is zero, the frequency in the moving coordinate system is simply ω_p) . The frequency of oscillation does not depend on the variation of the disturbance with the transverse, or y, coordinate. Fields which go with this type of solution are localized within the beam, and are not coupled to external electromagnetic circuits (gridded cavities excepted). This type of solution is similar to the solution $(\omega - \beta u)^2 = \omega_p^2$ found by Rigrod and Lewis[4] in their study of wave propagation along a magnetically focused cylindrical electron beam.

The charge density modulation in the interior of the beam is zero for solutions of the second type, and the differential equation for E_{1z}

is especially simple. The nature of these solutions is discussed in Section IV, following the discussion of boundary conditions in Section III.

When s is unity (intermediate values of s will not be discussed), it is convenient to express II.21 in terms of dimensionless variables,

$$r = \frac{\omega_p}{\omega_c} \qquad \text{II.38}$$

$$\xi = -\frac{\omega - \beta u}{\Delta} \qquad \text{II.39}$$

or

$$\omega - \beta u = -\Delta\xi = -\frac{\omega_p^2}{\omega_c} \quad .$$

The dependence of ξ on y is through the dependence of u on y. With the aid of II.4, it is easily shown that

$$d\xi = \beta\, dy \, . \qquad \text{II.40}$$

With these substitutions the differential equation for E_{1z} becomes

$$\left[1 - \frac{r^2}{r^4\xi^2 - 1 + r^2}\right]\frac{d^2E_{1z}}{d\xi^2} + \frac{2r^6}{(r^4\xi^2 - 1 + r^2)^2}\frac{dE_{1z}}{d\xi} - \left[1 - \frac{r^2}{r^4\xi^2 - 1 + r^2} + \frac{2r^4}{(r^4\xi^2 - 1)}\right]E_{1z} = 0 \qquad \text{II.41}$$

which may be rewritten

$$\frac{d^2E_{1z}}{d\xi^2} + \frac{2r^6}{(r^4\xi^2 - 1 + r^2)(r^4\xi^2 - 1)}\frac{dE_{1z}}{d\xi} - \left[1 + \frac{2r^4}{(r^4\xi^2 - 1 + r^2)(r^4\xi^2 - 1)}\right]E_{1z} = 0 \quad . \qquad \text{II.42}$$

The second instance in which a simplification is obtained is when ω_p and ω_c are equal, $(r = 1)$. When $r = 1$ II.42 becomes

$$\frac{d^2E_{1z}}{d\xi^2} + \frac{2}{\xi(\xi^2 - 1)} \frac{dE_{1z}}{d\xi} - \left[1 + \frac{2}{\xi^2(\xi^2 - 1)}\right] E_{1z} = 0 \quad . \qquad \text{II.43}$$

The substitution, $E_{1z} = \xi\Psi$, further simplifies this to

$$\frac{d^2\Psi}{d\xi^2} + \frac{2}{\xi^2 - 1} \frac{d\Psi}{d\xi} - \Psi = 0 \quad . \qquad \text{II.44}$$

II.44 has also been obtained by Macfarlane and Hay (13) in their analysis of wave propagation along a slipping stream of electrons using an action function Ψ. Their results apply only to the case $r = s = 1$ and to forward wave electromagnetic circuits. Although the case $r = s = 1$ is of interest in the analysis of the backward wave oscillator the use of the functions defined by II.44 complicates the analysis considerably. Since the numerical work of this report deals only with the simpler cases, a detailed discussion of the properties of these functions is not given here. It will suffice to note that $\xi = -1$ and $\xi = +1$ are regular singular points of the equation, and $\xi = \infty$ is an irregular singular point. Two linearly independent solutions of equation II.43 in the range $-1 < \xi < 1$, together with their derivatives have been obtained by numerical integration of II.44 and are shown in Figure 3. One of these solutions has been chosen to be an even function of ξ and the other to be odd. Both are singular at $\xi = 1, -1$, although there exists a linear combination which is not.

The third instance in which II.42 simplifies is when r^4 is small compared with unity, and only waves whose phase velocity is approximately

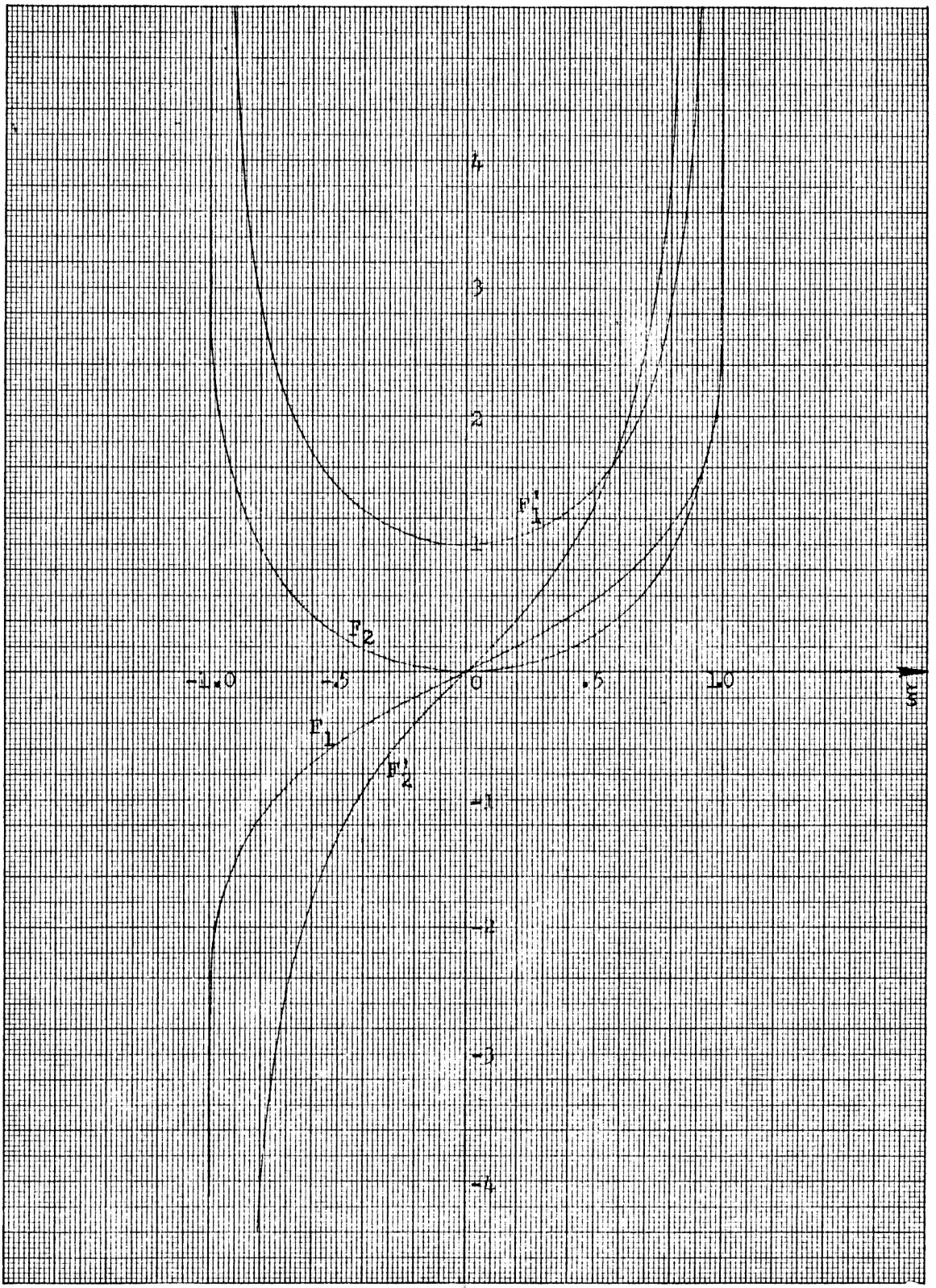

FIGURE 3. TWO SOLUTIONS OF THE DIFFERENTIAL EQUATION FOR E_{1z}, AND THEIR DERIVATIVES, FOR THE CASE r = s = 1.

equal to the electron velocity are considered. The latter restriction may be expressed more precisely by $|\xi| \ll 1$. When these two conditions are satisfied, the coefficient of the first derivative term in II.42 is small, and the coefficient of E_{1z} is approximately equal to one so that the following approximate differential equation is obtained,

$$\frac{d^2E_{1z}}{d\xi^2} - E_{1z} = 0 . \qquad \text{II.45}$$

With the aid of the relation $d\xi = -\beta dy$, this becomes

$$\frac{d^2E_{1z}}{dy^2} - \beta^2 E_{1z} = 0 \qquad \text{II.46}$$

which is the same equation as obeyed by E_{1z} outside the beam. In later sections it is primarily this third special case that will be of interest.

It should be noted that in this special case, as in the first special case, the a.c. charge density in the beam vanishes. The previously cited error in the French work, together with an error in the sign of the force given by the second term of II.27, prevented them from obtaining this simple equation for the field in the interior of the electron beam.

Conditions at the Surfaces of the Beam. The equations applying to the interior of the beam have been derived. In the free space between the beam and the sole, and between the beam and the slow-wave circuit, E_{1z} obeys the free space equation

$$\frac{d^2E_{1z}}{dy^2} - \beta^2 E_{1z} = 0 \qquad \text{II.47}$$

which is obtained from II.14 by setting ρ_1 equal to zero. The joining of the solutions in three principal regions is accomplished by means of the equivalent surface charge method used by Hahn (1) and Feenberg (3) and others. The motion of edge electrons may be rather complicated, but the effect is to produce a rippling of the boundary as shown in Figure 4a. As far as an interior electron is concerned, the difference between this situation and the unmodulated situation can be represented by a charge distribution as shown in Figure 4b or 4c. While it may be difficult to calculate the exact motion of the edge electrons, only the total excess charge which accumulates on the boundary influences motion of the interior electrons, and for this purpose it is sufficiently accurate to use

$$\sigma_{\pm} = \pm \rho_o y_1 = \pm \rho_o \frac{v_{1y}}{j(\omega - \beta u_{\pm})} \qquad \text{II.48}$$

for the surface charge density. The upper signs apply at the upper surface of the beam while the lower signs apply at the lower surface of the beam. u_+ is the velocity of the upper edge electrons and u_- is the velocity of the lower edge electrons. At a boundary E_{1y} is discontinuous by an amount $\sigma_{\pm}/\epsilon_o$ and E_{1z} is continuous.

Solutions in the three regions may be written

$$\begin{aligned} E_{1z} &= C_1 \sinh \beta(y + t + a) && -(a+t) < y < -t \\ &= C_2 F_1(\xi) + C_3 F_2(\xi) && -t < y < 0 \\ &= C_4 \cosh \beta y + C_5 \sinh \beta y && 0 < y < d \end{aligned} \qquad \text{II.49 abc}$$

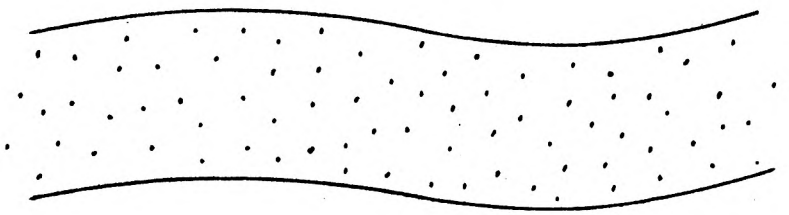

Figure 4a. Deformation of Beam when Modulated

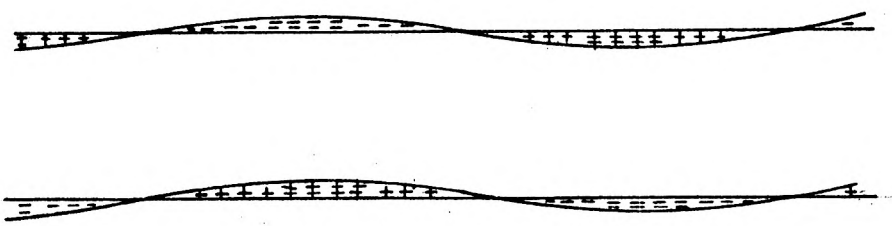

Figure 4b. Time-varying Part of Charge Density When Beam is Modulated

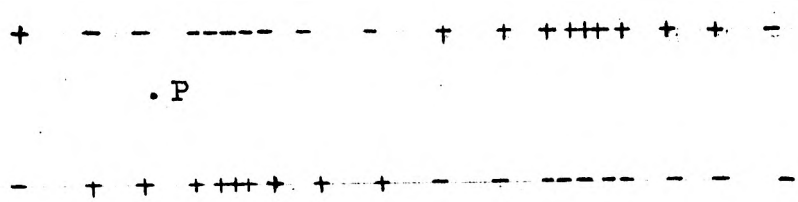

Figure 4c. Equivalent Surface Charge Density which is used to Represent the Charge Density of 4b in Computing the Field at an Interior Point, P.

$$E_{1y} = jC_1 \cosh \beta(y+t+a) \qquad -(a+t) < y < -t$$
$$= j\left[C_2 F'_1(\xi) + C_3 F'_2(\xi)\right] \qquad -t < y < 0 \qquad \text{II.50 abc}$$
$$= j\left[C_4 \sinh \beta y + C_5 \cosh \beta y\right] \qquad 0 < y < d$$

where $F_1(\xi)$ and $F_2(\xi)$ denote the two fundamental solutions of II.37, II.43, or II.46. In the first and third cases $F_1(\xi)$ and $F_2(\xi)$ may be regarded as standing for $\cosh \beta y$ and $\sinh \beta y$, respectively. In all three cases, $\frac{dF(\xi)}{dy} = \beta F'(\xi)$.

Requiring E_{1z} to be continuous at $y = -t$ and $y = 0$ ($\xi = \xi_-$ and ξ_+ respectively) gives two relationships among the five constants,

$$C_1 \sinh \beta a = C_2 F_1(\xi_-) + C_3 F_2(\xi_-) \qquad \text{II.51}$$

$$C_2 F_1(\xi_+) + C_3 F_2(\xi_+) = C_4 \quad . \qquad \text{II.52}$$

Requiring E_{1y} to be discontinuous by an amount $\sigma_\pm/\epsilon_o$ gives two more relationships among the five constants,

$$C_2 F'_1(\xi_-) + C_3 F'_2(\xi_-) =$$
$$C_1 \cosh \beta a + \frac{\omega_p^2}{\Omega_-^2}\left[C_2 F'_1(\xi_-) + C_3 F'_2(\xi_-) + \frac{\omega_c}{\omega - \beta u_-} C_1 \sinh \beta a\right] \qquad \text{II.53}$$

$$C_5 = C_2 F'_1(\xi_+) + C_3 F'_2(\xi_+) - \frac{\omega_p^2}{\Omega_+^2}\left[C_2 F'_1(\xi_+) + C_3 F'_2(\xi_+) + \frac{\omega_c}{\omega - \beta u_+} C_5\right] \qquad \text{II.54}$$

Two boundary conditions at $y = d$ must still be applied: E_{1y} and E_{1z} may be specified. Actually, only the ratio of E_{1y} to E_{1z} is significant in determining the allowed values of β , since specifying either E_{1y} or E_{1z} in addition to the ratio only determines the amplitude of the wave. With the four equations II.51, II.52, II.53 and

II.54, and the ratio of E_{1y} to E_{1z} at $y = d$, it is possible to eliminate all five constants and obtain a transcendental equation which determines the allowed or characteristic values of β and hence the characteristic waves of the system.

The characteristic waves when the circuit is absent will be discussed in the next section.

III. THE ADMITTANCE METHOD AND SPACE CHARGE WAVES

The Admittance Method. It is sometimes more convenient to use the admittance method (14),(15), to satisfy the boundary conditions at beam edges. The normalized admittance will be defined as

$$P + jQ \equiv \frac{E_{1y}}{E_{1z}} \qquad \text{III.1}$$

where P is the real part of the admittance, or conductance, and Q is the imaginary part, or susceptance. This normalized admittance is related to the usual E-mode admittance (14),(15),

$$Y_E = - \frac{H_{1x}}{E_{1z}} \qquad \text{III.2}$$

through the equation

$$Y_E = + \frac{k}{\beta} \sqrt{\frac{\epsilon_o}{\mu_o}} \; (P + jQ) \qquad \text{III.3}$$

where $\frac{k}{\beta}$ is the phase velocity of the wave divided by the velocity of light (which is small) and $\sqrt{\frac{\epsilon_o}{\mu_o}}$ is the characteristic admittance of free space. $P + jQ$ is normalized in the sense that the surface admittance of free space is given by

$$P + jQ = \pm j \qquad \text{III.4}$$

This is easily seen from the following consideration:

For $y<0$ an appropriate solution of II.47 which is bounded at $-\infty$ is

$$E_{1z} = C_1 e^{\beta y}$$

Using II.12

$$E_{1y} = jC_1 e^{\beta y}$$

Consequently

$$P + jQ = \frac{E_{1y}}{E_{1z}} = j \quad .$$

Similarly, for $y>0$,

$$E_{1z} = C_1 e^{-\beta y} \qquad E_{1y} = jC_1 e^{-\beta y} \quad .$$

Hence $P + jQ = -j$.

The normalized admittance of a conducting plane at a distance d is $\pm j \coth \beta d$. It is easily shown that if the admittance at a particular plane is $(P + jQ)_1$, the admittance at distance d above this plane is

$$(P + jQ)_2 = \frac{(P + jQ)_1 + j \tanh \beta d}{1 - j \tanh \beta d \, (P + jQ)_1} \qquad \text{III.5}$$

or when P is zero simply

$$Q_2 = \frac{Q_1 + \tanh \beta d}{1 + Q_1 \tanh \beta d} \qquad \text{III.6}$$

The usefulness of the normalized admittance lies in the fact that only the ratio E_{1y}/E_{1z} is important in determining the characteristic waves of the system. This method is used in this section to obtain the propagation constants of the space charge waves which propagate on a beam between two conducting planes. Throughout the remainder of this section it will be assumed that the fields E_{1z} and E_{1y} obey the free space equation II.47 inside, as well as outside the beam, and that the slow wave circuit at $y = d$ in Figure 2 is replaced by a conducting plane.

The boundary condition at the lower edge of the beam may be written

$$\left.\frac{E_{1y}}{E_{1z}}\right|_{y=-t^+} = \left.\frac{E_{1y}}{E_{1z}}\right|_{y=-t^-} + \frac{\sigma_-}{\epsilon_o E_{1z}} \qquad \text{III.7}$$

The first term is the admittance just above the lower surface, the second term is the admittance just below the lower surface (and equal to $j \coth \beta a$), and the third term is the discontinuity in surface admittance provided by the equivalent surface charge. The latter term may be expressed in terms of the admittances with the aid of II.48, II.18, and the definition of ω_p^2,

$$\frac{\sigma_-}{\epsilon_o E_{1z}} = \frac{\omega_p^2}{\Omega_-^2}\left[\left.\frac{E_{1y}}{E_{1z}}\right|_{y=t^+} - \frac{\omega_c}{j(\omega - \beta u_-)}\right] . \qquad \text{III.8}$$

In terms of the susceptance Q,

$$Q_{t^+}\left[1 - \frac{\omega_p^2}{\Omega_-^2}\right] = Q_{t^-} + \frac{\omega_p^2\,\omega_c}{\Omega_-^2(\omega - \beta u_-)}$$

or

$$Q_{t^+} = \frac{Q_{t^-}}{1 - \dfrac{\omega_p^2}{\Omega_-^2}} + \frac{\omega_p^2\,\omega_c}{(\Omega_-^2 - \omega_p^2)(\omega - \beta u_-)} \qquad \text{III.9}$$

Since $Q_{-t^-} = \coth a$, III.9 may be written

$$Q_{-t^+} = \frac{\Omega_-^2(\omega - \beta u_-)\coth \beta a + \omega_p^2\,\omega_c}{(\Omega_-^2 - \omega_p^2)(\omega - \beta u_-)} \qquad \text{III.10}$$

Using the transformation formula III.6, since the fields obey the free space equation in the beam, this admittance appears as

$$Q_{o-} = \frac{\left[\Omega_-^2(\omega-\beta u_-)\coth\beta a+\omega_p^2\omega_c\right]+\left[(\Omega_-^2-\omega_p^2)(\omega-\beta u_-)\right]\tanh\beta t}{\left[\Omega_-^2(\omega-\beta u_-)\coth\beta\beta a+\omega_p^2\omega_c\right]\tanh\beta t+\left[(\Omega_-^2-\omega_p^2)(\omega-\beta u_-)\right]} \qquad \text{III.11}$$

just below the upper edge of the beam. The boundary condition at the upper edge of the beam can be written,

$$\left.\frac{E_{1y}}{E_{1z}}\right|_{y=0^+} = \left.\frac{E_{1y}}{E_{1z}}\right|_{y=0^-} + \frac{\sigma_+}{\epsilon_o E_{1z}} \qquad \text{III.12}$$

which may be expressed in terms of the admittances with the aid of II.48, II.18, and the definition of ω_p^2 ,

$$\frac{\sigma_+}{\epsilon_o E_{1z}} = -\frac{\omega_p^2}{\Omega_+^2}\left[\left.\frac{E_{1y}}{E_{1z}}\right|_{y=0^-} - \frac{\omega_c}{j(\omega-\beta u_+)}\right]. \qquad \text{III.13}$$

In terms of the susceptance Q ,

$$Q_{o+} = Q_{o-}\left[1-\frac{\omega_p^2}{\Omega_+^2}\right] - \frac{\omega_p^2\,\omega_c}{\Omega_+^2(\omega-\beta u_+)} \qquad \text{III.14}$$

Thus the normalized susceptance just above the upper edge of the beam is

$$Q_{o+} = \left\{\frac{\left[(\Omega_-^2(\omega-\beta u_-)\coth\beta a+\omega_p^2\omega_c\right]+\left[(\Omega_-^2-\omega_p^2)(\omega-\beta u_-)\right]\tanh\beta t}{\left[\Omega_-^2(\omega-\beta u_-)\coth\beta a+\omega_p^2\omega_c\right]\tanh\beta t+\left[\Omega_-^2-\omega_p^2)(\omega-\beta u_-)\right]}\right\} \qquad \text{III.15}$$

$$\cdot\left\{1-\frac{\omega_p^2}{\Omega_+^2}\right\} - \left\{\frac{\omega_p^2\,\omega_c}{\Omega_+^2(\omega-\beta u_+)}\right\}.$$

Finally, this admittance must be transformed to $y=d$ by means of

$$Q_d = \frac{Q_{o+}+\tanh\beta d}{1+Q_{o+}\tanh\beta d}. \qquad \text{III.16}$$

The resulting susceptance is a function of the propagation constant β .

The propagation constants of the characteristic waves of the system are obtained by equating this expression to the susceptance of the circuit at $y = d$. Since in this section the circuit is replaced by a conducting plane, the susceptance Q_d must be infinite. From III.16 this is easily seen to occur when

$$Q_{o+} = - \coth \beta d \qquad \text{III.17}$$

Space Charge Waves of the Non-slipping Beam. When $s = 0$, all electrons have the same velocity, $u_+ = u_- = u_o$. If the beam is very thick, $\beta t \gg 1$, the fields generated by the equivalent surface charge on the upper edge of the beam will be negligible at the lower edge of the beam and the fields generated by the equivalent surface charge on the lower edge of the beam will be negligible at the upper edge, and the waves associated with the upper and lower boundaries of the beam may be analyzed separately. The waves associated with the upper boundary may be found by setting $\tanh \beta t = 1$ in III.15 and equating this to III.17,

$$1 - \frac{\omega_p^2}{\Omega^2} - \frac{\omega_p^2 \, \omega_c}{\Omega^2 (\omega - \beta u)} = - \coth \beta d \; . \qquad \text{III.18}$$

Using the definition of Ω^2 and rearranging slightly, this becomes,

$$(\omega - \beta u - \omega_c)(\omega - \beta u) = \frac{\omega_p^2}{1 + \coth \beta d} \; . \qquad \text{III.19}$$

Solving for β

$$\beta_1 = \beta_e - \frac{\beta_c}{2} + \sqrt{\left(\frac{\beta_c}{2}\right)^2 + \frac{\beta_p^2}{1 + \coth \beta d}} \qquad \text{III.20}$$

$$\beta_2 = \beta_e - \frac{\beta_c}{2} - \sqrt{\left(\frac{\beta_c}{2}\right)^2 + \frac{\beta_p^2}{1 + \coth \beta d}} \qquad \text{III.21}$$

where the usual traveling wave tube notation is employed:

$$\beta_e = \frac{\omega}{u} \qquad \beta_c = \frac{\omega_c}{u} \qquad \beta_p = \frac{\omega_p}{u} \quad .$$

The first wave has a phase velocity which is less than the electron velocity, while the second wave has a phase velocity which is greater than the electron velocity. The electron velocity field corresponding to these waves can be found from II.18 and II.19. Rewriting them as

$$\frac{u\, v_{1y}}{\eta} = -\frac{j(\beta - \beta_e)\, E_{1y} + \beta_c\, E_{1z}}{(\beta - \beta_e)^2 - \beta_c^2} \qquad \text{III.22}$$

$$\frac{u\, v_{1z}}{\eta} = -\frac{j(\beta - \beta_e)\, E_{1z} - \beta_c\, E_{1y}}{(\beta - \beta_e)^2 - \beta_c^2} \qquad \text{III.23}$$

and using the ratio of E_{1y} to E_{1z} in the interior of the beam $(+j)$

$$\frac{u\, v_{1y}}{\eta} = \frac{E_{1z}}{\beta - \beta_e + \beta_c} \qquad \text{III.24}$$

$$\frac{u\, v_{1z}}{\eta} = \frac{-jE_{1z}}{\beta - \beta_e + \beta_c} \quad . \qquad \text{III.25}$$

Since the electric field decays exponentially $(e^{\beta y})$ in the interior of the beam, electrons near the surface of the beam deviate further from their equilibrium paths than do electrons in the interior of the beam. Because these waves are, in a sense, supported by the electrons near the surface of the beam, they are called surface waves. Comparison of III.25 with III.24 shows that the phase of the z velocity differs from the phase of the y velocity by $\frac{\pi}{2}$, but the amplitude of the two components of velocity are equal. Thus the motion of each electron is the combination of a drift at the

electron is the combination of a drift at the velocity u and a circular motion. A given amplitude of the electric field, E_{1z}, produces a greater velocity modulation of the electrons for wave 2 than for wave 1 since the denominators of III.24 and III.25 are smaller for wave 2 than for wave 1.

In a coordinate system which moves with the electrons the frequency of oscillation is higher for wave 2

$$\omega'_2 = \omega - \beta_2 u = \frac{\omega_c}{2} + \sqrt{\left(\frac{\omega_c}{2}\right)^2 + \frac{\omega_p^2}{1 + \coth \beta d}} \qquad \text{III.26}$$

than for wave 1

$$\omega'_1 = \omega - \beta_1 u = \frac{\omega_c}{2} - \sqrt{\left(\frac{\omega_c}{2}\right)^2 + \frac{\omega_p^2}{1 + \coth \beta d}} \quad . \qquad \text{III.27}$$

Electrons execute many more circles in drifting a fixed distance when wave 2 is excited than when wave 1 is excited. In addition ω'_2 is positive and the electrons execute counter-clockwise circular motion, when wave 1 is present, while ω'_1 is negative and the electrons execute clockwise motion.

The waves associated with the lower boundary may be found by setting normalized susceptance, III.10, equal to -1, since the fields in the beam may be assumed to be proportional to $e^{-\beta y}$. The resulting equation can be written,

$$(\omega - \beta u + \omega_c)(\omega - \beta u) = \frac{\omega_p^2}{1 + \coth \beta u} \qquad \text{III.28}$$

and its solutions are

$$\beta_3 = \beta_e + \frac{\beta_c}{2} - \sqrt{\left(\frac{\beta_c}{2}\right)^2 + \frac{\beta_p^2}{1+\coth \beta d}} \qquad \text{III.29}$$

$$\beta_4 = \beta_e + \frac{\beta_c}{2} + \sqrt{\left(\frac{\beta_c}{2}\right)^2 + \frac{\beta_p^2}{1+\coth \beta d}} \; . \qquad \text{III.30}$$

The electron velocity field is given by

$$\frac{u\, v_{1y}}{\eta} = \frac{-E_{1z}}{\beta - \beta_e - \beta_c} \qquad \text{III.31}$$

$$\frac{u\, v_{1z}}{\eta} = \frac{-j\, E_{1z}}{\beta - \beta_e - \beta_c} \; . \qquad \text{III.32}$$

As before, the velocities are equal in magnitude but differ in phase by $\frac{\pi}{2}$. For wave 3

$$\omega'_3 = \omega - \beta_3 u = \frac{\omega_c}{2} - \sqrt{\left(\frac{\omega_c}{2}\right)^2 + \frac{\omega_p^2}{1+\coth \beta a}} \qquad \text{III.33}$$

the frequency is negative and the circular motion is clockwise; while for wave 4

$$\omega'_4 = \omega - \beta_4 u = \frac{\omega_c}{2} + \sqrt{\left(\frac{\omega_c}{2}\right)^2 + \frac{\omega_p^2}{1+\coth \beta a}} \qquad \text{III.34}$$

the frequency is positive and the motion is counterclockwise. The circular motion is greatest for edge electrons, less for electrons in the interior of the beam, being practically negligible for electrons which are more than a small fraction of an electronic wavelength (distance measured in units $\lambda_e = \frac{2\pi}{\beta_e}$) from the boundary of the beam.

It is interesting to note that when $\omega_p^2 \ll \omega_c^2$ the propagation constants of the four waves are given by

$$\beta_1 = \beta_e + \frac{\beta_p^2/\beta_c}{1 + \coth \beta d} \qquad \text{III.35}$$

$$\beta_2 = \beta_e - \beta_c - \frac{\beta_p^2/\beta_c}{1 + \coth \beta d} \qquad \text{III.36}$$

$$\beta_3 = \beta_e - \frac{\beta_p^2/\beta_c}{1 + \coth \beta a} \qquad \text{III.37}$$

$$\beta_4 = \beta_e + \beta_c + \frac{\beta_p^2/\beta_c}{1 + \coth \beta a} \qquad \text{III.38}$$

Waves 1 and 3 have phase velocities approximately equal to the electron velocity and are similar to those to be discussed later in the slipping stream analysis. Waves 2 and 4 are sometimes referred to as the fast and slow cyclotron waves, respectively, since their phase velocities are less than and greater than the electron velocity and the frequency in the moving coordinate system is approximately equal to the cyclotron frequency. As the charge density of the beam approaches zero, the frequency of these waves in a system moving with the average velocity of the electrons approaches ω_c and these waves describe the natural circular motion which an electron executes in a magnetic field, which is counterclockwise for the sense of magnetic field assumed here. Similarly, as the charge density of the beam decreases the frequency of waves 1 and 3 tends to zero and these waves describe the natural drift motion which an electron executes in crossed electric and magnetic fields.

To discuss the waves it is convenient to introduce a new variable, $\delta = \beta/\beta_e$. The susceptance just above the beam III.15 can be written

$$Q_{o+} =$$

$$\frac{\left\{\left[(\delta-1)^2-m^2\right]\left[\delta-1\right]\coth \beta_e a\delta - r^2m^3\right\} + \left\{\left[\delta-1\right]\left[(\delta-1)^2-m^2-m^2r^2\right]\right\}\tanh \beta_e t\delta}{\left\{\left[(\delta-1)^2-m^2\right]\left[\delta-1\right]\coth \beta_e a\delta - r^2m^3\right\}\tanh \beta_e t\delta + \left\{\left[\delta-1\right]\left[(\delta-1)^2-m^2-m^2r^2\right]\right\}}$$

$$\cdot\left\{\frac{(\delta-1)^2-m^2-m^2r^2}{(\delta-1)^2-m^2}\right\} + \frac{r^2m^3}{\left[\delta-1\right]\left[(\delta-1)^2-m^2\right]} \quad . \qquad \text{III.39}$$

Upon putting this over a common denominator, a common factor $(\delta-1)^2-m^2$ may be cancelled from numerator and denominator, so that Q may be written

$$Q_{o+} =$$

$$\frac{\left\{\delta-1\right\}\left\{\left[\delta-1\right]\left[(\delta-1)^2-m^2-m^2r^2\right]\left[1+\tanh(\beta_e t\delta)\right] - r^2m^2(\delta-1)\tanh(\beta_e t\delta) + r^2m^3\tanh(\beta_e t\delta)\right\} + m^4r^4\tanh \beta_e t\delta}{\delta-1\left[\left\{\left[(\delta-1)^2-m^2\right]\left[\delta-1\right]-r^2m^3\right\}\tanh \beta_e t\delta + \left[\delta-1\right]\left[(\delta-1)^2-m^2-m^2r^2\right]\right\}\right]}$$

where $\coth \beta_e a\,\delta$ has been taken equal to 1 $(a=\infty)$ for simplicity. To find the modes of propagation when there is a conducting plane at a distance d above this beam it is necessary to equate this expression to $-\coth \beta_e d\,\delta$ and find the values of δ which satisfy the resulting relation. The solution may be effected by plotting the susceptance of the beam and $-\coth \beta_e d\,\delta$ as a function of δ and locating the intersections of the two curves. This procedure is illustrated in Figure 5, where it has been assumed that $\coth \beta_e a\,\delta = 1$, $\beta_e t = .50$, $m = 1/2$, and $r = 1$. The susceptance at a distance $d = \frac{.50}{\beta_e}$ above the beam is also shown. Intersections of the beam susceptance curve with the free space curve, $Q = -1$ occur at

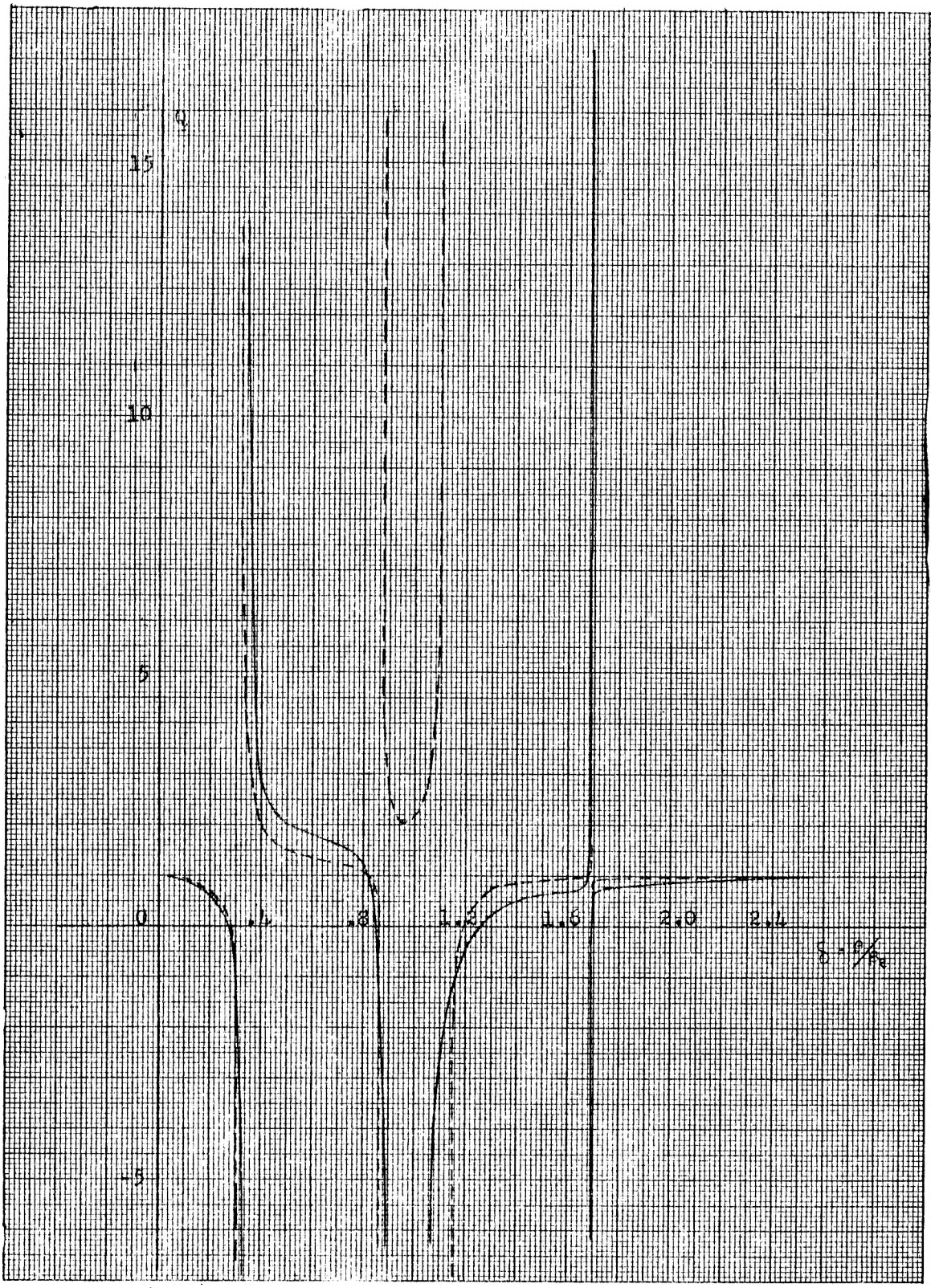

Figure 5. Normalized Susceptance of a Non-slipping Beam of Finite Thickness, $\omega_n = \omega_c = \frac{1}{2}\omega$.

$$\delta = \frac{\beta}{\beta_e} = 0.30,\ 0.86,\ 1.16,\ 1.69 \ .$$

The waves for which $\delta = .30,\ 1.69$ may be termed the fast and slow cyclotron waves respectively while the waves for which $\delta = .86,\ 1.16$ are similar to the waves whose phase velocities were approximately equal to electron velocity which were found in the thick beam case.

Figure 6 shows the distribution of E_{1z} across the beam for each of the four modes. The values calculated from the thick beam formulas III.20, III.21, III.29, and III.30 are

$$\delta = \frac{\beta}{\beta_e} = 0.134,\ 0.634,\ 1.366,\ 1.866 \ ,$$

and are in qualitative agreement with above results. In both cases there is one fast cyclotron wave, one slow cyclotron wave, and two waves with a phase velocity near the electron velocity, one a little faster and one a little slower than the electrons. Previous investigators have found only one wave (8),(9), or claim that only one of the two waves near the electron velocity can couple to external circuits (6). The field analysis shows that there are two waves near the electron velocity which can couple to external circuits. In many other respects the curves of Figure 5 are similar to those obtained from an equivalent circuit theory (8),(9).

Connection between Energy Transfer and $\frac{\partial Q}{\partial \beta}$. The power extracted from the electron beam can be obtained by integrating the Poynting vector over a surface just above the beam. The time average of the Poynting vector is

$$\Pi = \frac{1}{2} \mathrm{Re}\ (E^*_z\ H_x) \qquad \text{III.41}$$

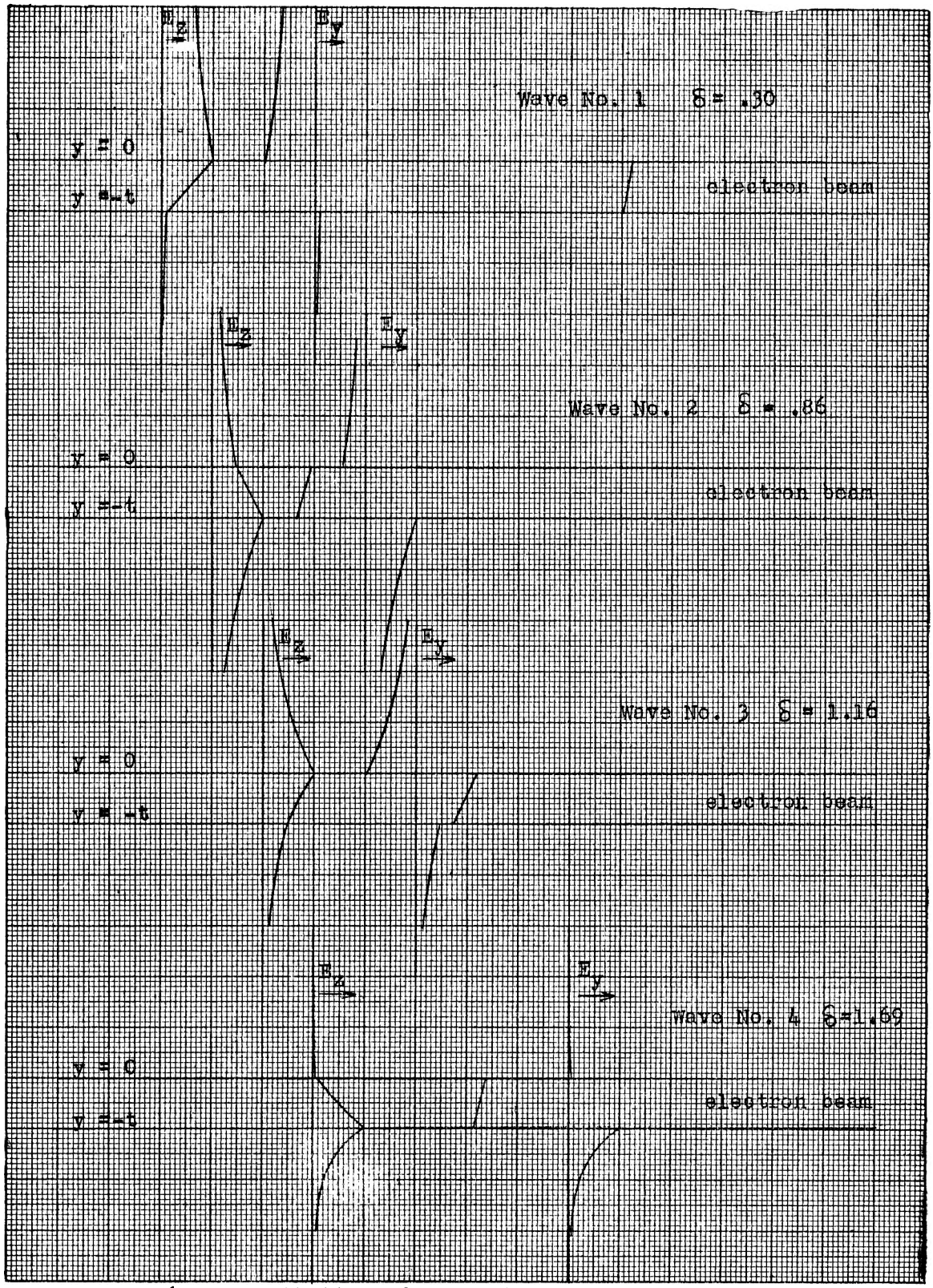

Figure 6. Distribution of Electric Field for Waves on a Non-slipping Beam of Finite Thickness

If a single wave whose space and time dependence $e^{j(\omega t - \beta z)}$ is present this may be rewritten

$$\overline{\Pi} = \frac{1}{2} E_z E^*_z \operatorname{Re}\left(\frac{H_x}{E_z}\right) = -\frac{1}{2} E_z E^*_z \operatorname{Re}(Y_E) \qquad \text{III.42}$$

According to III.3 Y_E is proportional to $P + jQ$ with a real constant of proportionality. In the preceding section it was found that P is zero for real values of the propagation constant. Thus the net energy transfer is zero since the time average of the Poynting vector is zero. Energy may be extracted from the beam if more than one wave is present or if the amplitude of the wave increases or decreases with z.

Increasing and decreasing waves can be represented by assuming the z dependence to be $e^{-(\alpha + j\beta)z}$; positive α represents a decreasing wave and negative α an increasing wave. III.42 is still valid. Since Y_E is analytic along the β axis, except at four points (see III.40 and Figure 5), the real part of the admittance can be found from the imaginary part in the following way:

In a neighborhood where Y_E is analytic,

$$Y_E(\beta - j\alpha) \approx Y_E(\beta) + (-j\alpha)\frac{\partial Y_E}{\partial \beta} \qquad \alpha \text{ small} \qquad \text{III.43}$$

Since $Y_E(\beta)$ and $\frac{\partial Y_E}{\partial \beta}$ are pure imaginary, the real part of $Y_E(\beta - j\alpha)$ is given by

$$\operatorname{Re} Y_E(\beta - j\alpha) \approx -j\alpha \frac{\partial Y_E}{\partial \beta}$$

or in terms of the normalized admittance

$$P(\beta - j\alpha) \approx \frac{\partial Q}{\partial \beta}\,\alpha \ . \qquad \text{III.44}$$

It may be concluded from this result that energy is extracted from the

beam if

$$\frac{\partial Q}{\partial \beta}\,\alpha < 0 \quad * \qquad \text{III.45}$$

The most interesting case is when $\alpha<0$, for in this case the wave increases with distance and the additional energy which appears in the field as the wave increases is obtained from the kinetic energy of the electrons. Reference to Figure 5 shows that $\frac{\partial Q}{\partial \beta}$ is positive only if β is greater than β_e, that is, if the wave velocity is slower than the electron velocity.

When two constant amplitude waves are present,

$$E_z = E_{z1}\, e^{-j\beta_1 z} + E_{z2}\, e^{-j\beta_2 z}$$

$$H_x = -Y_{E1}\, E_{z1}\, e^{-j\beta_1 z} - Y_{E2}\, E_{z2}\, e^{-j\beta_2 z}$$

and the time average of the Poynting vector is given by

$$\overline{\Pi} = -\frac{1}{2}\,\mathrm{Re}\Big[Y_{E1}\, E_{z1}\, E_{z1}^{*} + Y_{E2}\, E_{z2}\, E_{z2}^{*} + Y_{E1}\, E_{z1}\, E_{z2}^{*}\, e^{-j(\beta_1-\beta_2)z} + Y_{E2}\, E_{z2}\, E_{z1}^{*}\, e^{+j(\beta_1-\beta_2)z} \Big] .$$

---

* In some respects this condition is analogous to a theorem for electrical networks: the z coordinate replaces the time variable and $-(\alpha + j\beta)$ replaces the complex frequency variable $p = \sigma + j\omega$ (the frequency is a constant in the electron beam problem). In the electron beam problem the admittance is pure imaginary along the β axis ($\alpha = 0$); this corresponds to a reactance network. The susceptance slope $\frac{\partial \beta}{\partial \omega}$ of a passive reactance network is positive. If the susceptance slope is negative over any part of the frequency range, energy can be extracted from the network. Energy can be extracted from the electron beam if $\frac{\partial Q}{\partial \beta}$ is positive; the difference in sign arises from the negative sign preceding β in the exponential z dependence.

Writing $Y_{e1} = jB_{e1}$ and $Y_{e2} = jB_{e2}$ where B_{e1} and B_{e2} are pure real,

$$\overline{\Pi} = -\frac{1}{2} \mathrm{Re}\left[jB_{e1} E_{z1} E^*_{z2} e^{-j(\beta_1 - \beta_2)z} + jB_{e2} E_{z2} E^*_{z1} e^{j(\beta_1 - \beta_2)z} \right] \qquad \text{III.46}$$

This expression has oscillatory z dependence and energy may be imagined to flow out of the electron beam at one point and into the beam at another. Since the length of the beam is finite, it is possible to obtain a net extraction of energy.

Space Charge Waves of the Slipping Beam: ω_p^2 Small Compared with ω_c^2, Waves Near the Electron Velocity. The restriction to waves near the electron velocity can be stated more precisely,

$$(\omega - \beta u)^2 << \omega_c^2 \quad . \qquad \text{III.47}$$

Since for the waves discussed in this and later sections

$$(\omega - \beta u)^2 \approx \frac{\omega_p^4}{\omega_c^2} \quad .$$

III.47 is satisfied if ω_p^2 is small compared with ω_c^2. Under these circumstances,

$$\Omega^2 = (\omega - \beta u)^2 - \omega_c(\omega_c - \Delta) \approx -\omega_c^2 \qquad \text{III.48}$$

and the surface charge density on the lower edge of the beam is

$$\frac{\sigma_-}{\epsilon_o E_{1z}} = \frac{\omega_p^2}{\omega_c} \frac{1}{j(\omega - \beta u_-)} \qquad \text{III.49}$$

while the surface charge density on the upper edge of the beam is

$$\frac{\sigma_+}{\epsilon_o E_{1z}} = -\frac{\omega_p^2}{\omega_c}\,\frac{1}{j(\omega - \beta u_+)} \qquad \text{III.50}$$

The last two equations are obtained from III.8 and III.13 by neglecting E_{1y}/E_{1z} in comparison with $\omega_c/(\omega - \beta u)$ since the former is of order of magnitude unity and the latter will be of order of magnitude $(\frac{\omega_c}{\omega_p})^2$.

The normalized susceptance just above the beam is

$$Q_{o+} = \frac{(\omega - \beta u_-)(\tanh \beta t + \coth \beta a) - \frac{\omega_p^2}{\omega_c}}{(\omega - \beta u_-)(1 + \tanh \beta t \coth \beta a) - \frac{\omega_p^2}{\omega_c}\tanh \beta t} + \frac{\omega_p^2}{\omega_c(\omega - \beta u_+)} \qquad \text{III.51}$$

which may also be written

$$Q_{o+} = \frac{(\beta - \beta_-)(\tanh \beta t + \coth \beta a) - r^2 m \beta_-}{(\beta - \beta_-)(1 + \tanh \beta t \coth \beta a) - r^2 m \beta_- \tanh \beta t} - \frac{r^2 m \beta_+}{(\beta - \beta_+)} \qquad \text{III.52}$$

where $\beta_- = \frac{\omega}{u_-}$ $\beta_+ = \frac{\omega}{u_+}$.

To simplify the writing of this expression, a new variable ν , is defined by

$$\beta = \beta_+ (1 + r^2 m \nu) \qquad \text{III.53}$$

and the following additional definitions are made,

$$\tanh \beta t \equiv T \qquad \coth \beta a \equiv C$$

$$\epsilon = \frac{u_+ - u_-}{u_-} = \frac{\Delta t}{u_-} = s m r^2 \frac{\omega t}{u_-}$$

ϵ is the fractional velocity spread and is assumed to be small compared to unity. The slip parameter, s, will be retained in order that subsequent expressions will apply to both the slipping or non-slipping cases. Since T and C are slowly varying functions of β , they may be taken

as constants, evaluated at

$$\beta = \frac{\omega}{\sqrt{u_+ u_-}} \approx \frac{\omega}{u_+} \approx \frac{\omega}{u_-} \quad .$$

The expression for the normalized susceptance, III.52 becomes

$$Q_{o+} = \frac{(\nu - s\beta_- t)(T + C) + 1}{(\nu - s\beta_- t)(1 + TC) + T} - \frac{1}{\nu}$$

$$= \frac{T + C}{1 + TC} \frac{\nu^2 - \nu\left[s\beta_- t + \frac{TC}{1 + TC}\right] + \frac{s\beta_- t(1 + TC) - T}{T + C}}{\nu\left[\nu - s\beta_- t + \frac{T}{1 + TC}\right]} \quad . \qquad \text{III.55}$$

III.55 is subject to obvious simplification if the beam does not slip ($s = 0$ or if the conducting plane below the beam is far removed ($C = 1$). When $C = 1$

$$Q_{o+} = \frac{\nu^2 - \nu\left[s\beta_- t + \frac{T}{1 + T}\right] + s\beta_- t - \frac{T}{1 + T}}{\nu\left[\nu - s\beta_- t + \frac{T}{1 + T}\right]} \quad . \qquad \text{III.56}$$

Figure 7 shows a plot of III.56. The slipping and non-slipping cases are shown separately. Two features which are common to both curves should be noted: (a) the normalized susceptance is very nearly equal to $+1$, the free space value if $\nu \gtrsim 1$, and (b) the slope of the susceptance curve is positive in the vicinity of $\nu = 0$, indicating a range of wave velocities in which it is possible to extract energy from the beam. Intersections of these curves with line $Q = -1$, the normalized susceptance of the free space above the beam, determines the propagation constants of the waves when the upper conductor is also far removed. It can be seen that when $s = 1$, no intersections are obtained. An analytical solution may be

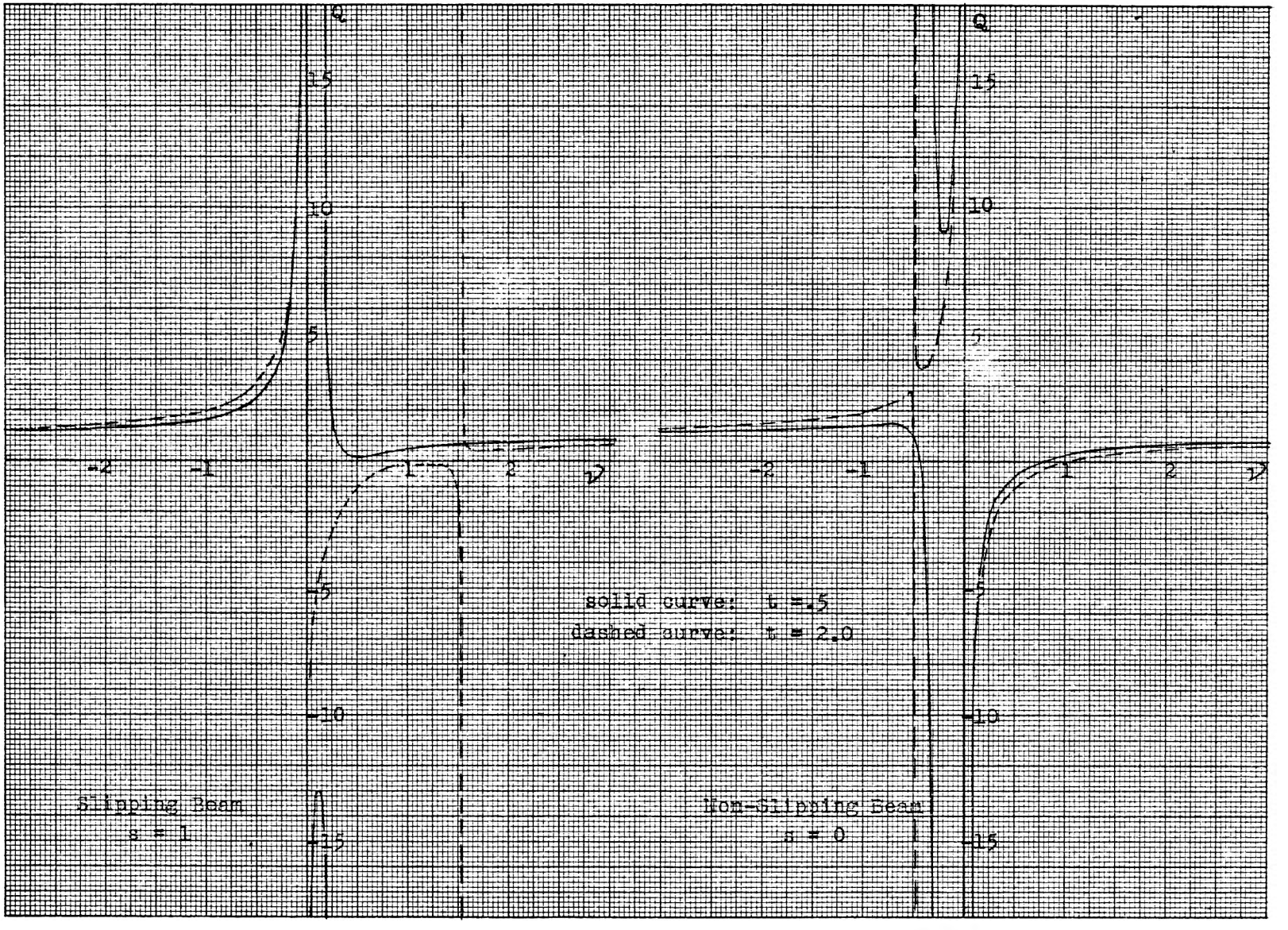

FIGURE 7 NORMALIZED SUSCEPTANCE OF THE SLIPPING AND NON-SLIPPING BEAMS

obtained by setting III.56 equal to -1 . After a slight amount of algebraic manipulation the resulting equation can be written

$$\nu^2 - (s\,\beta_- t)\,\nu + \tfrac{1}{2}\left(s\,\beta_- t - \frac{T}{1+T}\right) = 0 \quad . \qquad \text{III.57}$$

The solutions of this equation are

$$\nu = \frac{s\beta_- t}{2} \pm \sqrt{\left(\frac{s\beta_- t}{2}\right)^2 - \frac{s\beta_- t}{2} + \frac{T}{2(1+T)}} \quad . \qquad \text{III.58}$$

When the beam does not slip ($s = 0$) this reduces to

$$\nu = \pm\sqrt{\frac{T}{2(1+T)}} \qquad \text{III.59}$$

and upon substituting into III.53

$$\beta = \beta_+ \left(1 \pm r^2 m \sqrt{\frac{T}{2(1+T)}}\right) \qquad \text{III.60}$$

(note $\beta_+ = \beta_-$ when $s = 0$)

One wave has a phase velocity which is slightly greater than the electron velocity (lower sign) and the wave has a phase velocity which is slightly less than the electron velocity. When the beam is thick ($T \approx 1$) III.59 gives the same result as III.35 and III.39 derived earlier,

$$\beta = \frac{\omega}{u} \pm \frac{\omega_p^2}{2\omega_c u} \qquad \text{III.61}$$

When the beam slips ($s = 1$) III.58 becomes

$$\nu = \frac{\beta_- t}{2} \pm \sqrt{\left(\frac{\beta_- t}{2}\right)^2 - \frac{\beta_- t}{2} - \frac{T}{2(T+1)}} \quad . \qquad \text{III.62}$$

Furthermore when the beam is thick ($T \approx 1$) the solution of this equation is

$$\nu_1 = \frac{1}{2}$$

$$\nu_2 = \beta_- t - \frac{1}{2} \quad . \qquad \text{III.63}$$

Using III.53 and III.54 the corresponding propagation constants are found to be

$$\beta_1 = \frac{\omega}{u_+} + \frac{\omega_p^2}{2\omega_c u_+} \qquad \text{III.64}$$

$$\beta_2 = \frac{\omega}{u_-} - \frac{\omega_p^2}{2\omega_c u_-} \quad . \qquad \text{III.65}$$

The first wave is a surface wave associated with the upper surface and has a phase velocity a little less than the velocity of the upper edge electrons. The second wave is also a surface wave associated with the lower surface and it has a phase velocity which is a little greater than the velocity of the lower edge electrons. These waves are similar to the waves described by III.61 except that the velocity of the appropriate edge electrons are different.

It is interesting to note that most of the longitudinal current in the electron beam is the surface current:

$$i_{\pm} = \sigma_{\pm} u_{\pm} = \pm j \frac{\epsilon_o E_{1z_{\pm}}}{2} u_{\pm} \qquad \text{III.66}$$

where $E_{1z_{\pm}}$ is the longitudinal field at appropriate edge of the beam. III.66 is obtained by substituting III.64 or III.65 into III.50 or III.49. The current in the body of the beam is obtained by integrating $\rho_o v_{1z}$

$$i = \int \rho_o v_{1z} \, dy$$

$$= \pm j \frac{\omega_p^2}{\omega_c \omega} \epsilon_o E_{1z} u_{\pm} \quad .$$

Thus the body current is $2\frac{\omega_p^2}{\omega\omega_c}$ times the surface current in the thick beam.

When the beam thickness is less than an amount given by $\beta t \approx 1.3$, III.62 gives complex conjugate values of γ. Consequently one wave increases with distance and the other decreases with distance, and small perturbations may grow as they are propagated along the electron beam. It is important to note that a source of disturbances at $z = 0$ sets up <u>both</u> the increasing wave and decreasing wave in the region $z > 0$. Small disturbances will grow large until the growth is limited by nonlinear effects or until the electrons are collected. Figure 8 shows the rate of growth of the disturbance with distance as a function of the beam thickness:

$$\alpha = \frac{\omega_p^2}{\omega_c u_+}\sqrt{\left(\frac{\beta_- t}{2}\right) - \left(\frac{\beta_- t}{2}\right)^2 - \frac{1}{2}\frac{T}{1+T}} \quad . \qquad \text{III.67}$$

This result can be understood in terms of Pierce's theory of coupling of modes of propagation (16). The increasing and decreasing waves come about through the coupling at the upper surface wave with the lower surface wave. When the beam is not very thick, the fields of the upper and lower surface waves overlap and the waves become coupled. The arguments of the preceding section indicate that the electron beam gives up energy to the field by being modulated with the upper surface wave and receives energy from the field by being modulated with the lower surface wave. Thus in the wave which increases with distance, the source of energy which appears in the field comes primarily from the upper edge electrons. The energy exchange takes place in the same way as in a magnetron: the electrons move into a region of higher d.c.

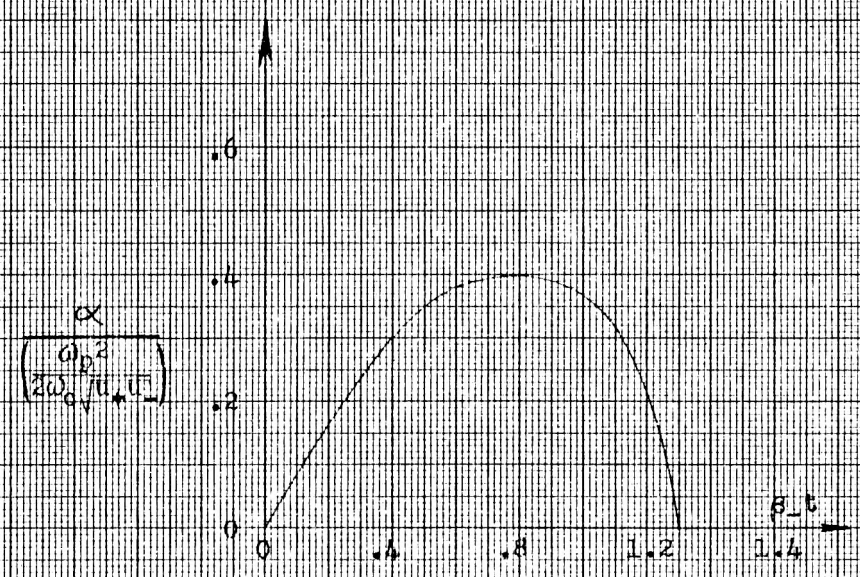

Figure 8. Slipping Beam Gain versus Beam Thickness and Frequency

potential without appreciable change in velocity by interaction with the high frequency field.

The critical thickness for growing waves is independent of the plasma frequency and hence of the current density in the beam. This result can be explained in the following way. Ordinarily, an increase in current increases the coupling between space charge waves but, in the slipping beam type of flow, an increase in current also increases the difference in velocity of the upper and lower edge electrons and hence increases the difference in velocity between the two surface waves. These two effects change the coupling in opposite directions with the net result that the coupling is independent of current.

Similarly, the beam thickness enters in two ways: the thicker the beam the greater the velocity separation $u_+ - u_-$ and, the less the fields of the two surface waves overlap. Both effects tend to reduce the coupling between the two surface waves.

The tendency for small perturbations to grow larger as they propagate along the electron beam has been termed the "diocotron" effect by French workers. A fundamental error in their analysis (12) of this effect has already been pointed out. This led to a prediction that the rate of growth of perturbations is proportional to the square root of the beam thickness for thin beams,

$$\alpha = \frac{\omega_p^2}{\omega_c u_+} \sqrt{\left(\frac{\beta_- t}{2}\right)} .$$

This result is incorrect. The analysis of the present paper furthermore shows that there exists a maximum thickness, beyond which growth does not occur.

Two of the results derived here are easily compared with the results of Macfarlane and Hay's(13) analysis which applies when $\omega_p = \omega_c$. The latter predicts a maximum rate of growth and a maximum frequency at which amplification can occur

$$\alpha_{max} \approx .24 \frac{\omega_p}{\left(\frac{u_+ + u_-}{2}\right)} \qquad \frac{u_+ - u_-}{u_+ + u_-} < .42$$

$$\omega_{max} \approx .707\, \omega_p \frac{u_+ + u_-}{u_+ - u_-} \quad .$$

while the analysis of this paper predicts

$$\alpha_{max} \approx .20 \frac{\omega_p^2}{\omega_c \left(\frac{u_+ + u_-}{2}\right)}$$

$$\omega_{max} \approx .65 \frac{\omega_p^2}{\omega_c} \frac{u_+ + u_-}{u_+ - u_-} \quad .$$

It is seen that the theory presented here would actually give fairly accurate results when applied to the extreme case, $\omega_p = \omega_c$, even though the principal assumption made in the derivation $(\omega_p^2 \ll \omega_c^2)$ does not apply.

Susceptance of the Beam at the Circuit. In the subsequent analysis it will be assumed that the lower plane is far removed. It will be necessary to know the normalized susceptance of the beam at a distance d above its upper surface, minus the normalized susceptance of free space at this same point. Using the susceptance transformation formula III.6 on III.56 gives

$$Q_d = \frac{\nu^2 + \nu\left[\frac{T}{1+T}\frac{T'-1}{T'+1} - s\beta_- t\right] + \frac{1}{T'+1}\left[s\beta_- t - \frac{T}{1+T}\right]}{\nu^2 + \nu\left[\frac{T}{1+T}\frac{1-T'}{T'+1} - s\beta_- t\right] + \frac{T'}{T'+1}\left[s\beta_- t - \frac{T}{1+T}\right]} \qquad \text{III.68}$$

where $T' \equiv \tanh \beta d$

$$Q_b - 1 = \frac{-\nu\left[\frac{2T}{1+T}\frac{1-T'}{1+T'}\right] + \frac{1-T'}{1+T'}\left[s\beta_- t - \frac{T}{1+T}\right]}{\nu^2 + \nu\left[\frac{T}{1+T}\frac{1-T'}{1+T'} - s\beta_- t\right] + \frac{T'}{1+T'}\left[s\beta_- t - \frac{T}{1+T}\right]} \qquad \text{III.69}$$

To determine the characteristic waves of the system when a slow wave circuit is present at $z = d$, it is necessary to match this susceptance to a similar susceptance for the circuit. This concludes the discussion of the electron beam characteristics. In the following section the circuit characteristics are discussed.

IV THE SURFACE ADMITTANCE OF THE SLOW WAVE CIRCUIT

Characteristics of a Periodic Circuit. The surface admittance of the electron beam which is a function of the propagation constant of the wave and other parameters, was derived in the preceding section. This section will deal with the characteristics of the slow wave circuit. The structure shown in Figure 9 is analyzed and these results are then generalized to include other types of slow wave circuits. The principal result of this analysis is the determination of the surface admittance which such a slow wave circuit presents to the electron beam, particularly when the electrons have a velocity nearly equal to phase velocity of one of the space harmonics of the circuit. Only the transverse magnetic modes will be discussed.

In some respects this analysis is similar to one made by Parzen (17) of the same type of circuit. His analysis applies only to very low current electron beams focused by a very large axial magnetic field, while in the treatment presented here it is not necessary to specify the beam conditions specifically when deriving the circuit properties. Parzen's treatment can be shown to be equivalent to a presentation of the circuit by a fixed admittance wall (15), and thus backward wave circuits are not treated correctly. This is equivalent to the neglect of the sum in IV.39. The sum turns out to be very important, even though it is zero for waves which propagate at exactly the circuit velocity. The analysis of this section differs from a previous analysis of the same type of circuit by the author (18).

While it is possible to write down the complete set of equations which determine the fields and propagation constants of this structure,

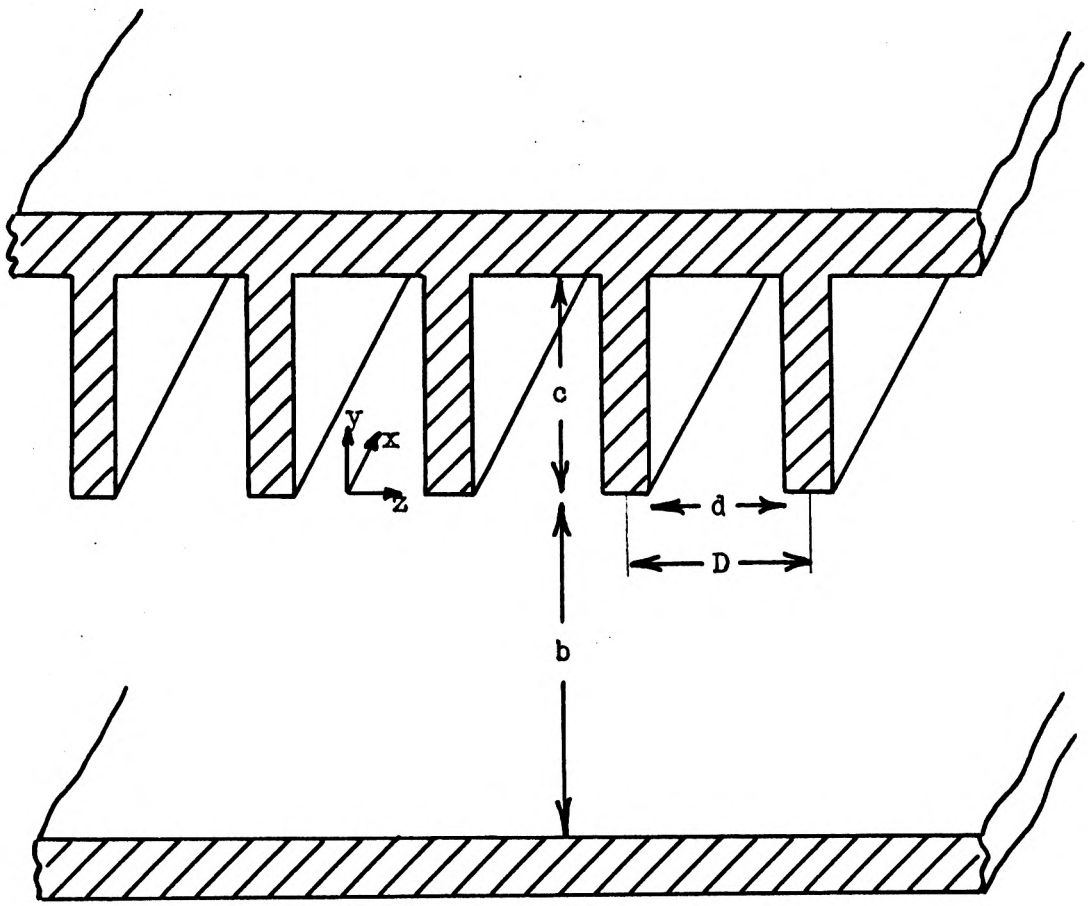

Figure 9. Cross-Section of the Slow Wave Circuit

with or without the electron beam, the boundary conditions are mixed and the solution of the set of equations requires the solution of an infinite determinant (19). Instead of following this procedure a variational method will be used in which the longitudinal electric field at $y = 0$ is the trial function. First, an integral equation for this field will be derived.

According to Bloch's (20) theorem the true fields of this structure satisfy the periodicity requirement

$$\begin{aligned} E_z(y,z+D) &= e^{-j\beta_o D} E_z(y,z) \\ E_y(y,z+D) &= e^{-j\beta_o D} E_y(y,z) \\ H_x(y,z+D) &= e^{-j\beta_o D} H_x(y,z) \end{aligned} \qquad \text{IV.1}$$

where the phase factor $e^{-j\beta_o D}$ is determined by the boundary conditions of the problem. E_z, E_y, H_x are the only field components present in the transverse magnetic modes when the fields are independent of the x coordinate. An expression for the electric field at $y = 0$ which satisfies periodicity condition IV.1 may be written

$$\mathcal{E}(z) = E_z(0,z) = e^{-j\beta_o z} \sum_{n=-\infty}^{+\infty} M_n e^{-j\frac{2\pi n z}{D}} \quad . \qquad \text{IV.2}$$

The inverse of IV.2 is obtained by multiplying IV.2 by $\frac{1}{D} e^{j\beta_o z} e^{+j\frac{2\pi m z}{D}}$ and integrating from $-\frac{D}{2}$ to $\frac{D}{2}$:

$$M_m = \frac{1}{D} \int_{-D/2}^{D/2} \mathcal{E}(z)\, e^{j\beta_o z} e^{j\frac{2\pi m z}{D}}\, dz \quad . \qquad \text{IV.3}$$

In the absence of the electron beam the electric and magnetic fields in the region $-b < y < 0$ are given by

$$E_z = e^{-j\beta_o z} \sum_{n=-\infty}^{+\infty} M_n \frac{\sinh \gamma_n (y+b)}{\sinh \gamma_n b} e^{-j\frac{2\pi n z}{D}} \qquad \text{IV.4}$$

$$E_y = e^{-j\beta_o z} \sum_{n=-\infty}^{+\infty} M_n \left(\frac{-j\beta_n}{\gamma_n}\right) \frac{\cosh \gamma_n (y+b)}{\sinh \gamma_n b} e^{-j\frac{2\pi n z}{D}} \qquad \text{IV.5}$$

$$H_x = e^{-j\beta_o z} \sum_{n=-\infty}^{\infty} M_n \left(\frac{-j\omega \epsilon_o}{\gamma n}\right) \frac{\cosh \gamma_n (y+b)}{\sinh \gamma_n b} e^{-j\frac{2\pi n z}{D}} \qquad \text{IV.6}$$

where $\gamma_n^2 = \beta_n^2 - k^2$ IV.7

$\beta_n = \beta_o + \frac{2\pi n}{D}$ IV.8

$k^2 = \omega^2 \mu_o \epsilon_o$. IV.9

These fields satisfy Maxwell's equations and the boundary condition at $y = -b$,

$$E_z = 0 .$$

The magnetic field at $y = 0$ is

$$H_x(0,z) = -e^{-j\beta_o z} \sum_{n=-\infty}^{\infty} Y_{no} M_n e^{-j\frac{2\pi n z}{D}} \qquad \text{IV.10}$$

where $Y_{no} = \frac{j\omega \epsilon_o}{\gamma_n} \coth \gamma_n b$ is the E-mode (transverse magnetic) surface admittance of free space for the n^{th} space harmonic.

When the electron beam is present IV.10 may be written

$$H_x(0,z) = -e^{-j\beta_o z} \sum_{n=-\infty}^{\infty} Y_n M_n e^{-j\frac{2\pi n z}{D}} \qquad \text{IV.11}$$

where Y_n is the E mode surface admittance at $y = 0$ with the electron beam present, and is determined by the methods of the previous sections. In this section, the total field in the region $-b < y < 0$ is the

superposition of an infinite number of partial waves or space harmonics as given by the summations in IV.4, IV.5 and IV.6 . Since the propagation constant of each space harmonic is different there is a different E mode admittance, Y_n , for each of these space harmonics. However, in the preceding section it was shown that when $s = 0$ the surface admittance with the beam present is practically equal to that of free space except when

$$\beta_n \approx \beta_e \ ,$$

$$\beta_n \approx \beta_e \pm \beta_c \ .$$

Thus most Y_n will not differ appreciably from Y_{no} . It is assumed that this is also the case when $s = 1$.

The fields in the slot which lies between $-\frac{d}{2}$ and $\frac{d}{2}$ may be written

$$E_z = \sum_{n=0}^{\infty} (2 - \delta_{no})\, B_n \frac{\sin q_n(c-y)}{\sin q_n c} \cos \frac{n\pi(z+\frac{d}{2})}{d} \qquad \text{IV.12}$$

$$E_y = \sum_{n=0}^{\infty} (2 - \delta_{no})\, B_n \left(\frac{n\pi}{q_n d}\right) \frac{\cos q_n(c-y)}{\sin q_n c} \sin \frac{n\pi(z+\frac{d}{2})}{d} \qquad \text{IV.13}$$

$$H = \sum_{n=0}^{\infty} (2 - \delta_{no})\, B_n \left(-\frac{j\omega\epsilon_o}{q_n}\right) \frac{\cos q_n(c-y)}{\sin q_n c} \cos \frac{n\pi(z+\frac{d}{2})}{d} \qquad \text{IV.14}$$

where $q_n^2 = k^2 - (\frac{n\pi}{d})^2$ $\qquad \delta_{no} = 1 \quad n = 0$

$\qquad\qquad\qquad\qquad\qquad\qquad\qquad\qquad\quad = 0 \quad n \neq 0$

Only the fields in one slot are specified, fields in adjacent slots differ only by the phase factor $e^{-j\beta_o D}$.

These fields have been chosen to satisfy the appropriate boundary

conditions at the conducting surfaces:

$$E_z = 0 \quad \text{at} \quad y = c$$

$$E_y = 0 \quad \text{at} \quad z = \pm \frac{d}{2} \quad .$$

At $y = 0$ IV.12 and IV.14 become,

$$E_z(0,z) = \sum_{n=0}^{\infty} (2 - \delta_{no})\, B_n \cos \frac{n\pi(z+\frac{d}{2})}{d} \qquad \text{IV.15}$$

$$H_x(0,z) = \sum_{n=0}^{\infty} (2 - \delta_{no})\, (-Y'_n) B_n \sin \frac{n\pi(z+\frac{d}{2})}{d} \qquad \text{IV.16}$$

where $Y'_n = \frac{j\omega\epsilon_o}{q_n} \cot q_n c$ is the admittance of the n^{th} harmonic in the slot.

The following boundary conditions must still be satisfied:

(a) $E_z(0,z)$ as given by IV.15 must be equal to $E_z(0,z)$ as given by IV.2 ,

(b) $H_x(0,z)$ as given by IV.16 must be equal to $H_x(0,z)$ as given by IV.11 ,

(c) $E_z(0,z)$ must vanish in the interval $\frac{d}{2} < |z| < \frac{D}{2}$.

The first of these conditions will be satisfied if

$$(z) = \sum_{n=0}^{\infty} (2 - \delta_{no})\, B_n \cos \frac{n\pi(z+\frac{d}{2})}{d} \quad . \qquad \text{IV.17}$$

Multiplying IV.17 by $\frac{1}{d} \cos \frac{m\pi(z+\frac{d}{2})}{d}$ and integrating from $-\frac{d}{2}$ to $\frac{d}{2}$ yields

$$B_m = \frac{1}{d} \int_{-d/2}^{d/2} \mathcal{E}(z) \cos \frac{m\pi(z+\frac{d}{2})}{d}\, dz \quad . \qquad \text{IV.18}$$

The second condition will be satisfied if

$$e^{-j\beta_o z} \sum_{n=-\infty}^{+\infty} Y_n M_n e^{-j\frac{2\pi n z}{D}} = \sum_{n=0}^{\infty} (2-\delta_{no}) + Y'_n B_n \cos\frac{n\pi(z+\frac{d}{2})}{d} \quad . \qquad \text{IV.19}$$

Upon substituting IV.3 and IV.18 for M_n and B_n, respectively, and interchanging the order of integration and summation, IV.19 becomes

$$\frac{1}{D}\int_{-D/2}^{D/2} \mathcal{E}(z') \sum_{n=-\infty}^{\infty} Y_n e^{-j(\beta_o + \frac{2\pi n}{D})(z-z')} dz' =$$

$$\frac{1}{d}\int_{-d/2}^{d/2} \mathcal{E}(z') \sum_{n=0}^{\infty} (2-\delta_{no}) Y'_n \cos\frac{n\pi(z'+\frac{d}{2})}{d} \cos\frac{n\pi(z'+\frac{d}{2})}{d} dz' \,. \qquad \text{IV.20}$$

This is an integral equation for $\mathcal{E}(z)$. $\mathcal{E}(z)$ must satisiy this integral equation in the region $-\frac{d}{2} < z < \frac{d}{2}$ and must vanish in the intervals $\frac{d}{2} < |z| < \frac{D}{2}$. Letting

$$G_I(z,z') = \frac{1}{D} \sum_{n=-\infty}^{\infty} Y_n e^{-j(\beta_o + \frac{2\pi n}{D})(z-z')} \qquad \text{IV.21}$$

$$G_{II}(z,z') = \frac{1}{d} \sum_{n=0}^{\infty} (2-\delta_{no}) Y'_n \cos\frac{n\pi(z+\frac{d}{2})}{d} \cos\frac{n\pi(z'+\frac{d}{2})}{d} \qquad \text{IV.22}$$

denote the Green's functions for regions I and II, the equation which $\mathcal{E}(z')$ must satisfy is conveniently written as,

$$\int_{-d/2}^{d/2} \left[G_I(z,z') - G_{II}(z,z')\right] \mathcal{E}(z')dz' = 0 \qquad |z| < \frac{d}{2}$$

$$\mathcal{E}(z') = 0 \qquad \frac{d}{2} < |z'| < \frac{D}{2} \quad . \qquad \text{IV.23}$$

In IV.23 $G_I(z,z')$ is a function of the propagation constant, β_o. Both $\mathcal{E}(z')$ and β_o are unknown. From the general theory of periodic

structures it is known that for a given set of dimensions and for a particular frequency the slow wave circuit of Figure 9 supports waves only for special values of β_o. Consequently, it is expected that IV-23 can be satisfied only for these special values of β_o. In other words, IV.23 determines the propagation constant β_o as well as the field $\mathcal{E}(z')$.

IV.23 may be converted to a stationary form for the determination of the propagation constant, β_o, by multiplying by $\mathcal{E}(-z)$ and integrating from $-\frac{d}{2}$ to $+\frac{d}{2}$,

$$\int_{-d/2}^{d/2}\int_{-d/2}^{d/2} \mathcal{E}(-z)\left[G_I(z,z') - G_{II}(z,z')\right]\mathcal{E}(z')\,dz'\,dz = 0 \qquad \text{IV.24}$$

For the true field $\mathcal{E}(z)$ and true propagation constant β_o this is a trivial operation since the integral IV.23 is identically zero for all z between $-\frac{d}{2}$ and $\frac{d}{2}$. However, if $\mathcal{E}(z)$ differs from the true field it will not, in general, be possible to satisfy IV.24, whereas it may be possible to satisfy IV.24 with a value of β_o which differs slightly from the true value. IV.24 is a weaker condition than IV.23; only a weighted average of the difference in tangential magnetic fields is required to vanish, the weighting function being $\mathcal{E}(-z)$.

By substituting various trial functions $\mathcal{E}(z)$ into IV.24, an implicit relation for the propagation constant β_o is obtained. It will now be shown that the value of β_o thus obtained is insensitive to small deviations in the trial function from the true field. Denoting the true field by $\mathcal{E}^o(z)$ and the true propagation constant by β_o^o, the first variation of IV.24 is

$$\int_{-d/2}^{d/2}\int \delta\mathcal{E}(-z)\left[G_I(z,z') - G_{II}(z,z')\right]_{\beta_o=\beta_o^o} \mathcal{E}^o(z')\,dzdz'$$

$$+ \delta\beta_o \int_{-d/2}^{d/2}\int \mathcal{E}^o(-z)\frac{\partial}{\partial\beta_o}\left[G_I(z,z') - G_{II}(z,z')\right]_{\beta_o=\beta_o^o} \mathcal{E}^o(z')\,dzdz'$$

$$+ \int_{-d/2}^{d/2}\int \mathcal{E}^o(-z)\left[G_I(z,z') - G_{II}(z,z')\right]_{\beta_o=\beta_o^o} \delta\mathcal{E}(z')\,dzdz' = 0 . \qquad \text{IV.25}$$

The first term vanishes because of the integral equation

$$\int_{-d/2}^{d/2}\left[G_I(z,z') - G_{II}(z,z')\right]_{\beta_o=\beta_o^o} \mathcal{E}^o(z')\,dz' = 0 . \qquad \text{IV.23}$$

The third term vanishes because

$$\int_{-d/2}^{d/2} \mathcal{E}^o(-z)\left[G_I(z,z') - G_{II}(z,z')\right]_{\beta=\beta_o^o} dz = 0 \qquad \text{IV.26}$$

vanishes for all z' . This follows from the symmetry properties of the Green's functions,

$$G_I(z,z') = G_I(-z',-z)$$
$$G_{II}(z,z') = G_{II}(-z',-z) \qquad \text{IV.27}$$

and the original integral equation IV.23 . IV.26 is proved by substituting IV.27 into IV.23, replacing $-z'$ by z and $-z$ by z', and interchanging the limits of integration.

Thus

$$\delta\beta_o \int_{-d/2}^{d/2}\int \mathcal{E}^o(-z)\,\frac{\partial}{\partial\beta_o}\left[G_I(z,z') - G_{II}(z,z')\right]_{\beta_o=\beta_o^o} \mathcal{E}^o(z')\,dz\,dz' = 0 \qquad \text{IV.28}$$

or $\delta\beta_o = 0$, provided the integral which multiplies $\delta\beta_o$ does not vanish. It seems unlikely that this integral vanishes and numerical calculation for the example discussed later bears out this conjecture. As a result, when IV.24 is used to determine the propagation constant, small errors in the trial function $\mathcal{E}(z)$ produce no error in the propagation constant to first order.

Substituting the series expansions for $\mathcal{E}(z)$ (IV.2 and IV.15) and the series expansion for the Green's functions (IV.21 and IV.22) into IV.24 and performing the indicated integrations yields

$$D\sum_{n=-\infty}^{\infty} Y_n M_n^2 + d\sum_{n=0}^{\infty}(2-\delta_{no})\,Y'_n B_n^2 = 0\,. \qquad \text{IV.29}$$

If the field is assumed to be uniform in the slot, $\mathcal{E}(z) = 1$,

$$M_n = \frac{1}{D}\int_{-d/2}^{d/2} e^{j\beta_o z}\, e^{j\frac{2\pi n z}{D}}\,dz = \frac{d}{D}\,\frac{\sin(\beta_o+\frac{2\pi n}{D})\frac{d}{2}}{(\beta_o-\frac{2\pi n}{D})\frac{d}{2}} \qquad \text{IV.30}$$

$$B_n = \frac{1}{d}\int_{-d/2}^{d/2} \cos\frac{n\pi\,(z+\frac{d}{2})}{d}\,dz = \delta_{no} \qquad \text{IV.31}$$

and IV.29 becomes

$$\sum_{n=-\infty}^{\infty} Y_n\left[\frac{d}{D}\,\frac{\sin(\beta_o+\frac{2\pi n}{D})\frac{d}{2}}{(\beta_o+\frac{2\pi n}{D})\frac{d}{2}}\right]^2 + \frac{d}{D}\,Y'_o = 0\,. \qquad \text{IV.32}$$

A better trial function, which takes into account the singular nature

of the fields at corners of the fins when $d \approx D$, is

$$\mathcal{E}(z) = \frac{\pi/2}{\sqrt{1-(\frac{2z}{d})^2}} \quad . \qquad \text{IV.33}$$

In this case $M_n = \frac{d}{D} J_o(\frac{\beta_o d}{2} + \frac{\pi n d}{D})$ IV.34

$$B_n = (-1)^{n/2} J_o(\frac{n\pi}{2}) \qquad n \text{ even}$$
$$= 0 \qquad n \text{ odd} \qquad \text{IV.35}$$

and IV.29 becomes

$$\sum_{n=-\infty}^{\infty} Y_n \frac{d}{D}\left[J_o(\frac{\beta_n d}{2} + \frac{\pi n d}{D})\right]^2 + \frac{d}{D} \sum_{\substack{n=0 \\ \text{odd}}}^{\infty} (2-\delta_{no}) Y'_n J_o^2(\frac{n\pi}{2}) = 0 \; . \qquad \text{IV.36}$$

Either IV.32 or IV.36 with the proper values of Y_n and Y'_n can be used to determine the propagation constant β_o. These two trial functions are not good approximations to the true field at very low frequencies, where the field, $\mathcal{E}(z)$, is nearly antisymmetric. In this region it would be better to employ a linear combination of a symmetric function and an antisymmetric function, determining the relative proportions by using the stationary property of IV.29. The solution of IV.32 for a particular set of dimensions is shown in Fig. 10. Computation is facilitated by converting IV.32 to a more rapidly converging series as discussed in ref.(17). The electron beam is assumed to be absent and only the propagation constant for the lowest mode has been determined. Curves of this type have been discussed by others, (21),(22),(23). A brief resume is given here.

Without loss of generality $\beta_o D$ may be assumed to lie between $-\pi$ and π. Since $\beta_n D = \beta_o D + 2\pi n$, the phase constants of the other space harmonics are obtained by simply displacing the fundamental curve ($n = 0$) by multiples of 2π. The velocity of energy propagation can be shown to be equal to the group velocity (24), which is given by

$$v_g = c \frac{\partial(kD)}{\partial(\beta_o D)} \qquad \text{IV.37}$$

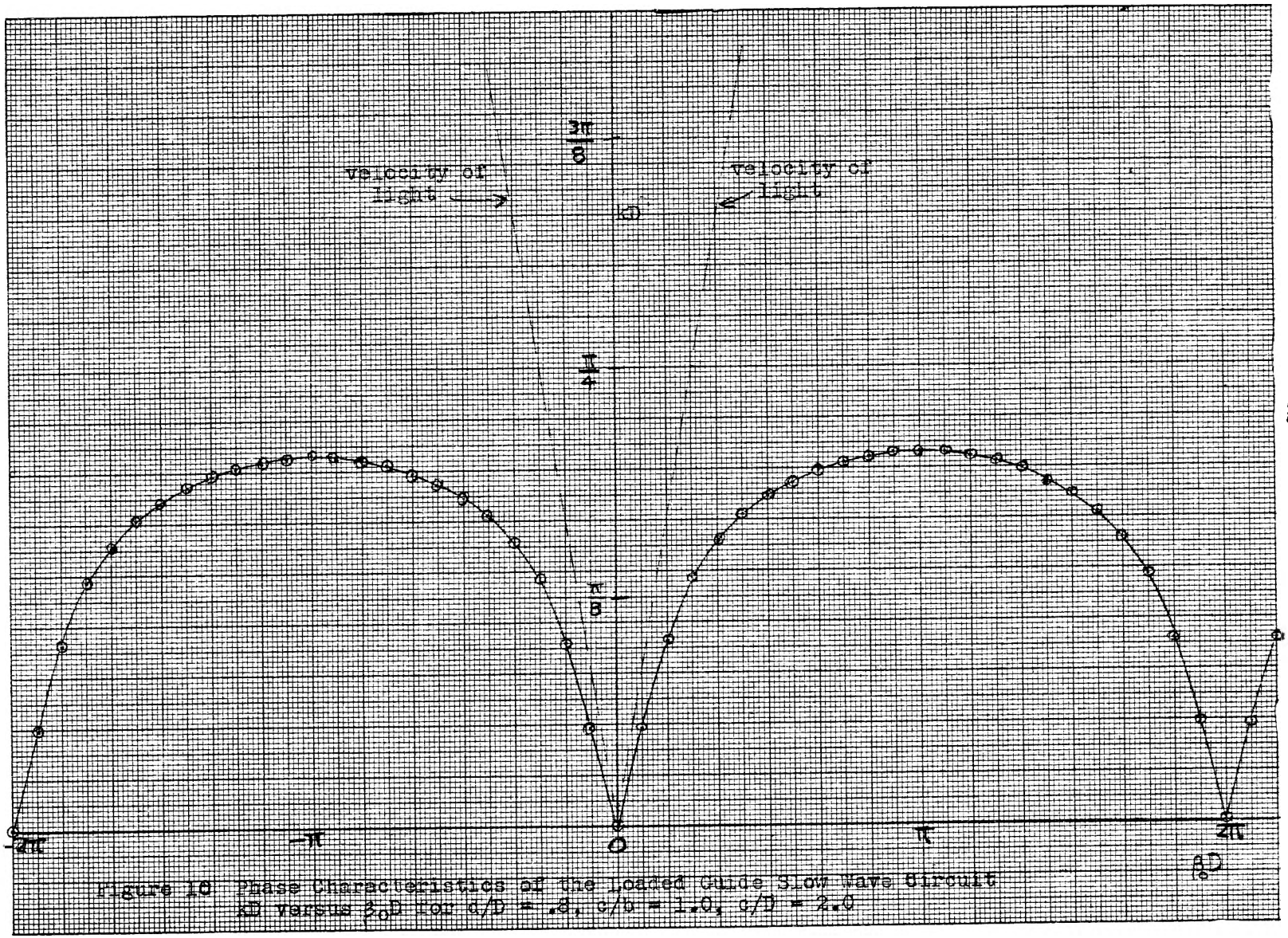

Figure 18 Phase Characteristics of the Loaded Guide Slow Wave Circuit
kD versus $\beta_0 D$ for d/D = .8, c/b = 1.0, c/D = 2.0

Thus when $\beta_o D$ is between 0 and π energy flows in the +z direction, while if $\beta_o D$ is between $-\pi$ and 0 energy flows in the -z direction. It should be noted that the phase velocity of space harmonics $\frac{\omega}{\beta_n}$ is not always of the same sign as the group velocity. For example, when $-\pi < \beta_o D < 0$ the group velocity is negative and the phase velocity of all space harmonics for which $n > 0$ is positive. A space harmonic whose phase velocity is of opposite sign from the group velocity at the wave is commonly called a backward space harmonic and sometimes, less precisely, a backward wave. When the phase velocity of a space harmonic has the same sign as the group velocity of the wave it is called a forward space harmonic or, sometimes, a forward wave. Backward space harmonics are of importance in oscillator tubes while forward space harmonics are of importance in amplifier tubes. At low frequencies (small kD, $kD = \frac{\omega D}{c}$), the behavior of this slow wave circuit is much like a strip transmission line, which propagates a transverse magnetic wave at the velocity of light. The effect of the fins is to capacitively load the line so as to decrease the phase velocity of the wave to about .65 times the velocity of light. As the frequency is increased, the phase shift per section increases until $\beta_o D = \pi$, where reflections from successive fins (or slots) reinforce and total reflection of the wave occurs. This is analogous to Bragg reflection of X-rays in crystal lattices. For a range of frequencies above the frequency at which total reflection occurs, no transmission occurs. Other transmission bends occur still higher in frequency but these are not of interest in the present discussion.

Solution with the Electron Beam Present. Solution of IV.29 is carried out in a similar manner when the electron beam is present, except

that the admittances Y_n are no longer the simple Y_{no}. In the preceding section it was found that the admittance with the beam present differs appreciably from that of free space only for certain rather narrow ranges of the propagation constant, β. The case of most interest in electron tubes is when the electron velocity is approximately equal to the phase velocity of one of the space harmonics, so that the electrons interact strongly with the circuit field. Under these circumstances the admittance for this particular space harmonic, $n = m$ for example, will differ drastically from the free space value, while the other space harmonic admittances will be practically equal to their free space values. An important exception to this situation occurs when other space harmonics have approximately the same phase velocity as the cyclotron waves of the beam. This effect will be discussed later in this section, and for the present it will be assumed that the space harmonic admittances Y_n are equal to their free space values Y_{no} except for $n = m$. IV.29 can then be written

$$(Y_m - Y_{mo})\, M_m^2 + \sum_{n=-\infty}^{\infty} Y_{no}\, M_n^2 + \frac{d}{D} \sum_{n=0}^{\infty} (2 - \delta_{no})\, Y'_n B_n^2 = 0 \qquad \text{IV.38}$$

by adding and subtracting a term $Y_{mo} M_m^2$. Solving IV.38 for Y_m

$$Y_m = Y_{mo} + \frac{1}{M_m^2}\left[\sum_{n=-\infty}^{\infty} Y_{no}\, M_n^2 + \frac{d}{D} \sum_{n=0}^{\infty} (2 - \delta_{no})\, Y'_n\, B_n^2 \right]. \qquad \text{IV.39}$$

This equation may be interpreted as follows. On the left stands the admittance of the electron beam at a plane which just grazes the circuit. The right side also has the dimensions of an admittance, and since the propagation constants of the system are found by equating this admittance

to the beam admittance, this expression is just the admittance which the circuit presents to the electron beam. In the remainder of the analysis it will be convenient to subtract Y_{mo} from both sides of IV.39 and denote the quantity in brackets by jS. The j has been used in the definition in order that S be real for real β. S is a susceptance.

$$Y_m - Y_{mo} = \frac{j\,S}{M_m^2} \quad . \qquad \text{IV.40}$$

The quantity

$$S = \frac{1}{j}\left[\sum_{n=-\infty}^{\infty} Y_{no}\, M_n^2 + \frac{d}{D} \sum_{n=0}^{\infty} (2-\delta_{no})\, Y'_n\, B_n^2 \right] \qquad \text{IV.41}$$

is closely connected with the problem of finding the propagation constants of the circuit in the absence of the electron beam; when β_o is equal to the propagation constant of the circuit in the absence of the beam, S is zero. If the propagation constant of the m^{th} space harmonic with the beam absence is denoted by β_m and the propagation constant of the m^{th} space harmonic with the beam present is denoted simply by β, S can be approximated by

$$S = \left(\frac{\partial S}{\partial \beta}\right)_{\beta_m} (\beta - \beta_m) + \frac{1}{2}\left(\frac{\partial^2 S}{\partial \beta^2}\right)_{\beta_m} (\beta - \beta_m)^2 \qquad \text{IV.42}$$

in a small neighborhood around β_m. Except when $\beta_m D \approx (2m \pm 1)\pi$, i.e., when operation is near the upper cutoff frequency of the circuit and the first derivative is small, the first derivative term by itself is a satisfactory approximation to S.

S is a periodic function of βD with period 2π. This is verified by noting that replacing $\beta_o D$ by $\beta_o D + 2\pi$ in IV.41 is equivalent to replacing n by n+1 in the first summation and does not affect the second summation. Since the first summation is over all values of n, this sum is also unchanged. Furthermore, S is an even function of βD. This may be demonstrated either by examining the terms in the sum in detail or by appealing to the symmetry properties of the circuit. Similarly $\frac{\partial S}{\partial \beta}$ is an odd periodic function of $\beta_o D$ with period 2π. Thus $(\frac{\partial S}{\partial \beta})_{\beta_m}$ does not depend on m since the different values of $\beta_m D$ differ by 2π.

As a result, if $-\pi < \beta_o D < 0$ so that the net energy flow of the wave is in the negative z direction, $(\frac{\partial S}{\partial \beta})_{\beta_m}$ will be equal in magnitude but opposite in sign from the value of $(\frac{\partial S}{\partial \beta})_{\beta_m}$ for the corresponding wave with energy flow in the positive z direction $(0 < \beta_o D < \pi)$ at the same frequency. Figure 11 shows $(\frac{\partial S}{\partial \beta})_{\beta_m}$ for the circuit whose characteristics are shown in Figure 10.

Thus when the electron beam has a velocity approximately equal to the phase velocity of the m^{th} space harmonic of the slow wave circuit, the circuit presents a susceptance to the beam given approximately by

$$B_m - B_{mo} = \frac{1}{M_m^2} \left(\frac{\partial S}{\partial \beta}\right)_{\beta_m} (\beta - \beta_m) \qquad \text{IV.43}$$

where the sign of $(\frac{\partial S}{\partial \beta})_{\beta_m}$ is negative for forward space harmonic interaction and positive for backward space harmonic operation. This is the principal result of this section. It gives a simple representation of the susceptance presented to the electron beam by the slow wave

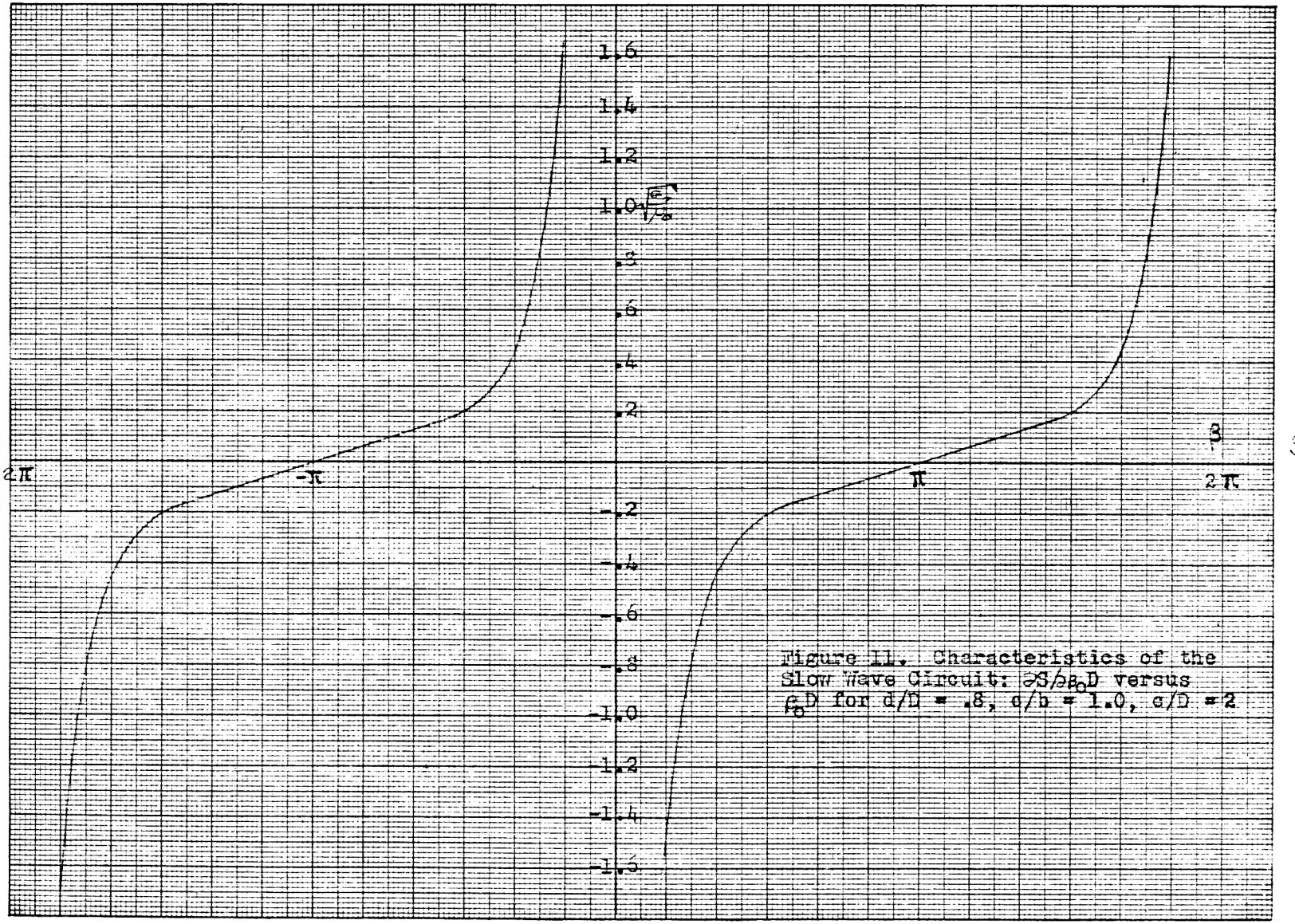

Figure 11. Characteristics of the Slow Wave Circuit: $\partial S/\partial \beta_0 D$ versus $\beta_0 D$ for d/D = .8, c/b = 1.0, c/D = 2

circuit. Fletcher (5) has shown that it is possible to represent the susceptance of a sheath helix, at the surface of the helix, in this manner. He has also demonstrated for the sheath helix, the equivalence between this type of representation and the Pierce equivalent circuit representation. It seems likely that most slow wave circuits can be represented approximately in this manner. Pierce (8) for example, assumes that this is possible. The treatment of this section demonstrates by means of a field analysis that this is possible for the loaded strip transmission line, a space harmonic circuit, and determines the pertinent constants of the representation. It is also possible to determine these constants experimentally (25) (26).

In Section V it will be assumed that the slow wave circuit may be represented by a susceptance

$$B_m = B_{mo} + C_m \frac{\beta - \beta_m}{\beta_m} \qquad \text{IV.44}$$

placed at the plane of the circuit. The values of C_m and β_m obtained in this section will not be used specifically in the computations, but rather a wider variety of values such as might be obtained with other types of slow wave circuits will be assumed.

Comparison with the Pierce Circuit Equation. Pierce derives a similar circuit equation using the normal mode theory (8) but the constants in his circuit equation must be evaluated from a field analysis (4),(5) or by experiment (25),(26). The difference in sign in the circuit equation between forward space harmonic operation and backward space harmonic operation can be deduced from the equivalent circuit approach, but the above analysis constitutes a proof of the validity of this type of circuit representation. The relationship between the

constant C_m in IV.49 and Pierce's traveling wave tube impedance parameter K will now be determined. Pierce's circuit equation for a thin beam is (see Figure 12)

$$\frac{V}{i} = \frac{\beta\,\beta_m\,K}{\beta^2-\beta_m^2} + \frac{\beta}{\omega C_1} \qquad \text{IV.45}$$

where V is the voltage at the electron beam, i is the convection current of the beam, and C_1 is the capacitance between beam and circuit in a unit length of circuit.

IV.45 gives the circuit impedance at the surface of the circuit if the second term is neglected.

$$\frac{V}{i} = \frac{\beta\,\beta_m}{\beta^2-\beta_m^2}\,K \quad .$$

Furthermore, if $\beta \approx \beta_m$ this may be written

$$\frac{V}{i} = \frac{\beta_m}{2(\beta-\beta_m)}\,K \quad \text{or} \quad \frac{i}{V} = \frac{2}{K}\,\frac{\beta-\beta_m}{\beta_m} \quad . \qquad \text{IV.46}$$

IV.46 is similar in form to IV.44. If the beam is a thin sheet beam of width w, the convection current in the z direction is related to the discontinuity in magnetic field by

$$i_z = \left[(H_{1x})_{\text{below}} - (H_{1x})_{\text{above}} \right] \cdot w \quad .$$

The longitudinal field is related to the voltage V by

$$V = \frac{E_{1z}}{j\beta} \approx \frac{E_{1z}}{j\beta_m}$$

so that IV.46 may be written

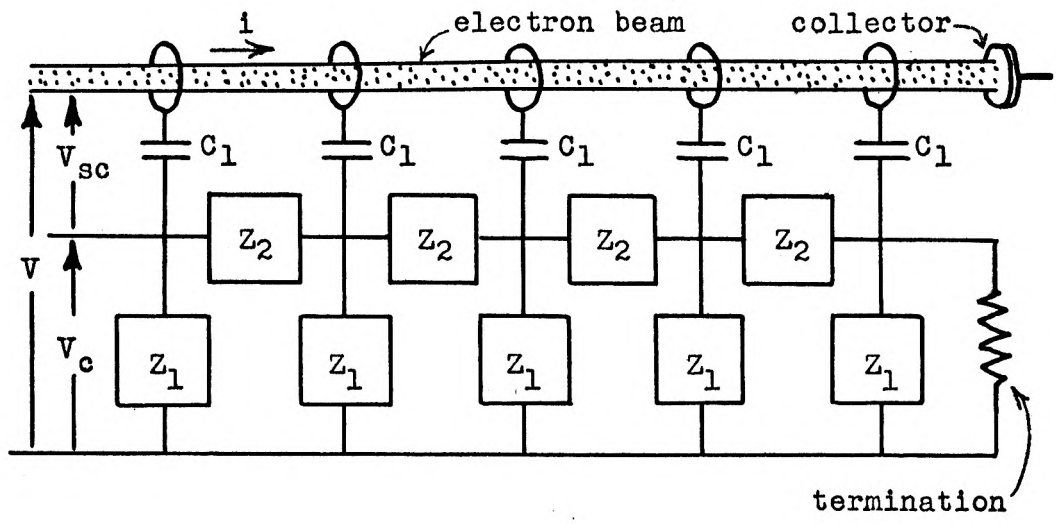

Figure 12. The Pierce Traveling Wave Tube Equivalent Circuit

$$\frac{i}{V} = \frac{2}{K}\frac{\beta - \beta_m}{\beta_m} = j\beta_m w \frac{(H_{1x})_{below} - (H_{1x})_{above}}{E_{1z}}$$

$$= j\beta_m w \left[Y_m - Y_{mo}\right] \qquad \text{IV.47}$$

$$= \beta_m w \left[B_{mo} - B_m\right] \qquad (Y_m = j\beta_m) \ .$$

Solving for $B_m - B_{mo}$,

$$B_m - B_{mo} = -\frac{2}{K}\frac{1}{\beta_m w}\frac{\beta - \beta_m}{\beta_m} \ . \qquad \text{IV.48}$$

Comparison of IV.48 with IV.44 shows that the Pierce traveling wave tube impedance parameter is inversely proportional to C_m ,

$$K = -\frac{2}{\beta_m w}\frac{1}{C_m} \ . \qquad \text{IV.49}$$

K is the value of the impedance parameter at a plane which just grazes the circuit. Thus IV.44 can also be written

$$B_m - B_{mo} = -\frac{2}{K}\frac{1}{\beta_m w}\frac{\beta - \beta_m}{\beta_m} \qquad \text{IV.50}$$

and, in terms of the normalized susceptance,

$$Q_m - Q_{mo} = \frac{2}{k w}\frac{\sqrt{\frac{\mu_o}{\epsilon_o}}}{K}\frac{(\beta - \beta_m)}{\beta_m} \ . \qquad \text{IV.51}$$

IV.51 can also be expressed in terms of the variable ν of the preceding section (III).

$$Q_m - Q_{mo} = \frac{1}{\aleph^2}(\nu - b) \qquad \text{IV.52}$$

where

$$\aleph^2 = \frac{kw}{2}\frac{K}{\sqrt{\frac{\mu_o}{\epsilon_o}}}\frac{1}{r^2_m} \qquad \text{IV.53}$$

and b is defined by

$$\beta_m = \beta_+ (1 + r^2 m b) \quad . \qquad \text{IV.54}$$

b is a measure of the difference in velocity of upper edge electrons and the phase velocity of the m^{th} space harmonic in the absence of the electron beam. When $b > 0$ the upper edge electrons travel faster than the space harmonic field. $\wp^2$ is a dimensionless parameter which is a measure of the strength of circuit field.

In Section V the circuit equation, IV.52, will be combined with the electronic equation, III.68, to find the waves of the electron beam in the presence of the circuit.

Operation Near the upper Cutoff Frequency, $\beta_m \approx \frac{2m+1}{D}\pi$.
In this region two space harmonics are important; one is a forward space harmonic and one is a backward space harmonic. It is necessary to retain both terms of IV.42 in approximating S . The consequences of the extra term and the conditions under which it must be retained will now be examined.

When the electron beam is absent, the phase constants of the circuit space harmonics may be found by setting S, as given by IV.42, equal to zero. Clearly, one solution is $\beta = \beta_m$, but this equation has two solutions. To the extent that third and higher order terms can be neglected, the other solution must represent the nearby space harmonic which has a propagation constant

$$\begin{aligned} \beta &= \frac{2m \pm 1}{D}\pi + \left(\frac{2m \pm 1}{D}\pi - \beta_m\right) \\ &= \frac{2m \pm 1}{D} 2\pi - \beta_m \quad . \end{aligned} \qquad \text{IV.55}$$

It should be noted that these two space harmonics are not space harmonics of the same wave. One is a space harmonic of a wave whose net energy flow is in the positive z direction and the other is a space harmonic of a wave whose net energy flow is in the negative z direction. As such, these space harmonics, together with the waves with which they are associated, can exist on the circuit independently of each other. With the aid of IV.55, IV.42 can be rewritten

$$S = \left(\frac{\partial S}{\partial \beta}\right)_{\beta_m} (\beta - \beta_m)\left(1 + \frac{\beta - \beta_m}{2\beta_m - \frac{2m \pm 1}{D} 2\pi}\right) \quad . \qquad \text{IV.56}$$

The second factor has been adjusted so as to vanish at the value given by IV.55 and still have the form given by IV.42. From IV.47 it can be seen that the one term approximation will be valid when the electron beam is present if all the propagation constants, β , which are determined using the one term approximation satisfy the condition

$$|\beta - \beta_m| << 2\left(\beta_m - \frac{2m \pm 1}{D}\pi\right) \quad . \qquad \text{IV.57}$$

For electron beams which have approximately the same velocity as the m^{th} space harmonic $|\beta - \beta_m|$ is generally between .01 β_m and .1 β_m . Finally, it should be noted that as $\beta_m \rightarrow \frac{2m \pm 1}{D}\pi$ the second term of the second factor in IV.56 becomes large compared with the first term, but that the factor $\left(\frac{\partial S}{\partial \beta}\right)_{\beta_m}$ approaches zero in such a manner that $\left(\frac{\partial^2 S}{\partial \beta^2}\right)_{\beta_m}$ is approximately constant.

The two term approximation is not used in subsequent analysis but is necessary for a correct analysis of operation near the high frequency cutoff.

Simultaneous Interaction of the Electron Beam with More Than One Space Harmonic of the Same Wave. This effect has been termed the rising sun effect by French workers (6), because of its similarity to an effect which occurs in rising sun magnetrons. It is observed to cause slight anomalies in the starting conditions. Although this effect is not studied in Section V, the formal modifications which would be required in the theory are presented here. It is possible to have simultaneous interaction with three space harmonics of the same wave if

$$\frac{\omega_c}{u} \approx \frac{2\pi}{D}\,\ell \qquad \ell = \text{integer}\,, \qquad \text{IV.58}$$

for under these circumstances when electrons have a velocity approximately equal to the phase velocity of the m^{th} space harmonic, the slow cyclotron wave is approximately in synchronism with the $m + \ell$ space harmonic and the fast cyclotron wave is in synchronism with the $m - \ell$ space harmonic. It is then necessary to treat three terms separately in IV.29 ,

$$\left[Y_{(m-\ell)} - Y_{(m-\ell)o}\right]M^2_{(m-\ell)} + \left[Y_m - Y_{mo}\right] M^2_m + \left[Y_{(m+\ell)} - Y_{(m+\ell)o}\right]M^2_{(m+\ell)} + jS = 0 \,. \qquad \text{IV.59}$$

The various admittances $Y_{m-\ell}$, Y_m, $Y_{m+\ell}$, etc. are functions of the propagation constants

$$\beta - \frac{2\pi\ell}{D}\,, \quad \beta\,, \quad \beta + \frac{2\pi\ell}{D}$$

respectively, where β is the propagation constant which is approximately equal to β_m, and must be determined from the theory given in the previous section. The approximation IV.42 for S may still be used.

V START OSCILLATION CONDITIONS FOR THE BACKWARD WAVE OSCILLATOR

Characteristic Waves of the System. The electronic equation, III.69 must be combined with the circuit equation IV.52 to determine the propagation constants of the waves of the beam in the presence of the circuit. The resulting equation is

$$\frac{1}{\mathcal{K}^2}(\nu - b) = \frac{-\nu\left[\frac{2T}{1+T}\frac{1-T'}{1+T'}\right] + \frac{1-T'}{1+T'}\left[s\beta_- t - \frac{T}{1+T}\right]}{\nu^2 + \nu\left[\frac{T}{1+T}\frac{1-T'}{1+T'} - s\beta_- t\right] + \frac{T'}{1+T'}\left[s\beta_- t - \frac{T}{1+T}\right]}. \qquad \text{V.1}$$

Since $T = \tanh \beta t$ and $T' = \tanh \beta d$ are slowly varying functions of β, they may be considered as constants in this equation. They are to be evaluated at $\beta = \frac{\omega}{\sqrt{u_+ u_-}} \approx \beta_+ \approx \beta_-$. IV.1 has three solutions, since it is of third degree in ν. When the coupling between the circuit and beam is weak, it is expected that these solutions will represent a circuit wave and an upper and lower surface wave of the beam. The solutions of this equation will be discussed in more detail in connection with the numerical examples.

The analysis which leads to V.1 neglects all waves except those which have a phase velocity nearly equal to the electron velocity. Thus many of the characteristic waves will not be obtained from V.1; the cyclotron waves and the waves with density modulation in the interior of the beam, found in the non-slipping beam, are omitted. Higher order waves of the circuit are also omitted.

Boundary Conditions at $z = 0, L$. The boundary conditions which must be satisfied at $z = 0$ and $z = L$ can be described loosely as

(a) The beam enters unmodulated at a plane $z = 0$. The y and z velocity and displacement of each electron from

its equilibrius position is zero. The electric field at $z = 0$ depends on the exact details of the coupling of circuit to an external waveguide or transmission line.

(b) The circuit is terminated with a perfect absorber of electromagnetic energy at $z = L$. In practice the circuit termination is confined to the immediate vicinity of the slow wave circuit and spread over a short distance in the z direction.

It is clear that even if these conditions could be stated more precisely, such as by specifying the exact shapes of all conductors and absorbers, it is only possible to meet three boundary conditions with the three waves that have been studied. For this reason this analysis is far short of a complete field analysis. Only certain aspects of the problem have been studied from the field point of view. It is, for example, possible to give a complete description of the fields associated with the three waves which have been studied.

Since the analysis has been reduced to a treatment of what are thought to be the three most important waves of the system, it is necessary to select the three most important boundary conditions. The electron beam propagates two waves in the absence of the circuit. One is associated with the upper boundary and one is associated with the lower boundary. Thus two conditions should probably be applied to the electron beam at $z = 0$ in such a manner as to determine the strength of these two surface waves. It is more important to have the a.c. current in the electron beam be zero at $z = 0$ than to have the velocity be zero there since current modulation produces a direct effect in the circuit while velocity modulation produces an effect only after it has

been converted to a current. In Section III it was shown that when $\omega_p^2 \ll \omega_c^2$ most of the a.c. beam current is in the form of surface current. Hence it seems reasonable to require that the surface current at the two beam edges be zero at $z = 0$.

It is interesting to note in this regard that J. W. Sedin (27) has shown that in the theory of Pierce and Muller it is sufficient to specify the current in the beam at $z = 0$. In this case there are only two waves near the electron velocity rather than three, so that only one condition is required at $z = 0$. Sedin also finds that the cyclotron waves, although they are excited only to a small extent and produce very little electric field, produce a velocity modulation of the beam which is comparable with that produced by the waves near the electron velocity. These waves are necessary to meet the boundary conditions on the velocity at $z = 0$. However, little error in the start oscillation conditions results by neglecting these waves and not satisfying the initial velocity conditions.

The third wave which is included in V.1 is the wave of the slow wave circuit whose group velocity and power flow are in the negative z direction. Thus the third boundary condition should probably be applied at $z = L$ in such a manner as to determine the strength of the circuit wave. This boundary condition is most easily formulated by analogy with the Pierce theory of traveling wave tubes. The Pierce equivalent circuit is shown in Figure 12. Since only the circuit wave with energy flow to the left is required, the absence of energy flow to the left at $z = L$ can be insured by taking V_c, the circuit

voltage, to be zero at this point. To be sure, the wave to the left is excited in the region between $z = 0$ and $z = L$ by the electron beam, and must be employed in that region.

By analogy it may be argued that the boundary condition which represents a termination at $z = L$ in the field analysis is: $E_z(d) = 0$, i.e., the electric field at the surface of the circuit must be zero. It is permissible to use the electric field in this case since it differs from the potential only by the factor $+j\beta$, which is nearly the same for all waves. Notice also that zero longitudinal field at the circuit does not imply zero longitudinal field at the beam, since these points are generally separated by a small distance. Similarly, in the Pierce equivalent circuit, $V_c = 0$ does not imply $V = 0$ since there can be a voltage drop V_{sc} across the capacitance C_1, which represents the space between the beam and the circuit.

The Starting Conditions. The amplitudes of the three waves will be specified by giving the strength of the longitudinal electric field of each wave at the upper edge of the beam. Denoting these amplitudes by $E^{(1)}$, $E^{(2)}$, and $E^{(3)}$, the total longitudinal field at the upper edge may be written,

$$E_{1z}(o) = E^{(1)} e^{-j\beta_1 z} + E^{(2)} e^{-j\beta_2 z} + E^{(3)} e^{-j\beta_3 z} \quad . \qquad V.3$$

The surface current density on the upper edge of the beam for a single wave of propagation constant β is

$$i_+ = u_+ \sigma_+ = - \frac{\omega_p^2 u_+ \epsilon_o E_{1z}(o)}{j(\omega - \beta u_+)\omega_c} \quad .$$

This may be rewritten in terms of the variable ν as

$$i_+ = -j \frac{u_+ \epsilon_o E_{1z}(o)}{\nu} \quad . \qquad V.4$$

Hence the total surface current of the upper edge of the beam when all three waves are present is

$$i_+ = -j u_+ \epsilon_o \sum_{i=1}^{3} \frac{E^{(i)} e^{-j\beta_i z}}{\nu_i} \quad . \qquad V.5$$

Since this must vanish at $z = 0$, one of the three boundary conditions is expressed by

$$\sum_{i=1}^{3} \frac{E^{(i)}}{\nu_i} = 0 \quad . \qquad V.6$$

To express the other two boundary conditions, E_{1z} at the lower edge of the beam and at the circuit must be expressed in terms of $E^{(i)}$. To do this note that, for a single wave, E_{1z} and E_{1y} in the interior of the beam are given by

$$E_{1z} = E^{(1)} \left[\cosh \beta_1 y + A_1 \sinh \beta_1 y\right] \qquad V.7$$

$$E_{1y} = jE^{(1)} \left[\sinh \beta_1 y + A_1 \cosh \beta_1 y\right] . \qquad V.8$$

A_1 may be determined as follows. At $y = -t$, the lower edge of the beam,

$$E_{1z} = E^{(1)} \left[\cosh \beta_1 t - A_1 \sinh \beta_1 t\right] \qquad V.9$$

$$E_{1y} = jE^{(1)} \left[-\sinh \beta_1 t + A_1 \cosh \beta_1 t\right]. \qquad V.10$$

Equating $\frac{E_{1y}}{E_{1z}}$ obtained from the quotient of these two expressions to

$$j\left[1 - \frac{\omega_p^2}{\omega_c(\omega - \beta_1 u_-)}\right] \approx j \left[1 - \frac{1}{s\,\beta_- t - \quad 1}\right] \qquad V.11$$

the admittance just above the lower edge of the beam, the following relationship is obtained

$$\frac{-T + A_1}{1 - TA_1} = 1 - \frac{1}{s\beta_- t - \nu_1} = \frac{s\beta_- t - \nu_1 - 1}{s\beta_- t - \nu_1} \quad .$$

Solving for A_1,

$$A_1 = \frac{\nu_1 - s\beta_- t + \frac{1}{1+T}}{\nu_1 - s\beta_- t + \frac{T}{1+T}} \quad . \qquad \text{V.12}$$

The total longitudinal field of lower edge of the beam $E_{1z}(-t)$ is found by substituting V.12 into V.9 and summing over all three waves

$$E_{1z} = \cosh \beta t \left[1 - T\right] \sum_{i=1}^{3} E^{(i)} e^{-j\beta_i z} \frac{\nu_i - s\beta_- t}{\nu_i - s\beta_- t + \frac{T}{1+T}} \quad . \qquad \text{V.13}$$

The surface current density at the lower edge of the beam when a single wave is present, is given by

$$i_- = u_- \sigma_- = -j \frac{u_- \omega_p^2 \epsilon_o E_z}{(\omega - \beta u_-)\omega_c} \quad ,$$

which may be rewritten

$$i_- = j \frac{u_- \epsilon_o E_{1z}}{\nu - s\beta_- t} \quad . \qquad \text{V.14}$$

The total surface current density at the lower edge of the beam is given by summing the contributions from the three waves

$$i_- = j u_- \epsilon_o \cosh \beta t \left[1 - T\right] \sum_{i=1}^{3} \frac{E^{(i)} e^{j\beta_i z}}{\nu_i - s\beta_- t + \frac{T}{1+T}} \quad . \qquad \text{V.15}$$

Since this also must vanish at $z = 0$, the second of the three boundary

conditions is expressed by,

$$\sum_{i=1}^{3} \frac{E^{(i)}}{\nu_i - s\beta_- t + \frac{T}{1+T}} = 0 \quad . \qquad \text{V.16}$$

The fields in the region above the beam may be written

$$E_{1z} = E^{(1)} \left[\cosh \beta_1 y + A_2 \sinh \beta_1 y\right] \qquad \text{V.17}$$

$$E_{1y} = jE^{(1)} \left[\sinh \beta_1 y + A_2 \cosh \beta_1 y\right] \qquad \text{V.18}$$

where A_2 may be determined as follows. From V.7, V.8, V.17, and V.18

$$\left.\frac{E_{1y}}{E_{1z}}\right|_{y=0_+} = jA_2 \quad \text{and} \quad \left.\frac{E_{1y}}{E_{1z}}\right|_{y=0_-} = jA_1 \quad .$$

These ratios differ by the normalized admittance of the equivalent surface charge density at $y = 0$

$$jA_2 = jA_1 + j \frac{\omega_p^2}{(\omega - \beta_1 u_+)\omega_o} \quad .$$

Using the value of A_1 given by V.12

$$A_2 = A_1 - \frac{1}{\nu_1} = \frac{\nu_1 - s\beta_- t + \frac{1}{1+T}}{\nu_1 - s\beta_- t + \frac{T}{1+T}} - \frac{1}{\nu_1} \quad . \qquad \text{V.19}$$

Denoting A_2, which is a function of ν, by $A_2(\nu)$, the total longitudinal field at the circuit may be written as

$$E_{1z} = \cosh \beta d \sum_{i=1}^{3} \left[1 + A_2(\nu_i)T'\right] E^{(i)} e^{-j\beta_i z} \qquad \text{V.20}$$

where $T' \equiv \tanh \beta d$.

This must vanish at $z = L$. Thus the third boundary condition is expressed by

$$\sum_{i=1}^{3} \left[1 + A_2(\nu_i)T'\right] E^{(i)} e^{-j\beta_i L} = 0 \qquad \text{V.21}$$

To obtain the start oscillation condition V.6, V.16 and V.21 must be satisfied simultaneously with non-zero $E^{(1)}$, $E^{(2)}$, or $E^{(3)}$. This will only be possible for certain values of b and L.

From V.6 and V.16 it is easily established that $E^{(1)}$, $E^{(2)}$, and $E^{(3)}$ must be in the ratio

$$\frac{1}{\nu_2(\nu_3 - s\beta_- t + \frac{T}{1+T})} - \frac{1}{\nu_3(\nu_2 - s\beta_- t + \frac{T}{1+T})} ,$$

$$\frac{1}{\nu_3(\nu_1 - s\beta_- t + \frac{T}{1+T})} - \frac{1}{\nu_1(\nu_3 - s\beta_- t + \frac{T}{1+T})} ,$$

$$\frac{1}{\nu_1(\nu_2 - s\beta_- t + \frac{T}{1+T})} - \frac{1}{\nu_2(\nu_1 - s\beta_- t + \frac{T}{1+T})} ,$$

so that V.21 may be written

$$\sum_{i=1}^{3} \left[1 + A_2(\nu_i)T'\right]\left[\frac{1}{\nu_j(\nu_k - s\beta_- t + \frac{T}{1+T})} - \frac{1}{\nu_k(\nu_j - s\beta_- t + \frac{T}{1+T})}\right] e^{-j\beta_i L} = 0 \qquad \text{V.22}$$

where $i\ j\ k$ are cyclical permutations of 1, 2, and 3. Since

$$\beta_i = \beta_+ (1 + mr^2\nu_i)$$

a common, non-zero factor $e^{-j\beta_+ L}$ can be removed from V.22 leaving

$$\sum_{i=1}^{3}\left[1+A_2(\nu_i)T'\right]\left[\frac{1}{\nu_j(\nu_k - s\beta_- t+\frac{T}{1+T})} - \frac{1}{\nu_k(\nu_j - s\beta_- t+\frac{T}{1+T})}\right]e^{-j\nu_i\theta} = 0 \qquad \text{V.23}$$

where $\theta \equiv \beta_+ L mr^2$. The roots, ν_i , of V.1 are functions of the geometrical parameters of the circuit and the beam, the beam current, and the parameter b , which denotes the difference in velocity between the upper edge electrons and the circuit space harmonic in the absance of the electrons. The procedure which will be adopted here is to assume that the beam current and all the geometrical parameters, except the length of the tube, are known. The length of the tube at which oscillation begins to occur is found by adjusting θ , the length parameter, and b , the velocity difference parameter until V.23 is satisfied.

Numerical Solution of the Start Oscillation Conditions. The following more or less typical conditions have been assumed for the numerical work which follows

$$\begin{aligned} \beta t &= .50 \quad T = .4621 \\ \beta d &= .50 \quad T' = .4621 \\ \beta a &= \infty \quad C = 1.0000 \ . \end{aligned} \qquad \text{V.24}$$

The circuit impedance, represented in dimensionless form by $\aleph^2$, is varied since it is expected that when it is small space charge effects will be important and when it is large space charge effects will be unimportant. Although the circuit analyzed in Section IV is capable of providing only a limited range of values of $\aleph^2$, a rather wide range of $\aleph^2$ is likely to be encountered when other circuits are also considered. Calculations have been made for the non-slipping case (s = 0) as well as the slipping beam case (s = 1) .

The first stage of the computation is to solve V.1 for ν_1, ν_2, and ν_3, for a number of values of b. Figures 13, 14, and 15 are plots of the solutions of V.1 versus b for $\kappa^2 = -.1$, $-.01$, $-.001$ and the remaining parameters given by V.24. As $|b|$ increases all curves are asymptotic to straight lines. Two of the asymptotes are the solutions which would be obtained by replacing the circuit by a conducting plane and the third asymptote is $\nu = b$, the circuit solution in the absence of the electron beam. Thus in these regions the solutions represent waves similar to those studied in Sections III and IV. In the intermediate regions where the curves deviate considerably from the asymptotes, the waves of the beam and the wave of the circuit are coupled together and are of an intermediate nature.

It is interesting to note that in the slipping stream case the waves of the beam are described by complex conjugate values of ν, hence one wave increases and one wave decreases with z. This effect was described in Section III and it is found to affect the starting conditions significantly. In the non-slipping case ($s = 0$) the waves of the beam are constant amplitude waves, one faster than the electrons and one slower than the electrons. In Figures 13b, 14b, and 15b, it can be seen that when the phase velocity of the unperturbed circuit wave is approximately equal to the phase velocity of the faster of the two beam waves (ν_3), an increasing and decreasing pair of waves results. A similar situation occurs in the ordinary backward wave oscillator (28), (29).

To find the zeros of V.23 it is convenient to plot the function

$$\frac{F(b,\theta)}{F(b,0)}$$

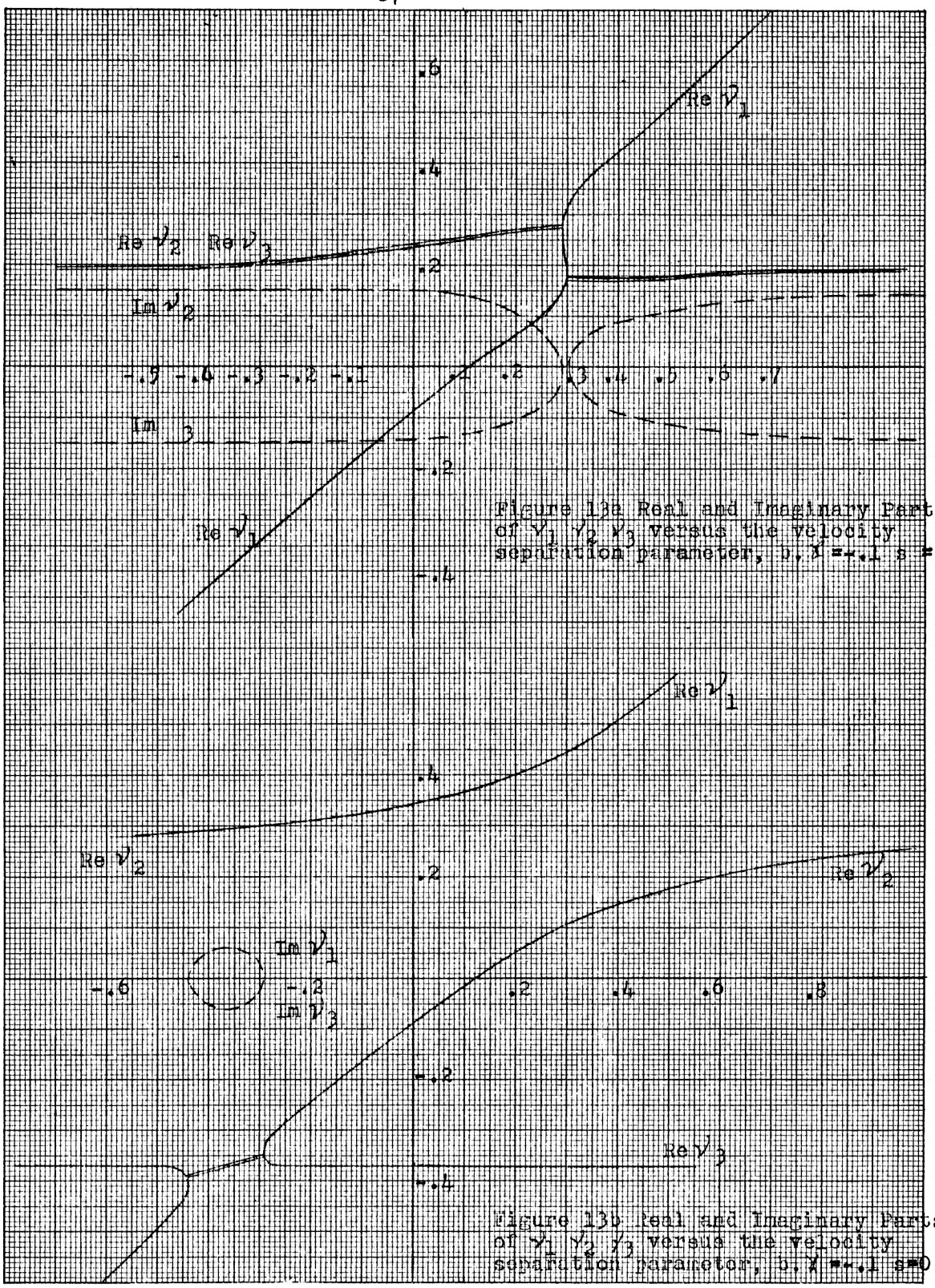

Figure 13a Real and Imaginary Parts of ν_1 ν_2 ν_3 versus the velocity separation parameter, b, λ =-.1 s = 1

Figure 13b Real and Imaginary Parts of ν_1 ν_2 ν_3 versus the velocity separation parameter, b, λ =-.1 s=0

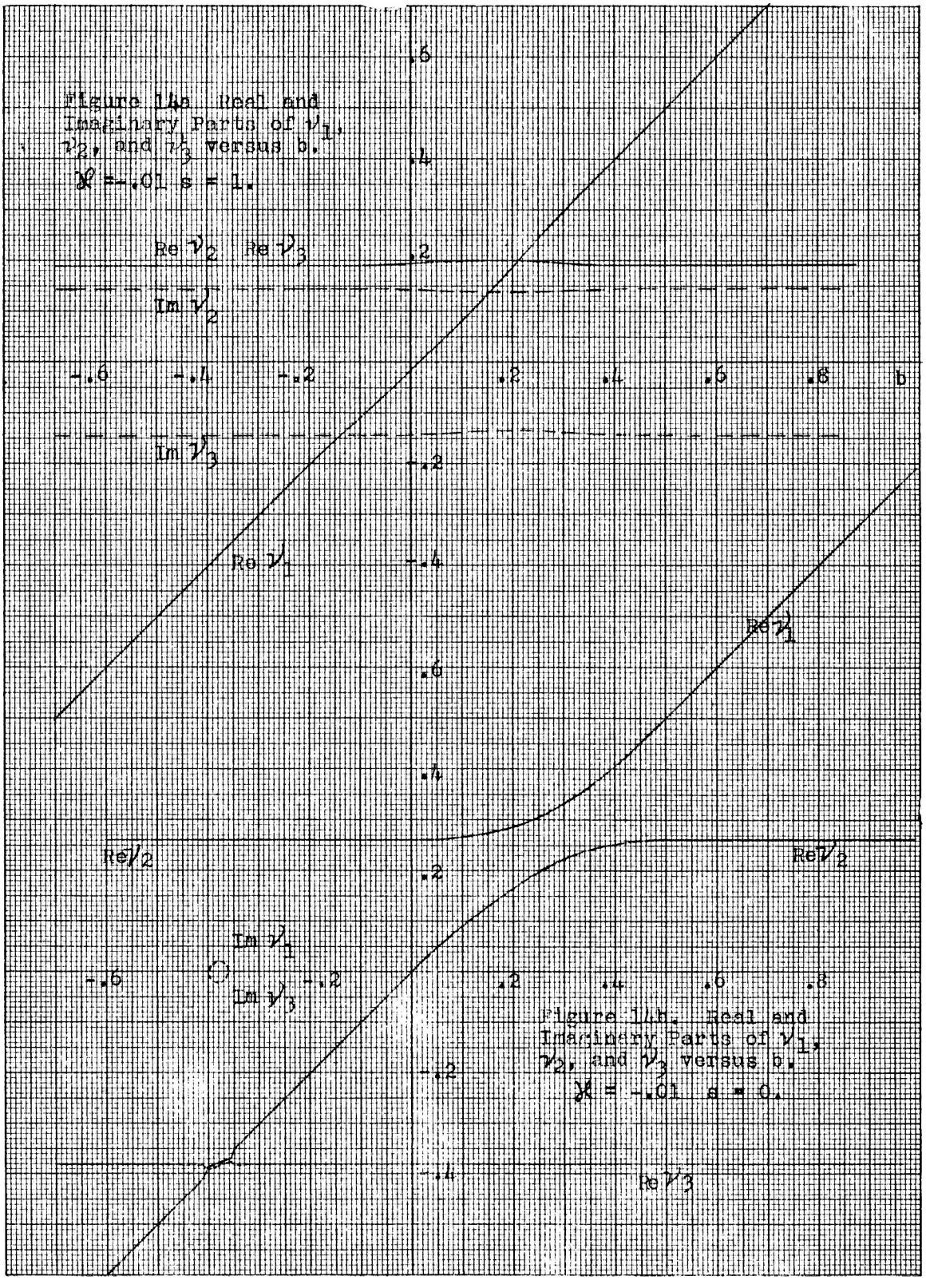

Figure 14a. Real and Imaginary Parts of ν_1, ν_2, and ν_3 versus b.
$\mathcal{K} = -.01$ s = 1.

Figure 14b. Real and Imaginary Parts of ν_1, ν_2, and ν_3 versus b.
$\mathcal{K} = -.01$ s = 0.

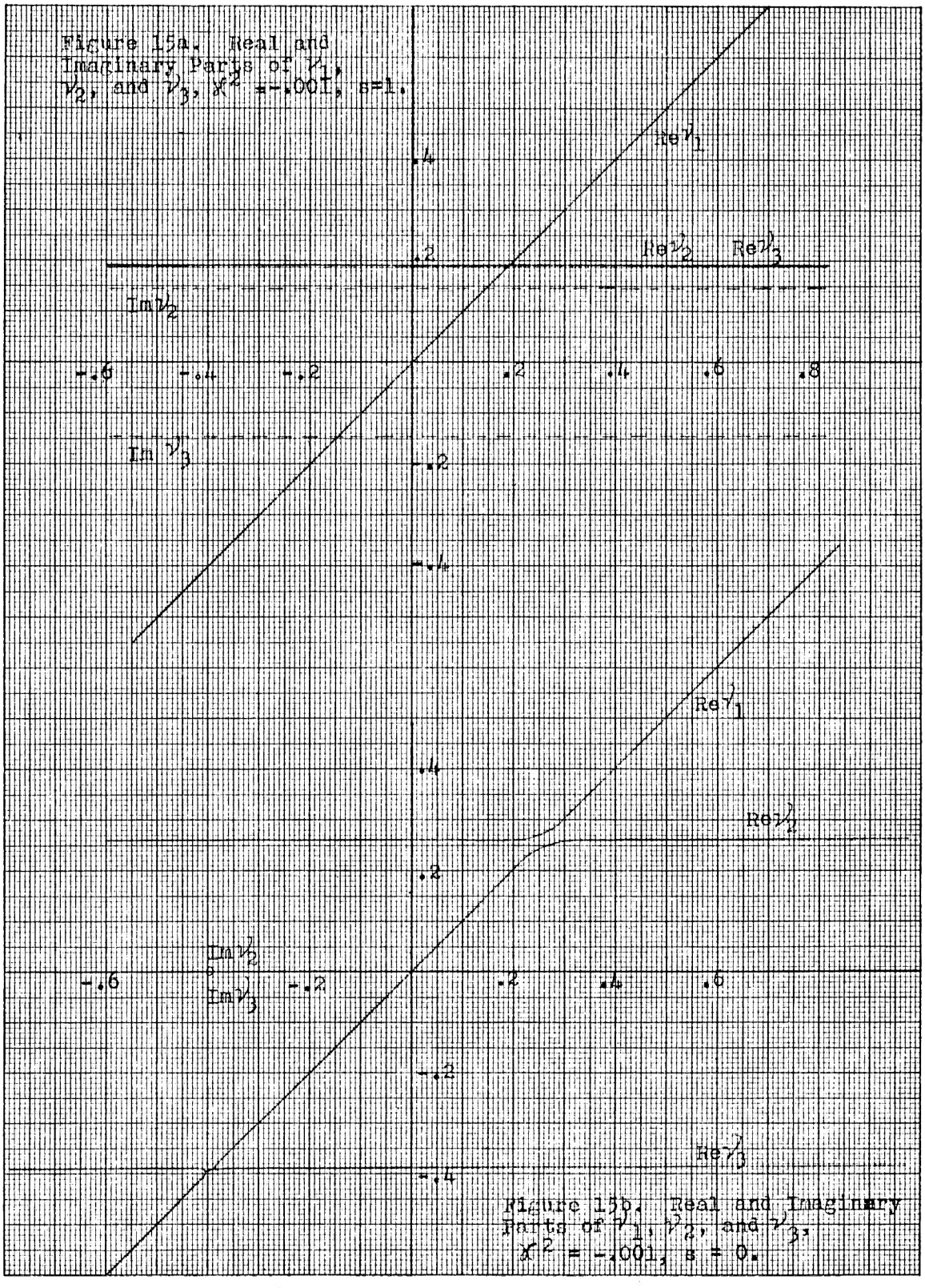

Figure 15a. Real and Imaginary Parts of ν_1, ν_2, and ν_3, $\chi^2 = -.001$, s=1.

Figure 15b. Real and Imaginary Parts of ν_1, ν_2, and ν_3, $\chi^2 = -.001$, s = 0.

where

$$F(b,\theta) = \sum_{i=1}^{3} \left[1 + C_2(\nu_i)T'\right]\left[\frac{1}{\nu_j(\nu_k - s\beta_- t + \frac{T}{1+T})} - \frac{1}{\nu_k(\nu_j - s\beta_- t + \frac{T}{1+T})}\right] e^{-j\nu_i\theta} \qquad V.16$$

in the complex plane with b and θ as parameters. Figure 16 shows a typical plot from which it is possible to determine the values of b and θ that make $F(b,\theta)$ equal to zero. Although there is more than one pair of b and θ which make $F(b,\theta)$ equal to zero (not shown in Figure 16), only the solution with the smallest value of θ has been obtained. This corresponds to the minimum length of tube for oscillation. If the tube is considerably longer than this minimum length, other modes of oscillation are possible, but these will not be discussed.

Solutions have been obtained for $\gamma^2 = -.10$, $-.01$, and $-.001$ (γ^2 is negative for backward space harmonic operation) with $s = 0$ and $s = 1$. The results are summarized in Table I.

Comparison with the Pierce-Muller Theory. Muller (9) has adapted Pierce's (8) theory of interaction between a forward wave circuit and a thin electron beam focused with crossed electric and magnetic fields to backward wave interaction and finds for the M type backward wave oscillator starting conditions

$$-(\beta_e L)^2 \frac{\omega}{\omega_c} \alpha \phi^2 \frac{KI_o}{2V_o} = (\frac{\pi}{2})^2 \qquad V.17$$

where I_o is the beam current, V_o is beam voltage (not the circuit voltage), K is impedance parameter at the plane of the circuit, ϕ is the ratio of the field (E_{1z}) at the beam to the field at the circuit and $\alpha = \frac{E_{1y}}{jE_{1z}}$ at the beam. Space charge effects were neglected in

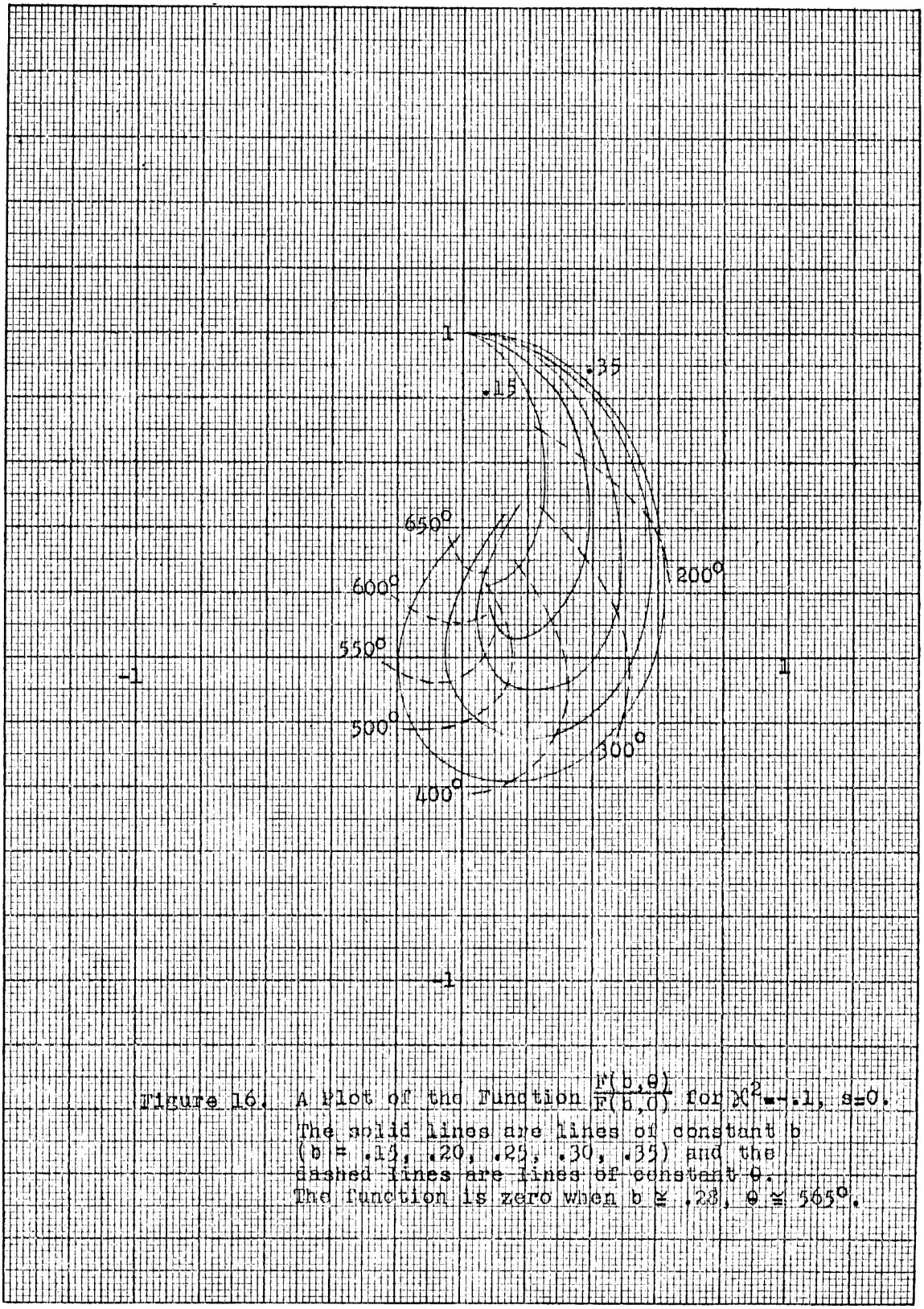

Figure 16. A plot of the function $\frac{F(b,\theta)}{F(b,0)}$ for $\chi^2=-.1$, $s=0$. The solid lines are lines of constant b (b = .15, .20, .25, .30, .35) and the dashed lines are lines of constant θ. The function is zero when $b \cong .23$, $\theta \cong 565^\circ$.

TABLE I

M-Type Backward Wave Oscillator Start Oscillation Conditions

Summary of Numerical Computations

case	b	θ	$E^{(1)}$	$E^{(2)}$	$E^{(3)}$
$\kappa^2 = -.1$, $s = 1$	.11	550°	j.736	$.209 \angle 55°$	$.209 \angle -55°$
$\kappa^2 = -.01$, $s = 1$	.16	1250°	j1.016	$.042 \angle -12°$	$.042 \angle 12°$
$\kappa^2 = -.001$, $s = 1$	.165	1975°	j1.009	$.0064 \angle -35°$	$.0064 \angle 35°$
$\kappa^2 = -.1$, $s = 0$	.28	565°	.47	.45	.08
$\kappa^2 = -.01$, $s = 0$	.27	1720°	.50	.50	.001
$\kappa^2 = -.001$, $s = 0$	.265	5430°	.50	.50	0

deriving this expression. V.17 can be written in terms of the parameters of this paper as

$$-\mathcal{K}^2 (\beta_e L\, mr^2)^2\, 2\beta t\ \alpha \phi^2 = \left(\frac{\pi}{2}\right)^2 \qquad \text{V.18}$$

or

$$\theta_o = \beta_e L\, mr^2 = \frac{\pi/2}{\sqrt{-\mathcal{K}^2\,(2\beta t)\ \alpha\ \phi^2}} \qquad \text{V.19}$$

The subscript 0 is appended to θ to distinguish the value of θ calculated in this manner from that obtained from the field analysis. When the beam is not thin it is appropriate to average ϕ^2 over the beam cross section,

$$\bar{\phi}^2 = \frac{1}{t}\int_{-t}^{0} \phi^2\, dy$$

$$= \frac{1}{t}\int_{-t}^{0} e^{+2\beta(y-d)}\, dy = e^{-2\beta d}\ \frac{1-e^{-2\beta t}}{2\beta t}\ .$$

Taking $\alpha = 1$, and substituting for $\bar{\phi}^2$ V.17 becomes

$$-\mathcal{K}^2(\beta_e L\, mr^2)^2\ \ e^{-2\beta d}(1-e^{-2\beta t}) = \left(\frac{\pi}{2}\right)^2$$

or

$$\theta_o = \frac{\pi/2}{\sqrt{-\mathcal{K}'^2}}\ ,$$

where

$$\mathcal{K}'^2 = e^{-2\beta d}(1-e^{-2\beta t})\mathcal{K}^2 = \frac{2T}{1+T}\,\frac{1-T'}{1+T'}\,\mathcal{K}^2\ . \qquad \text{V.20}$$

For the numerical examples $\beta t = .5$ $\beta d = .5$ this becomes

$$\theta_o = \frac{\pi/2}{\sqrt{-.2325\mathcal{K}^2}} \qquad \text{V.21}$$

The results of the field analysis given in Table I have been compared to the thin beam result of Pierce and Muller given by V.21. This comparison is shown in Figure 17 where θ/θ_o is plotted versus $\aleph^2$. θ/θ_o is the length of the tube at start oscillation as predicted by the field analysis of this paper divided by length predicted by the Pierce-Muller thin beam theory. The comparison is made when the beam slips (s = 1) and when it does not slip (s = 0).

Also shown is the result of an approximate analysis of space charge effects by Epsztein. His result is discussed at the end of this section.

From the definition of $\aleph^2$ (IV.53) it is seen that the $\aleph^2$ is increased by increasing the circuit impedance and decreasing the plasma frequency of the beam (and hence by decreasing the current). In the region of large $\aleph^2$ the circuit fields are much stronger than the fields produced by the space charge so that space charge effects are negligible. In this region the field analysis and the Pierce-Muller analysis should agree, and they do.

Figure 17 shows that when the slipping of the beam is ignored (s = 0) the results of the field analysis agree relatively well with the Pierce-Muller theory for all values of $\aleph^2$ whereas if the slipping is taken into account and $\aleph^2$ is small, the field analysis predicts a considerably shorter length of tube. Although no specific experimental data is available to check this curve, the magnitude of the effect is large enough to explain the French observations. Roughly speaking, the factor by which the current is reduced is the square of the factor by which the length is reduced.

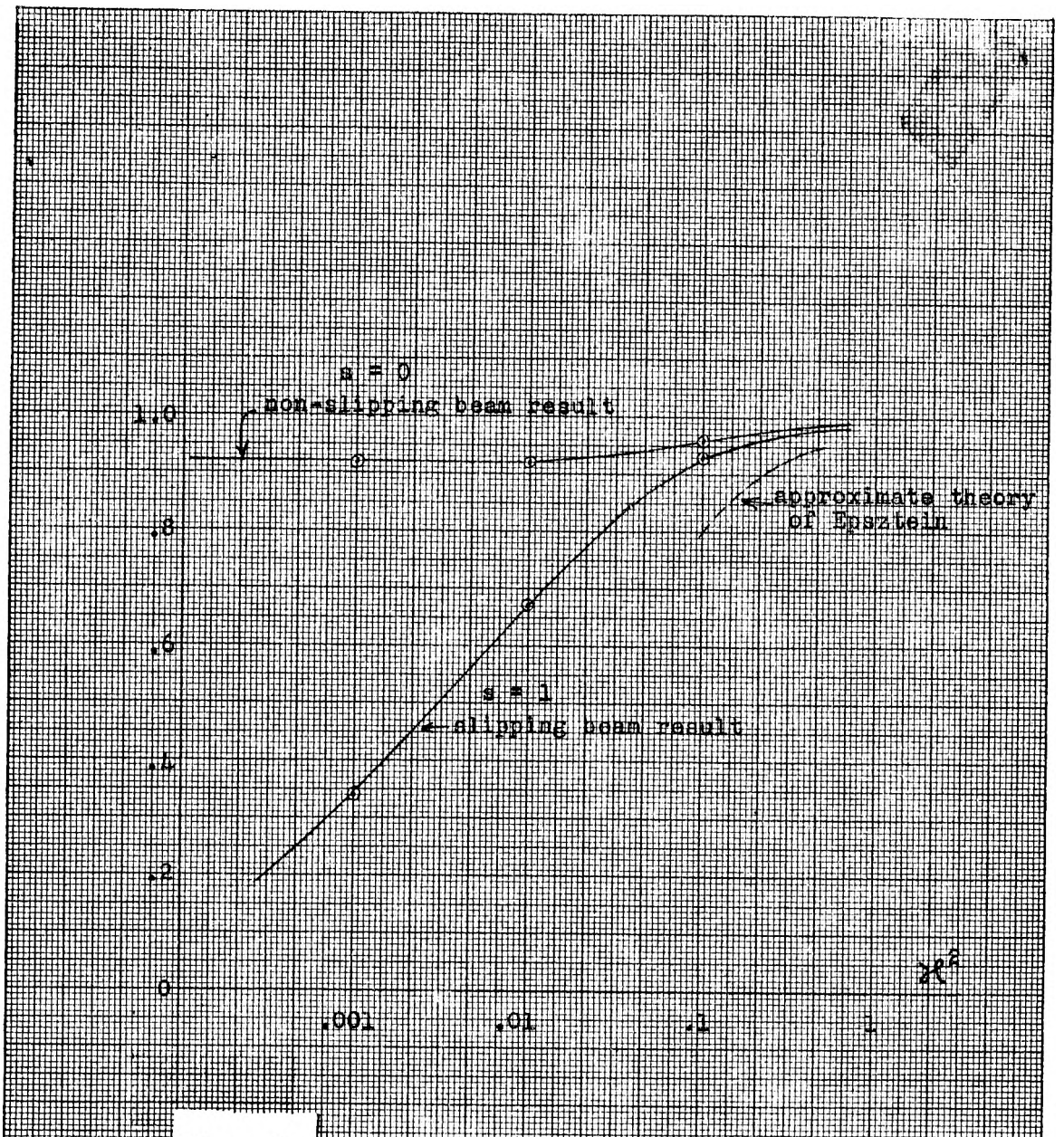

Figure 7. A comparision of the Results of the Field Analysis with the results of the Thin Beam Theory of Pierce and Muller. The ordinate is tube length for Start Oscillation, as predicted by the Field Analysis, divided by the Length as predicted by the Thin Beam Theory. The Dashed Curve shows the Results of Epsztein's Theory.

This result seems plausible on the following grounds. The backward wave oscillator may be considered as a continuous amplifier with modulation at the electron beam by circuit fields along the entire length of the tube. The slow wave circuit feeds back energy to the beginning of the tube to sustain this modulation. Due to the slipping beam effect small perturbations in the beam conditions at $z = 0$ modulate the beam more and more as it drifts through the tube, even in the absence of the slow wave circuit. Thus when the slipping beam effect is present the circuit can be coupled more loosely to the beam than is otherwise possible, and still have oscillation occur.

Discussion of the French Theory of Space Charge Effects. Recently Epsztein (6),(10), has modified the thin beam theory to include the effects of space charge. In this theory the electrons in the thin beam are assumed to move in the field of the circuit plus the field generated by the electronic charge. The beam is assumed to have a finite but small thickness and the field at the center of the beam is computed by assuming that the density of the beam is constant and using an equivalent surface charge density to represent deformations of the beam boundaries. The space charge field computed in this manner is then assumed to act on all electrons. This causes a modification of the propagation constants of the two waves in thin beam theory. This in turn causes a decrease in the length (or current) of the tube required for start oscillation. The reduction computed in this manner is said to be in agreement with the experimental results.

Although Epsztein's theory applies only to thin beams, it may be compared with the results of this paper by replacing the thick beam of

this paper by a thin beam with the same current at the average position of the thick beam. His result can be written in terms of the parameters of this paper as follows:

$$\frac{L}{L_o} = \frac{\theta}{\theta_o} = 1 + \frac{3}{32} \frac{m^2(\beta t)^2}{\gamma'^2} \quad . \qquad \text{V.22}$$

Only the first two terms in a series expansion are given and the formula applies only when the second term is small compared to unity. This result is plotted in Figure 17.

Epsztein's treatment is an attempt to include a.c. space charge effects. It does not take into account the d.c. space charge effect or slipping beam effect, since when the beam is thin all electrons have substantially the same velocity. The $s = 0$ analysis of this paper is undoubtedly a better description of the same situation and it does not predict an appreciable reduction in starting length or current. Only when the slipping beam, or diocotron, effect is taken into account are the predicted starting currents much less than given by the simple thin beam theory. Thus there is considerable doubt as to the correctness of Epsztein's explanation of space charge effects.

The analysis presented in this paper, although requiring lengthier calculations, offers the possibility of studying the effect of other parameters, such as beam thickness, distance from the circuit, etc. on the characteristics of the M-type backward wave oscillator. Although it has not been discussed here, the magnetron amplifier can be analyzed in a similar manner.

BIBLIOGRAPHY

1. Hahn, W. C. "Small Signal Theory of Velocity Modulated Electron Beams" General Electric Review 42 258 (1939).

2. Ramo, S. "Space Charge Waves and Field Waves in an Electron Beam" Phys. Rev. 56 276 (1939).

3. Feenberg, E. "Notes on Velocity Modulation" Sperry Gyroscope Co. Report No. 5221-1043, (1945).

4. Rigrod, W. W. and Lewis, J. A. "Wave Propagation along a Magnetically Focused Electron Beam" Bell System Tech. J. 33 399 (1954).

5. Fletcher, R. C. "Helix Parameters in Traveling Wave Tube Theory" Inst. of Radio Engineers 38 413 (1950).

6. Warnecke, R. R., Guenard, P., Doehler, O., and Epsztein, B. "The M-Type Carcinotron Tube" Inst. of Radio Eng. 43 413 (1955).

7. Brillouin, L. "A Theorem of Larmor and Its Importance for Electrons in Magnetic Fields" Phys. Rev. 67 260 (1945).

8. Pierce, J. R. "Traveling Wave Tubes" D. Van Nostrand (1950).

9. Muller, M. "Traveling-Wave Amplifiers and Backward-Wave Oscillators" Inst. of Radio Eng. 42 1651 (1954).

10. Epsztein, B. "Influence des effets de la charge d'espace sur la courant d'accrochage d'un oscillateur carcinotron type magnetron" C.R. (Acad des Sci) 240 408 (1955).

11. Lamb, H. "Hydrodynamics" Cambridge University Press (1932).

12. Warnecke, R. R., Doehler, O., and Bobot, D. "Les Effets de la Charge d'espace dans les Tubes a Propagation d'onde a Champ Magnetic" Ann. de Radio. 22 (1950).

13. MacFarlane and Hay "Wave Propagation in a Slipping Stream of Electrons: Small Amplitude Theory" Proc. Royal Soc. 63 B 409 (1953).

14. Shelkunoff, S. "Impedance Concept in Waveguides" Quart. App. Math. 2 1 (1944).

15. Birdsall, C. K. and Whinnery, J. R. "Waves in an Electron Stream with a General Admittance Wall" Jour. App. Phys. 24 315 (1953).

16. Pierce, J. R. "Coupling of Modes of Propagation" Jour. App. Phys. 25 179 (1954)

17. Gould, R. W. "Interaction of an Electron Beam with a Periodic Circuit" Calif. Inst. of Tech. Electron Tube and Microwave Laboratory Tech. Report No. 1, March 1955.

18. Parzen, P. "Field Theory of Space Harmonic Traveling Wave Structures" Johns Hopkins Univ. Rad. Lab. Report No. AF-6, Sept. 25, 1954.

19. Chodorow, M. and Chu, E. L. "Cross-wound Twin Helices for Traveling Wave Tubes" Jour. App. Phys. 26 33 (1955).

20. Bloch, F. "Über die Quantenmechanik der Elektronen in Kristallgittern" Zeitschrift für Physik 52 555 (1928).

21. Brillouin, L. "Wave Propagation in Periodic Structures" McGraw-Hill (1946).

22. Slater, J. C. "Microwave Electronics" D. Van Nostrand (1950).

23. Goldstein, H. "Cavity Resonators and Waveguides Containing Periodic Elements" PhD Thesis, Mass. Inst. of Tech. 1943

24. Stark, L. "Electromagnetic Waves in Periodic Structures" Mass. Inst. of Tech. Res. Lab. of Electronics, Tech. Report No. 208, Dec. 9, 1952.

25. Nalos, E. J. "Measurement of Circuit Impedance of Periodically Loaded Structures by Frequency Perturbations" Inst. of Radio Eng. 42 1508 (1954).

26. Watkins, D. A. and Siegman, A. E. "Helix Impedance Measurements Using an Electron Beam" Jour. App. Phys. 24 917 (1954).

27. Sedin, J. W., private communication.

28. Heffner, H. "Analysis of the Backward-Wave Travoling-Wave Tube" Inst. of Radio Eng. 42 930 (1954).

29. Johnson, H. R. "Backward-Wave Oscillators" Inst. of Radio Eng. 43 684 (1955).

LIST OF SYMBOLS

α attenuation constant in z direction

β propagation constant in z direction

$$\beta_e = \frac{\omega}{u}, \quad \beta_c = \frac{\omega_c}{u}, \quad \beta_p = \frac{\omega_p}{u}, \quad \beta_+ = \frac{\omega}{u_+}, \quad \beta_- = \frac{\omega}{u_-}$$

β_o propagation constant of the fundamental space harmonic of the periodic slow-wave circuit

β_n propagation constant of the n^{th} space harmonic of the periodic slow wave circuit

$\gamma_n = \sqrt{\beta_n^2 - k^2}$, transverse separation constant for the n^{th} space harmonic of the periodic slow wave circuit

$\delta = \beta/\beta_e$, normalized propagation constant

$\Delta = \frac{\partial u}{\partial y}$, transverse velocity gradient in electron beam

$\epsilon = \frac{u_+ - u_-}{u_-}$, fractional velocity difference in electron beam

ϵ_o permittivity of free space

$\mathcal{E}(z)$ z component of electric field at a plane which just grazes the slow wave circuit

η charge to mass ratio of the electron $(\eta > 0)$

$\theta = \beta_+ L m r^2$, length of backward wave oscillator at start oscillation in dimensionless units

θ_o length of backward wave oscillator at start oscillation as predicted by the thin beam theory, in dimensionless units

κ^2 dimensionless constant of coupling between circuit waves and space charge waves of the electron beam

μ_o permeability of free space

$\nu = \frac{\beta - \beta_+}{r^2 m \beta_+}$, dimensionless variable representing the propagation constant β

$\xi = \frac{\beta u - \omega}{\Delta}$, dimensionless variable which is a linear function of the y coordinate in the electron beam

ρ_o steady or d.c. component of the charge density of the electron beam

ρ_1 perturbation or a.c. component of the charge density of the electron beam

σ_+ equivalent surface charge density which represents the deformation of the upper boundary of the electron beam

σ_- equivalent surface charge density which represents the deformation of the lower boundary of the electron beam

ω radian frequency of sinusoidal oscillations

$\omega_c = B_{ox}$, radian cyclotron frequency of electrons in a magnetic field B_{ox}

$\omega_p = \sqrt{-\frac{\rho_o}{\epsilon_o}\eta}$, radian plasma frequency of the electron beam

$\Omega = \sqrt{(\omega - \beta u)^2 - \omega_c(\omega_c - \Delta)}$, a quantity with the dimensions of frequency (sec^{-1}) which appears in the solution of the electronic equations.

a distance from lower edge of beam to conducting plane

$b = \frac{\beta_m - \beta_+}{mr^2 \beta_+}$ difference in the m^{th} space harmonic phase velocity and electron velocity in dimensionless units

B_E E-mode, or transverse magnetic, surface susceptance

B_m E-mode surface susceptance for the m^{th} space harmonic at the plane of the slow wave circuit, of the space below the circuit with the electron beam present

B_{mo} E-mode surface susceptance for the m^{th} space harmonic at the plane of the slow wave circuit, of the space below the circuit with the electron beam absent

$\underline{B}_o$ steady part of the magnetic field vector

B_{ox} x component of steady magnetic field

$C = \coth \beta a$

C_1 "space charge" capacitance in the Pierce equivalent circuit

D period of the slow wave circuit

$\underline{E}_o$ steady part of the electric field vector

$\underline{E}_1$ time-varying part of the electric field vector

E_{oy} y component of the steady electric field

E_{1y} y component of the time-varying electric field

E_{1z} z component of the time-varying electric field

i_+ equivalent surface current on upper beam edge

i_- equivalent surface current on lower beam edge

$k = \omega\sqrt{\mu_o \epsilon_o}$, free space wave number

K Pierce traveling wave tube circuit impedance

L length of backward wave oscillator at start oscillation

$m = \frac{\omega_c}{\omega}$ ratio of cyclotron frequency to oscillation frequency

P normalized surface conductance

Q normalized surface susceptance

$\underline{r}$ vector position of an electron in the Lagrangian description

$\underline{r}_o$ unperturbed position of an electron in the Lagrangian description

$\underline{r}_1$ perturbation position of an electron in the Lagrangian description

$r = \frac{\omega_p}{\omega_c}$ ratio of plasma frequency to cyclotron frequency

s slip parameter

S sum which arises in determining propagation characteristics of the slow wave circuit

t thickness of electron beam

$T = \tanh \beta t$

$T' = \tanh \beta d$

$\underline{u}$ steady part of the velocity field

$u = u(y)$, z component of the steady velocity field

u_+ z component of velocity of the upper-beam edge

u_- z component of velocity of the lower-beam edge

$\underline{v}_1$ time-varying component of the velocity field

v_{1y} y component of the time-varying velocity field

v_{1z} z component of the time-varying velocity field

w width, or x dimension, of the tube

y_1 perturbation in y position of electron in Lagrangian description

z_1 perturbation in z position of electron in Lagrangian description

Y_E E-mode, or transverse magnetic, surface admittance

Y_m E-mode surface admittance for the m^{th} space harmonic, at the plane of the slow wave circuit, of the space below the circuit with the electron beam present

Y_{mo} E-mode surface admittance for the m^{th} space harmonic, at the plane of the slow wave circuit, of the space below the circuit with the electron beam absent

Y'_n Admittance of slow wave circuit slots to n^{th} harmonic

DISTRIBUTION LIST - Nonr 220(13)

TECHNICAL REPORTS

		Copies
Chief of Naval Research Navy Department Washington 25, D. C.	Code 427	2
Director Naval Research Laboratory Washington 25, D. C.	Code 5240 Code 7130 Code 2000 Code 5430	1 1 6 1
Commanding Officer Office of Naval Research Branch Office 1000 Geary Street San Francisco 9, California		1
Commanding Officer Office of Naval Research Branch Office 1030 E. Green Street Pasadena, California		2
Commanding Officer Office of Naval Research Branch Office The John Crerar Library Building 86 East Randolph Street Chicago 1, Illinois		1
Commanding Officer Office of Naval Research Branch Office 346 Broadway New York 13, New York		1
Officer-in-Charge Office of Naval Research Navy 100 Fleet Post Office New York, New York		3
Chief, Bureau of Aeronautics Navy Department Washington 25, D. C.	EL 4	1
Chief, Bureau of Ordnance Navy Department Washington 25, D. C.	Re 4 Re 9	1 1
Chief of Naval Operations Navy Department Washington, D. C.	Op 20X Op 421 Op 55	1 1 1
Director Naval Ordnance Laboratory White Oak, Maryland		1

Director Naval Electronics Laboratory San Diego 52, California		1
U.S. Naval Post Graduate School Monterey, California	Dept.of Electronics and Physics Prof. C.E. Menneken	1
Commander Naval Air Missile Test Center Point Mugu, California	Code 366	1
U. S. Naval Proving Ground Dahlgren, Virginia	W. H. Benson	1
Commander U. S. Naval Air Development Center Johnsville, Pennsylvania		1
Committee on Electronics Research and Development Board Department of Defense Washington 25, D. C.		1
Director National Bureau of Standards Washington 25, D. C.	Division 14.0 CRPL, Librarian	1
Commanding Officer Engineering Research and Development Lab. Ft. Belvoir, Virginia		1
Ballistics Research Laboratories Aberdeen Proving Ground, Md.	D.W.H.Delsasso	2
Chief, Ordnance Development Division National Bureau of Standards Connecticut Ave. and Van Ness St., NW Washington 25, D. C.		2
Commanding Officer Frankford Arsenal Bridesburg, Philadelphia, Pa.	COL Kundul	1
Supply Receiving Section Signal Corps Engineering Laboratories Evans Signal Laboratory Building 42 Belmar, New Jersey	Thermionics Branch	5
Commanding General Air Research and Development Command Post Office Box 1395 Baltimore 3, Maryland	RDRR RDDDE-3 RDDDE-5	1 1 1

Commanding General Wright Air Development Center Wright-Patterson Air Force Base, Ohio	WCLC WCLRC	1 1
Commanding General Air Force Cambridge Research Center 230 Albany Street Cambridge 39, Massachusetts	CRRE	1
Commanding General Rome Air Development Center Griffiss Air Force Base Rome, New York	RCRW	1
Armed Services Technical Information Agency Document Service Center Knott Building Dayton 2, Ohio	DSC-SA	5
Director Air University Library Maxwell Air Force Base, Alabama	CR4582	1
Chief, Western Division Air Research and Development Command Office of Scientific Research Post Office Box 2035 Pasadena, California		1
Microwave Laboratory Stanford University Stanford, California	F.V.L.Pindar	1
Engineering Library Stanford University Stanford, California		1
Massachusetts Institute of Technology Cambridge 39, Massachusetts	Research Laboratory of Electronics	1
Document Office of Government Research Contracts G-16, Littanuer Center Harvard University Cambridge, Massachusetts	M.L.Cox, Librarian	1
Sloane Physics Laboratory Yale University New Haven, Connecticut	R. Beringer	1
Department of Electrical Engineering Yale University New Haven, Connecticut	H. J. Reich	1

Electrical Engineering Department University of Illinois Champaign, Illinois	Electron Tube Section	1
Chairman, Div. of Electrical Engineering University of California Berkeley 4, California		1
Technical Report Collection 303a, Pierce Hall Harvard University Cambridge, 38, Massachusetts		1
Laboratory for Insulation Research Massachusetts Institute of Technology Cambridge 39, Massachusetts	A. von Hippel	1
Engineering Library California Institute of Technology		1
Lincoln Laboratory Massachusetts Institute of Technology Cambridge 39, Massachusetts		1
Signal Corps Resident Engineer Electronic Defense Laboratory Post Office Box 205 Mountain View, California	F. W. Morris Jr.	1
Cornell Aeronautical Laboratory Cornell Research Foundation Buffalo 21, New York		1
Director, Electronics Defense Group Engr. Research Institute University of Michigan Ann Arbor, Michigan		1
Georgia Institute of Technology Atlanta, Georgia	Mrs. J. F. Crosland Librarian	1
Varian Associates 611 Hansen Way Palo Alto, California	Fred D. Wilimek	1
Airborne Instrument Laboratory Mineola, New York	John Dyer	1
Bell Telephone Laboratories Murray Hill Laboratory Murray Hill, New Jersey	Leah E. Smith Librarian J. R. Pierce	1 1
Hughes Aircraft Company Culver City, California	John T. Milek Technical Librarian	1

RCA Laboratories Princeton, New Jersey	E. W. Herold and Harwell Johnson	1
Federal Tele. Laboratories, Inc. 500 Washington Avenue Nutley, New Jersey	W. Derick K. Wing	1 1
General Electric Microwave Laboratory 601 California Avenue Palo Alto, California	Technical Library	1
Columbia Radiation Laboratory 538 W 120th Street New York 27, New York		1
Countermeasures Laboratory Gilfillan Bros, Inc. 1815 Venice Boulevard Los Angeles, California		1
The Rand Corporation 1700 Main Street Santa Monica, California	Margaret Anderson Librarian	1
Research and Development Board Pentagon Building Washington 25, D. C.	Technical Library	1
The Motorola Riverside Research Lab. 8330 Indiana Avenue Riverside, California	Mr. John Byrne	1
Chief, Bureau of Aeronautics Department of the Navy Washington, D. C.	EL 43 EL 45	1 1
Chief, Bureau of Ships Department of the Navy Washington, D. C.	Code 816 820 840	1 1 1
Panel on Electron Tubes 346 Broadway (8th Floor) New York 13, New York		1
Supervisor of Research Laboratory Electrical Engineering Bldg. Purdue University Lafayette, Indiana	H.J.Oorthuys	1
University of Florida Department of Electrical Engineering Gainesville, Florida	W. E. Lear	1

Microwave Research Institute Polytechnic Institute of Brooklyn 55 Johnson Street Brooklyn 1, New York	E. Weber	1
New York Naval Shipyard Material Laboratory Library Brooklyn 1, New York	Code 912B	1
University of Washington Department of Electrical Engineering Seattle, Washington	E.A.Harrison A.V.Eastman	1 1
University of Colorado Department of Electrical Engineering Boulder, Colorado		1
Electrical Engineering Dept. Princeton University Princeton, New Jersey		1
National Union Radio Co. 350 Scotland Road Orange, New Jersey	Dr.A.M.Skellet	1
Sperry Gyroscope Company Great Neck, L.I., New York	J. E. Shepherd	1
W. L. Maxson Corporation 460 West 34th Street New York 1, New York	M. Simpson	1
Raytheon Corporation Waltham, Massachusetts	H.R. Argento	1
Electron Tube Div., Research Lab. General Electric Company The Knolls Schenectady, New York	E.D.McArthur	1
Office of Technical Services Department of Commerce Washington 25, D. C.		1
Extra copies for future requirements		25
Electronics Research Laboratory Stanford University Stanford, California	Librarian	1
Professor W. P. Dyke Linfield College McMinnville, Oregon		1